5-2014

VALUE-ADDED LIGNIN BASED CARBON FIBER FROM ORGANOSOLV FRACTIONATION OF POPLAR AND SWITCHGRASS

Andreas Attwenger
University of Tennessee - Knoxville, aattweng@utk.edu

To the Graduate Council:

I am submitting herewith a thesis written by Andreas Attwenger entitled "VALUE-ADDED LIGNIN BASED CARBON FIBER FROM ORGANOSOLV FRACTIONATION OF POPLAR AND SWITCHGRASS." I have examined the final electronic copy of this thesis for form and content and recommend that it be accepted in partial fulfillment of the requirements for the degree of Master of Science, with a major in Forestry.

Joseph J. Bozell, Major Professor

We have read this thesis and recommend its acceptance:

Timothy M. Young, Alexander Petutschnigg, David P. Harper

Accepted for the Council:
Carolyn R. Hodges

Vice Provost and Dean of the Graduate School

(Original signatures are on file with official student records.)

VALUE-ADDED LIGNIN-BASED CARBON FIBER FROM ORGANOSOLV FRACTIONATION OF POPLAR AND SWITCHGRASS

A Thesis Presented for the

Master of Science

Degree

The University of Tennessee, Knoxville

Andreas Attwenger

May 2014

Dedication

to my parents

Günter
Ursula

my brothers

Thomas & David

my sister-in-law & her beautiful boys

Silvia, Sebastian & Maximilian

Acknowledgements

I would like to express my graduation and appreciation for the many people that have guided me throughout my study.

First, I would like to thank my previous supervisor Dr. Darren A. Baker for giving me the opportunity to work in this interesting field. A special thank you goes to my major Professor Dr. Joe J. Bozell, and committee member Professor Dr. Timothy M. Young, without their guidance and assistance, this project could not be successfully completed. Thank you also to my other committee members Dr. Alexander Petutschnigg and Dr. David Harper who have provided extensive support.

I would further like to express my graduation towards Dr. Timothy G. Rials, Professor and Director of the Center for Renewable Carbon as well as Dr. Keith Belli, Professor and Head of the Department of Forestry, Wildlife and Fisheries.

I owe many thanks to Dr. Omid Hosseinaei who has always been helping me in my research. I am also very thankful to all people working at the Center for Renewable Carbon, staff and fellow students for their friendship and support. Hagen, Anton, Dominik, Alex, Tanu, Jimmy and Derek, thanks for being such good friends and support in the labs.

Ms. Ann Ryan, Ms. Amanda Silk Curde, Mr. Chris Helton and Mr. Nicolas André, thanks for your help your friendship and good times at the center.

Abstract

Carbon fibers have unique properties that include high strength, low density and excellent chemical and thermal resistance. However, they have a low level of utilization because of their high price; typically around $30/kg for an entry level polyacrylonitrile (PAN) based carbon fiber. Low-cost carbon fibers derived from lignin are currently being investigated at the University of Tennessee, because using lignin as a precursor could significantly reduce production costs. Lignins obtained from the pulp and paper and the emerging biofuel industries have the potential to be used for carbon fiber production, however, they are typically unsuitable because of the high levels of impurity and variable thermal properties. This research study examines the potential of a novel organosolv process to provide high purity lignin for carbon fiber production. This fractionation separates woody and herbaceous bioenergy crops into their three main components: cellulose, hemicellulose, and lignin, each of which can be used within the biorefinery for the production of fuels or chemicals. In this program, organosolv derived lignins from both tulip poplar (*Liriodendron tulipifera*) and Alamo switchgrass (*Panicum virgatum*) were recovered and compared as starting materials for carbon fiber. The organosolv derived lignin was analyzed using several different methods to assess quality differences for potential carbon fiber manufacture. Their purities, chemical structures, consistencies, thermal, and carbonization properties were evaluated and lignin exhibiting optimal properties was used for fiber spinning and conversion to carbon fiber. Lignin exhibiting the best thermal performance was achieved by isolation at 150°C to 170°C with an acid concentration of 0.05 and 0.1 M H_2SO_4, and a fractionation time of 120 and 180 minutes. Organosolv fractionation conditions and their influence on the properties of lignin-based carbon fiber are presented in this thesis.

Keywords: Organosolv fractionation, lignin analysis, carbon fiber, melt-spinning, lignin-based carbon fiber, biopolymers and renewable polymers

Table of Contents

List of Tables

List of Figures

List of Abbreviations

ANOVA	=	Analysis of variance
APR	=	Alcohol pulping and recovery
CF	=	Carbon fiber
CO_2	=	Carbon dioxide
CRC	=	Center for Renewable Carbon
CS	=	Combined severity
DOE	=	Department of Energy
DSC	=	Differential scanning calorimetry
H_2SO_4	=	Sulfuric acid
HW	=	Hardwood
LCF	=	Lignocellulosic feedstock
MIBK	=	Methyl isobutyl ketone
NMR	=	Nuclear magnetic resonance
PAN	=	Polyacrylonitrile
PEO	=	Poly ethylene oxide
SEM	=	Scanning electron microscopy
SGOL	=	Switchgrass organosolv lignin
SW	=	Softwood
TG	=	Glass transition temperature
TGA	=	Thermogravimetric analysis
TMA	=	Thermomagnetic analysis
UV	=	Ultraviolet

CHAPTER I. INTRODUCTION

Today there is great pressure to conserve naturally occurring fuel resources, decrease carbon dioxide (CO_2) emissions, and counteract global warming. A significant quantity of CO_2 emissions are caused by the utilization of petroleum products in transportation fuels, and therefore, there is great interest in providing low-cost lightweight materials for use in the automobile industry to improve fuel efficiencies and lower CO_2 emissions. Ultra-lightweight, fuel-efficient vehicles are needed and thus, there has been great enthusiasm about the potential for using carbon fiber (CF) reinforced composites in the automobile industry (Warren et al., 2009). According to the U.S. Department of Energy (DOE), reinforced composites using PAN-based carbon fiber could reduce the weight of car parts by up to 60%. The fact that these PAN carbon fibers are still too expensive, about $30/kg (Baker et al., 2012) and over-engineered for the task, opens up the possibility for evaluating new precursor materials that could significantly reduce carbon fiber costs while maintaining acceptable and/or comparable mechanical properties.

Carbon fiber has desirable properties such as high strength, low density, and high chemical resistance but is very expensive. It is therefore, mainly used in aerospace, motorsports, engineering and other industrial applications or the luxury automotive industry. Nonetheless, forecasts show that the demand on carbon fiber will dramatically increase in the near future.

Renewable resources such as agricultural residues and forest crops are potential sources of materials that are inexpensive and abundant and as such can be used in industrial production (Council, 2000). Current research at the University of Tennessee is examining the use of abundant and low cost lignin as a starting material for carbon fiber production. Lignin can be recovered from lignocellulosic biomass and can be further processed to improve its properties. Moreover, the large amount of lignin potential from biorefineries could make lignin the innovative material of the future. However, the feasibility of processing lignin to carbon fiber depends on the method used to separate the lignin from biomass. Any separation process must afford high purity lignin with specific thermal properties and narrow molecular weight distribution. The barrier for the transition of lignin-based starting materials to carbon fiber production has historically been the low mechanical properties achieved using typically available technical lignins (Baker et al., 2012). Recent work has revealed laboratory-scale efforts that have given lignin carbon fibers, which were anticipated to be very low in cost compared to petroleum-based carbon fibers and offered much improved mechanical properties compared to earlier lignin carbon fiber work (Baker et al., 2012). The current

challenge is therefore to improve the lignin used for carbon fiber manufacture further and then adapt the processes for industrial scale production.

1.1. Project Objectives

Previous research on lignin-based carbon fibers has documented low mechanical properties relative to carbon fibers obtained from petroleum-based sources. To manufacture low cost lignin-based carbon fiber with improved properties, a novel organosolv fractionation process is used to recover relatively pure lignin with improved thermal properties compared to lignin from other pretreatments. A requirement for lignin to be used in carbon fiber production is the feasibility to be melt-spun at high rates. This requirement demands a relatively clean lignin with a specific molecular weight distribution. The main objective of this research is to explore and quantify carbon fiber properties from organosolv lignin relative to the minimum requirements specified by the automobile industry (strength of 1.72 GPa and modulus of 172 GPa). Therefore, novel lignins recovered from poplar and switchgrass, both potential bioenergy feedstocks, were analyzed, spun, and converted to carbon fiber, and their mechanical properties were evaluated.

1.2. Research Hypotheses

H_1: The novel organosolv fractionation process will provide high purity lignins in comparison to those produced from other processes.

H_2: Lignin-based carbon fibers produced from these lignins have improved mechanical properties over those developed from other lignins.

1.3. Thesis Tasks

The study tasks necessary to test the research hypotheses are as follows:

- Design a matrix, based on previous research for poplar and switchgrass to obtain a maximum lignin yield as well as maximum lignin purity;
- Conduct organosolv fractionation of poplar and switchgrass biomass using the CRC reactor;
- Separate recovered black liquor to obtain lignin and determine purity and ash content;
- Carry out thermal characterization of lignin by Fisher Johns, differential scanning calorimetry (DSC) and thermogravimetric analysis (TGA);
- Use lignin with the best thermal properties for melt spinning to fabricate lignin fiber;
- Convert lignin fibers to carbon fiber using sequential thermal treatments;
- Evaluate lignin-based carbon fiber with optical and mechanical analysis;
- Compare mechanical properties of carbon fibers and give further recommendations.

1.4. Thesis Organization

The first chapter of this thesis is a literature review of carbon fiber derived from an environmentally friendly material, lignin. First, lignin itself will be described, followed by an overview of current carbon fiber production, its costs and requirements to serve as a precursor. The historical development of lignin-based carbon fiber will be explained starting with its origin in the 1960s. Suitable recovery processes for lignin will be explained giving an overview of biorefineries, which produce a variety of different chemical products and transportation fuels derived from biomass. The kraft, steam explosion and organosolv fractionation processes will be explained in detail as they are the most promising sources of lignin for further production to carbon fiber. A detailed explanation of the melt spinning process and the conversion of lignin fibers into carbon fiber will lead to the analytical and

thermal analyses. Methods used to determine purity, ash content, and elemental composition, as well as melting properties, transition temperature and decomposition temperatures are shown. Optical analysis and mechanical measurements of produced fibers are also defined in this section.

The next chapter addresses the materials and methods used for this study. The chemical analyses, laboratory equipment, and feedstocks are documented. The structure of this section outlines the basic steps of getting from lignocellulosic biomass to the point of actual carbon fiber production. The two different feedstocks used in the study are defined followed by the solvent composition. An explanation of the reactor and the workup of the gathered black liquor is given. Different matrixes define the experimental runs of tulip poplar (*Liriodendron tulipifera)* and Alamo switchgrass (*Panicum virgatum)*. All methods for lignin analysis are also given. The steps necessary to spin lignin for best performance as fibers, heat treatment and stabilization for carbonization, are defined. The techniques for carbon fiber verification and comparison are given as well.

Following chapter gives an overview of all analytical work that has been conducted for this research. First, an analysis of the investigated biomass is given, including the moisture and lignin content of tulip poplar and switchgrass, followed by the presentation of fractionation conditions. Organosolv fractionation conditions are shown separately for both feedstocks and then compared. The second part of the chapter presents the thermal analysis. Thermal properties including the glass-liquid transition, the decomposition temperature and melting properties give an idea for the operation of lignin and its utility for further processing to carbon fiber. This discussion is followed by the results of the second approach of this study, time dependent organosolv fractionations. Again, both feedstocks are discussed separately and then compared. The final portion of this chapter presents the conversion of lignin to carbon fiber, and evaluation of the morphology and mechanical properties using scanning electron microscopy and an Instron single filament-testing machine, respectively.

At the end the findings will be discussed and some further directions are given.

CHAPTER II. LITERATURE REVIEW

2.1. Lignin

The term lignin is derived from the Latin word *Lignum* for wood and was first mentioned by Augustin Pyramus de Candolle, a Swiss botanist in 1819 (Candolle et al., 1821). Natural lignin is a three-dimensional polymer that occurs in many plants at levels from 15 to 32 wt% (Table 1), and after cellulose, is the most abundant organic polymer on earth. Lignin's chemical structure is complex (Figure 1), is built upon phenylpropane units, and is mainly composed of carbon, hydrogen and oxygen. Lignin occurs between and within cell walls, gives rigidity to the cell and helps reduce dimensional changes in the wood.

Table 1. Composition of biomass.

Biomass	Cellulose	Hemicellulose	Lignin	Extractives	Reference
Hardwood	42±2 %	27±2 %	28±3 %	3±2 %	(1)*
Softwood	45±2 %	30±5 %	20±4 %	5±3 %	(1)*
Switchgrass	37±2 %	29±2 %	19±2 %	15±2 %	(2)*

*(1) (Sjostrom, 1993); (2) (Mani et al., 2006)

Lignin plays a number of important roles: one is providing strength in lignocellulosic biomass and serving as cement between the cellulose fibers in plants. Considering that nowadays there is a huge amount of lignin potentially available as a byproduct from pulp and paper industry, there is increasing interest in the development of economically viable new applications (Suhas et al., 2007). Lignin is biosynthesized from three primary monolignol precursors: *para*-coumaryl alcohol, coniferyl alcohol and sinapyl alcohol, which lead to the *para*-hydroxyphenyl (H), guaiacyl (G) and syringyl (S) subunits of lignin, respectively, as can be seen in Figure 1. The main structural differences in lignin are the amount and position of the methoxyl groups in the H, G and S units. During biosynthesis, the monolignols are linked through a variety of carbon-carbon bonds and different ether bonds leading to a complex structure comprising many substructures and interunit linkages (Adler, 1977). Hardwood lignins contain approximately equal amounts of sinapyl and coniferyl units while switchgrass is primarily derived from coniferyl, sinapyl and 10-20% p-coumaryl units (Bozell et al., 2007). With regard to the eventual use of lignin for carbon fiber production, (Baker et al.,

2012) described how the S, G and H contents in lignin affect the thermal properties and moreover, the performance in further processing.

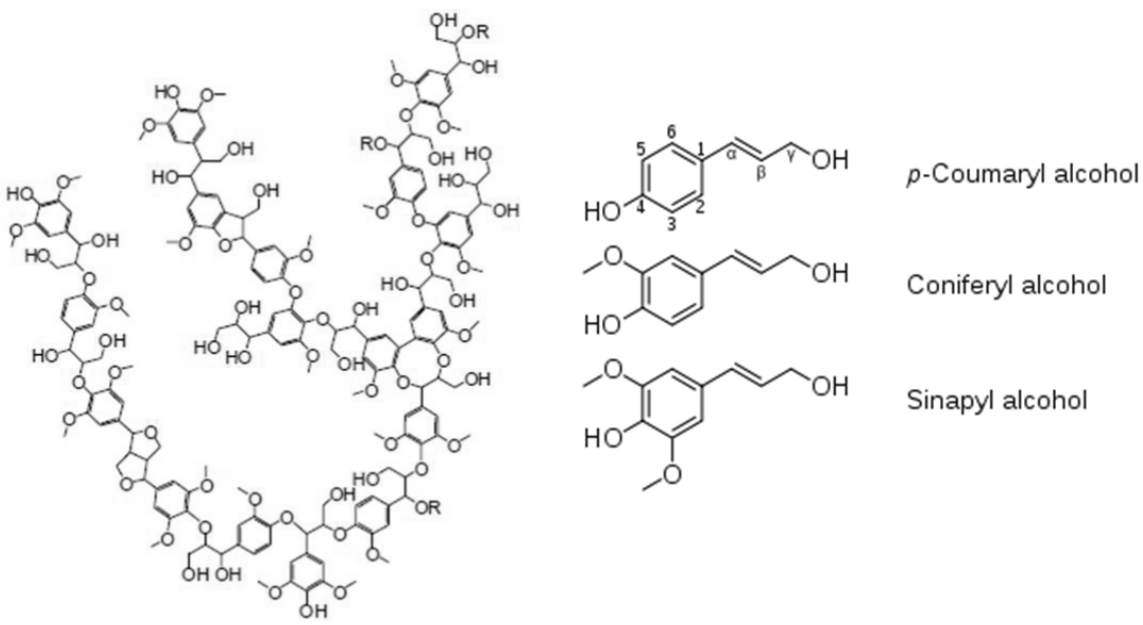

Figure 1. Chemical structure of hardwood lignin (left) and its monolignols (right).

During the manufacture of paper and biofuels, lignin can be recovered using separation processes explained in detail in section 2.4. Because processes mainly focus on the cellulose exploitation these separation processes change the chemical structure of the lignin to a certain extent. About 255 million tons of technical lignin, as a byproduct of pulp and paper industry, is produced in one year but is burned for process energy. However, lignocellulosic biomass requires some kind of pretreatment to liberate the desired components, thus limiting the adaptability in current industrial applications.

2.2. Carbon Fiber

Carbon fiber is a long, very thin strand consisting of carbon atoms arranged in a honeycomb crystal lattice, the so-called graphene (Figure 2).

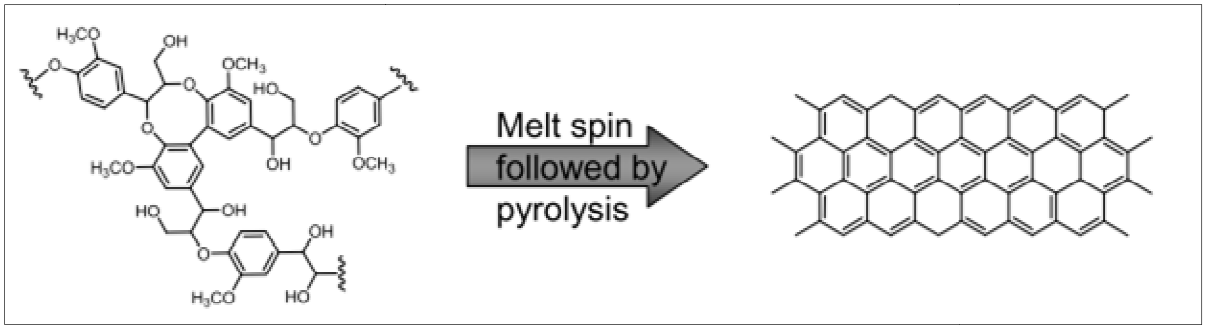

Figure 2. Scheme of converting melt-spun lignin into carbon fiber (Norberg et al., 2013).

A typical sequence of operations to produce carbon fiber based on a PAN precursor is usually divided into a few main steps depending on the company (Figure 3) but in general, carbon fiber production includes spinning the fiber, stabilization, carbonization and graphitization. Organic polymers such as PAN are melt spun into long strands and then heated to 1000ºC to 3000ºC for several minutes in an inert atmosphere. PAN is the most widely used precursor for carbon fiber production and accounts for almost 90% of carbon fiber produced annually (Chae et al., 2009). The final fibers are then slightly oxidized to enhance their bonding ability with different adhesives for further processing. After a sizing surface treatment, the fibers are wound onto cylinders and the final carbon fiber is ready to ship. For composite manufacture, these strands can be twisted into a yarn, woven into a fabric and impregnated with an epoxy to form a composite.

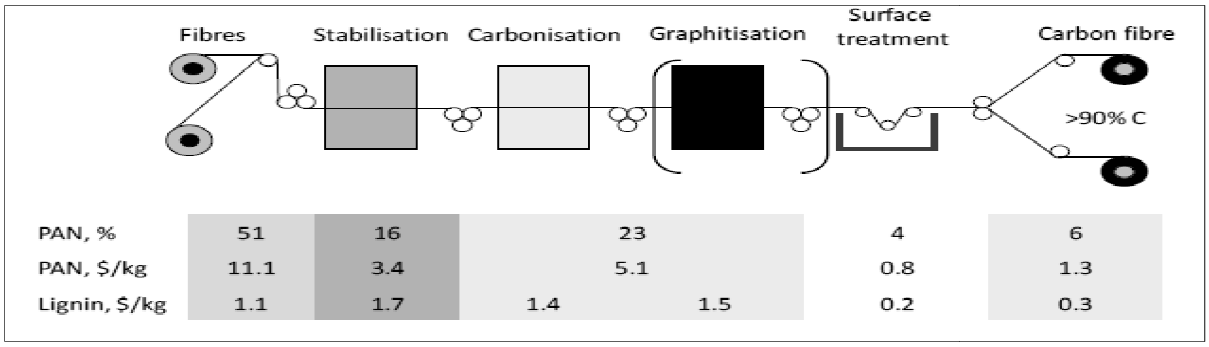

Figure 3. Processing steps for CF production and their estimated costs (Norberg, 2013).

The total amount of carbon fiber manufactured in the year 2000 was about 17,000 tons and currently has more than doubled to 35,000 tons of production (Frank et al., 2012). The forecast for carbon fiber demand by 2015 is 60,000 tons per annum (Lysenko et al., 2011). This forecasted supply and demand gap for carbon fiber has led to an increase in the research on a renewable alternative to petroleum-based carbon fiber (Frank et al., 2012). About 50% of the final carbon fiber costs from both PAN and lignin as starting material, results from the

cost of the precursor immediately after melt spinning, but before stabilization, carbonization and post treatment steps. Norberg et al. (2013) estimates those lignin fiber costs at $1.1 $/kg as can be seen in Figure 3, whereas Baker et al. (2012) predicts a price for one kilogram as low as $0.85 but both estimate the same cost of $6.2/kg for the finished carbon fiber. Thus, a focus on carbon fiber from low cost and sustainable materials could result in significantly lower final costs. The table below shows an experimental comparison of the costs of carbon fiber precursors related to the possible yield and the already measured mechanical properties (Table 2).

Table 2. Experimental cost estimation of carbon fiber precursor.

Precursor	**Cost/kg [$]**	**CF Yield [%]**	**Cost of CF ($/kg)**	**Tensile strength [GPa]**	**Tensile modulus [GPa]**
Lignin	0.85(1)*	55	6.2	1.069	82.7
Polyolefin	1.57 - 2.36(2)*	70	N/D	0.758(3)*	149
Textile grade PAN	4.4 - 13.2	50	12.25 - 25.43	2.516	173
Melt-spun PAN	6.3	50	$ 17.4	1.034	N/D

*(1) Baker et al., 2012, (2) Warren, 2012; (3) Paulaukas, 2010

As mentioned before, the cost of the carbon fiber after the melt spinning step is about 50% of the production and the equipment costs are estimated about 30% of the production costs (Warren et al., 2009). Remaining costs are, therefore, the costs for the separate production steps as can be seen in Figure 3. The cost estimations for lignin as precursor in carbon fiber production shows a huge potential in cost reduction compared to conventionally used petroleum-based starting material.

2.3. Lignin as a Raw Material for Carbon Fiber

The production of carbon fiber from lignin began in the 1960s and was first reported by Otani (1969). In his patent (US 3,461,082A) he provides a method for producing carbon fiber from lignin that was obtained by the chemical treatment of woody material. Several methods providing carbon fiber from lignin were disclosed which included the use of different mixtures of alkali lignin, kraft lignin and lignosulfonates from both hardwoods and softwoods, and lignin mixed with zinc chloride, glycerine and sulfuric acid. A kraft lignin from hardwood was spun into fiber using a hybrid solution/melt spinning process, which upon conversion was reported to give carbon fiber with strength of 0.785 GPa. In the early 1970s the Japanese company Nippon Kayaku Seizo Co., Ltd. started production of a commercial lignin-based carbon fiber (Kayacarbon) using lignosulfonates obtained from sulfite pulping.

A few years later the fine structure of a dry spun Kayacarbon fiber was investigated by Johnson et al. (1975). High angle X-ray diffraction and scanning electron microscopy were used to evaluate the crystallite size and the structure, respectively. The major finding of this investigation was that the lignin-based carbon fibers had a heterogeneous fine structure considered to be more distinct than in other carbon fibers. At about the same time inventors from Germany (Manfred et al., 1973) published a patent describing the process for the production of a lignin-based carbon fiber. The authors further delineated five basic requirements for carbon fiber production: 1) the starting material has to be readily producible, 2) the carbon content has to be as high as possible, 3) the original fiber must be readily available in a fibrous form, 4) the fiber must preserve flexibility and strength during thermal stabilization, and 5) the precursor should be inexpensive. Nine examples investigating the dry spinning of numerous starting materials such as regenerated cellulose, PAN, polyvinyl alcohol and polyvinyl chloride were reported, but none of them fulfilled all these conditions. Almost every example required a small quantity of high molecular weight linear polymer to achieve carbon fibers. Semi-structural automobile applications using lignin-based carbon fiber were initiated by ORNL in late 1990s. Other techniques to obtain lignin for carbon fiber production arose later through investigation on steam explosion lignin, kraft lignin and organosolv lignin (Chakar et al., 2004; de la Torre et al., 2013; Li et al., 2009)

At the end of the 20th century Kubo et al. (1998) discovered that carbon fiber from organosolv lignin could be upgraded and was even classified as a general performance grade suitable for midrange markets. This group removed infusible high molecular mass material from a softwood acetic acid lignin and spun the remainder by fusion spinning. Carbonizing these fibers without thermal stabilization successfully gave carbon fiber. The Klason method

and thermomagnetic analysis (TMA) were conducted to determine lignin content and thermal flow properties, respectively (Kubo et al., 1998). In 2002, Kadla et al. (2002) showed that commercially available kraft and organosolv lignin (Alcell) could be used to obtain general performance grade carbon fiber. The overall yield of the kraft-based carbon fiber was 45 wt% based on the starting material with a tensile strength of 400-550 MPa and a modulus of 30-60 GPa. They used a thermal treatment to decrease the lignin's hydroxyl content and remove volatile contaminants that disrupt fiber integrity during subsequent thermal spinning. The lignin investigated was used as a pure starting material, but was also blended with PEO (polyethylene oxide) in ratios of 95/5, 87.5/12.5 and 75/25 (lignin/PEO, w/w). Spinning temperature for the organosolv lignin was between 138°C and 165°C and for kraft lignin between 195°C and 228°C, for lignins that displayed glass transition temperatures of 68.2°C and 83.3°C respectively. Lignin fibers were heat treated at rates from 12°C to 180°C per hour to stabilization (at 250°C) and carbonization (at 1000°C) and delivered general performance grade carbon fiber.

Generally, all lignin can be processed to carbon fiber, given that basic requirements such as purity and molecular weight distribution are in a certain range and with adding of plasticizer (Christopher, 2009). A modified technical lignin was used by Warren (2012) to manufacture a carbon fiber with tensile strength of 1.07 GPa and a modulus of 82.7 GPa.

2.4. Lignin Recovery

This section demonstrates the diversity of lignin recovery processes suitable for carbon fiber production. Numerous reports can be found on different processes and their advantages and disadvantages (Bozell et al., 2007; Harmsen et al., 2010; Helander et al., 2013; Li et al., 2009). Lignin can be extracted from woody biomass using different methods as kraft pulping, steam explosion, organosolv processing and others. The kraft pulping procedure is based on chemicals as sodium hydroxide and sodium sulfide whereas the organosolv process works with organic solvents or their aqueous solutions to separate the lignin, but has not been successfully deployed in papermaking so far. Organosolv lignin is generally much purer than the commercial kraft lignin (Huang, 2009).

The different processes using biomass as feedstock to produce fuels, chemicals and biobased material are described with the term "biorefinery" (Hongbin et al., 2013). The biomass used can be anything from agricultural crops such as sugar cane and corn, dedicated energy crops such as grasses and various types of softwood and hardwood or industrial waste such as sludge from wastewater treatment processes. The objective of biorefineries is to

convert this biomass into biobased products. This can be done with a range of different conversion technologies like thermal processes, chemical processes or biotransformation. The product stream that the biorefinery can give us can be almost anything that is produced in the existing petrochemical industry e.g., paint, rubber, fabrics, polymers or biofuels such as ethanol.

The two main goals of biorefineries are high volume liquid fuels and high-value chemicals. Therefore, the development of new biorefinery concepts aiming for fuels, energy, chemicals and upgraded products are necessary (Kamm et al., 2009). Biorefineries are divided into first, second and third generation biorefineries. A first generation biorefinery produces a single primary product stream, for example, sugar cane going to bioethanol. Second generation biorefineries produce multiple product streams derived from sustainable biomass feedstocks. One of the major developments of second generation biorefineries is lignocellulosic-based processing, and a schematic is displayed in Figure 4.

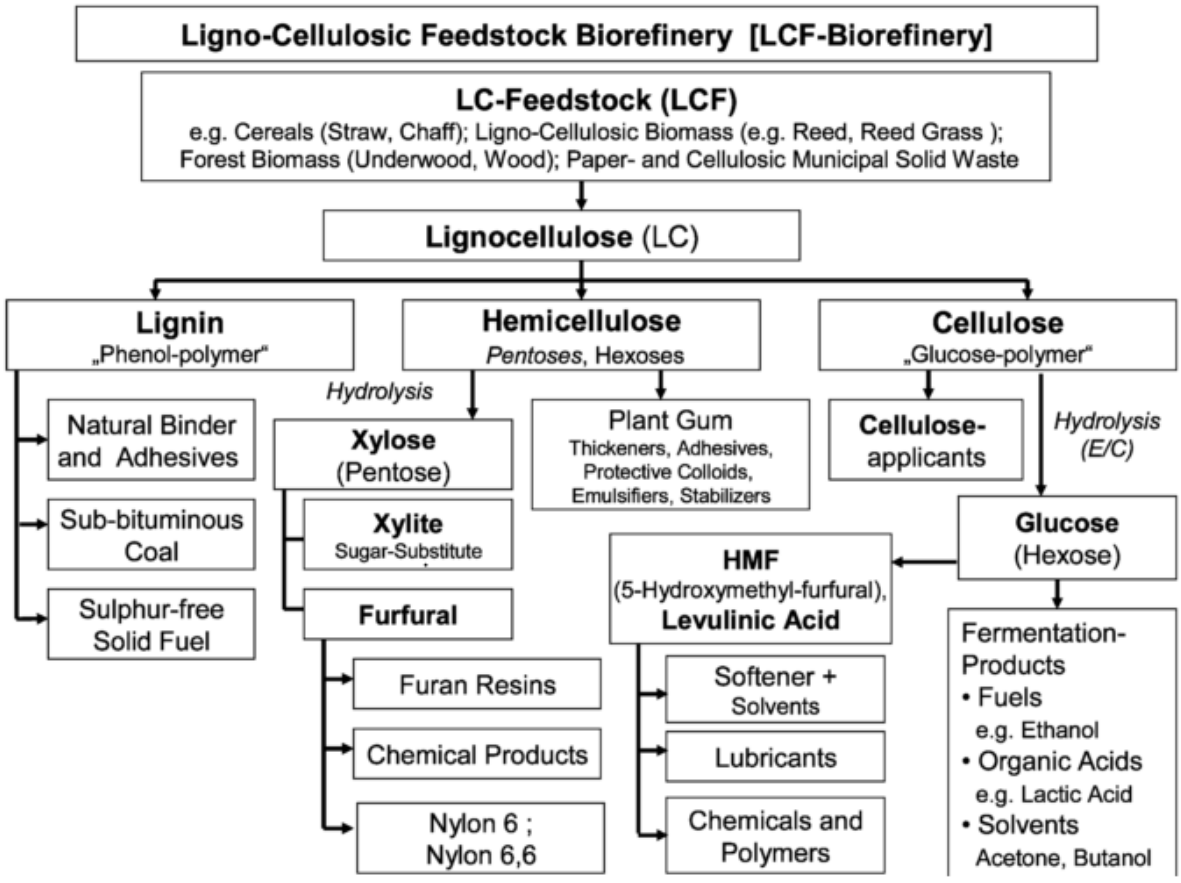

Figure 4. Conceptual lignocellulosic feedstock biorefinery (Cheng et al., 2009).

The objective of second generation biorefineries is to break down the lignocellulosic structures into their main components, refine them and then transform them into product streams. It is certain that this kind of biorefinery will be the future of chemical and energy

industry, although there are still some technical difficulties for its commercialization. Cellulose and hemicellulose are mostly converted into fuels, whereas the lignin can be used for chemicals and polymers or other high value products like carbon fiber. Within the biorefinery an initial separation provides cellulose, hemicelluloses, lignin and some residues. These residues include extractives, which can be used for resins or essential oils. The key advantage of a second generation biorefinery is that all of the biomass components are utilized for value-added products. Another advantage is that multiple processes can be integrated into the existing systems and can become competitive with other industries. However, the biggest challenge to successful operation of a second generation biorefinery is the fractionation of the biomass into its components. The existing processes are quite aggressive and aim mainly on the cellulose recovery and, therefore, break down the structure of the other components as lignin. The usage of this lignin is particularly difficult because its complex structure is very reactive and changes during separation. However the most advanced type of biorefinery is the third generation biorefinery, which uses multiple feedstocks as well as waste streams for conversion into multiple products. An LCF biorefinery has the potential to be a future phase III one, but before the lignocellulosic biomass can be converted into its main components and then further processed to fuels and value added biochemicals, all biorefineries require the implementation of a pretreatment step. The proper choice of the pretreatment depends mainly on the feedstock used (Menon et al., 2012) and the most promising as kraft, steam explosion and organosolv fractionation are explained below.

2.4.1. Kraft Lignin

In the kraft process, woody biomass is processed at 150-180°C with a mixture of aqueous sodium hydroxide and sodium sulfide (white liquor) at high pH levels to remove lignin. The kraft pulping process is the dominant global process in terms of chemical modification of lignin. The objective of any chemical pulping process is to remove enough lignin to separate the cellulosic fraction, producing a pulp suitable for the manufacture of paper and other related products. (Davies, 1984). Kraft pulping could be the most available source of lignin today. However, separated kraft lignin is mainly burned in the recovery furnace to regenerate the pulping chemicals used for pulp and paper production.

Delignification occurs in three individual phases, i.e., an initial phase, the bulk phase, and the residual phase. These phases cause the lignin to react and to fragment into smaller water/alkali-soluble fragments that can be washed out of the cellulose to form the so-called ‘”black liquor”. Each of these phases has a characteristic set of lignin reactions that helps

determine the final structure of kraft lignin, and thus, the potential reactivity of kraft lignin as a carbon fiber source. Nowadays kraft lignin is mainly used as an energy source for biorefineries, but forecasts show that will change soon into a precursor for modern biorefineries. The work of Hamaguchi et al. (2013) showed two easy ways to implement techniques to convert a kraft pulp mill into a multi-production biorefinery as described before. In one example, lignin removal from black liquor after pulping was considered, and in a second example a hemicellulose extraction from the wood prior to pulping was examined. They used a softwood pulp mill in Finland as a reference and came to the conclusion that even though additional outflows are available to increase the mill revenue, the mill must compensate for operational costs as well as possible losses. That means it is strongly dependent on the feasibility of hemicellulose extraction and the influence on the pulp quality but could be a promising technique for future biorefineries.

The vision of a modern biorefinery is still under discussion, but a broad vision includes a manufacturer that produces paper, energy and a variety of chemical feedstocks that will be the basis of future biomaterials, like carbon fiber out of lignin (Wyman et al., 1993). The possibility of converting kraft lignin into a host for alternative materials is already studied by (Kadla, 2002) and others, however, this process is not suitable to deliver a reasonable source for value-added lignin-based products so far.

2.4.2. Steam Explosion Lignin

High pressure steam applied on lignocellulosic material for a short period of time, followed by sudden decompression (explosion) delivers fiberization of the biomass (Ibrahim et al., 1999). An apparatus for and process of explosion fiberization of lignocellulosic material (later referred to as “steam explosion”) was invented by Mason (1928). The steam explosion process is a pretreatment to enable easier fiber accessibility and has been shown to be a fundamental technology for biomass separation. Mason’s (1928) technique used steamed wood chips at 285°C at a pressure level of 3.5 MPa for about 2 min (Mason, 1928). The usual temperature range for steam explosion today is between 180°C and 240°C. Steam explosion is a procedure that can use no additional chemicals besides water, gives a good yield of hemicellulose, and shows disruption of the solid residues from bundles to individual fibers (Garrote et al., 1999). As a pre-treatment for microbial bioethanol or biogas production, steam explosion of biomass can be used as an environmental friendly pulping process (Cara et al., 2006).

The application of steam explosion in biomass conversion, the techniques and their advantages were described by Wang et al. (2010). Steam explosion requires less energy compared to many other techniques and has low environmental impact, but because the lignin (~60%) is poorly solubilized (Hergert et al., 1992) and its structure is significantly broken down, steam explosion is not a suitable recovery process for further lignin processing so far.

2.4.3. Organosolv Lignin

Organosolv fractionation is a process that can provide low cross-contamination between lignin and cellulose fractions. Organic solvents or their aqueous solutions are used to solubilize hemicellulose and lignin and remove them from cellulose, providing relatively clean fractions. Organosolv pulping involves contacting a lignocellulosic feedstock such as chipped wood or grasses with an organic solvent at temperatures ranging from 130°C to 200°C. A benefit of organosolv solvents is that they are easily recovered by distillation leading to less water pollution and elimination of the odor usually associated with kraft pulping. In 1998, Black et al. (1998) disclosed a method for separating lignocellulosic material into its three major components for further processing. They showed that lignin is present in the organic solvent as well as in the aqueous phase.

However, there are also disadvantages to this process that have to be considered. Organic solvents are expensive and require a highly accurate processing environment as temperature and pressure ranges and increase the energy costs dramatically. But investigations are ongoing to solve those problems and to open the way for this promising technique. A detailed rationale for the organosolv process is given by Hergert et al. (1992) describing all relevant work since 1987. They conclude that two of many organosolv pulping processes are most promising, the Alcell process for hardwoods and the Organocell process for softwoods. A modified alcohol pulping and recovery process using 50% ethanol at 195°C called alcohol pulping and recovery process (APR) was further improved by the company Alcell Developments Inc. The Organocell process is owned by Organocell GmbH and was the most advanced new process to be implemented on an industrial scale in the year 1992.

The lignin investigated in this work was recovered using an organosolv fractionation developed at the National Renewable Energy Laboratory by Bozell et al. (2011). This fractionation separates lignocellulosic biomass into its three main components: cellulose, hemicellulose and lignin (Figure 5). In this process, an experimental reactor at the University of Tennessee's Center for Renewable Carbon performs the organosolv fractionation of the raw material using a mixture of MIBK, ethanol and water in the presence of an acid promoter.

After the fractionation, a solid fraction and a liquid fraction are separated. The solid fraction is the remaining cellulose. The liquid fraction is called black liquor and includes lignin and hemicellulose. The black liquor is then separated into an aqueous phase, containing mainly hemicellulose and an organic phase, containing mainly lignin (Figure 6).

Investigation from Astner (2012) investigated optimization of lignin yield over a range of process temperatures from 120°C to 160°C and a sulfuric acid concentrations of 0.025 to 0.1M. That work found a maximum lignin yield of 81% at a fractionation time of 90 min at 160°C using 0.1M sulfuric acid concentration with a feedstock ratio of 90% switchgrass and 10% tulip poplar.

Another investigation on the CRC organosolv fractionation process was performed by Maraun (2013). The main findings of this work describe run conditions as temperature, duration and solvent composition in the presence of feedstock contamination. A maximum mean lignin yield of 85.7% could be achieved at a fractionation time of 56 min at 160°C using 0.1M sulfuric acid and a feedstock mixture containing 10% switchgrass and 90% tulip poplar.

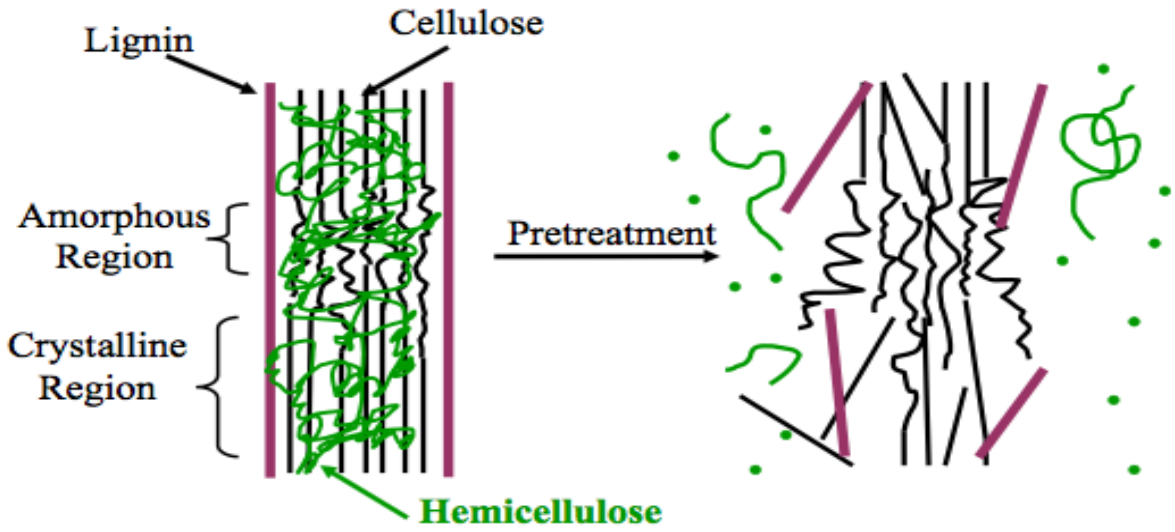

Figure 5. Organosolv fractionation schematic.

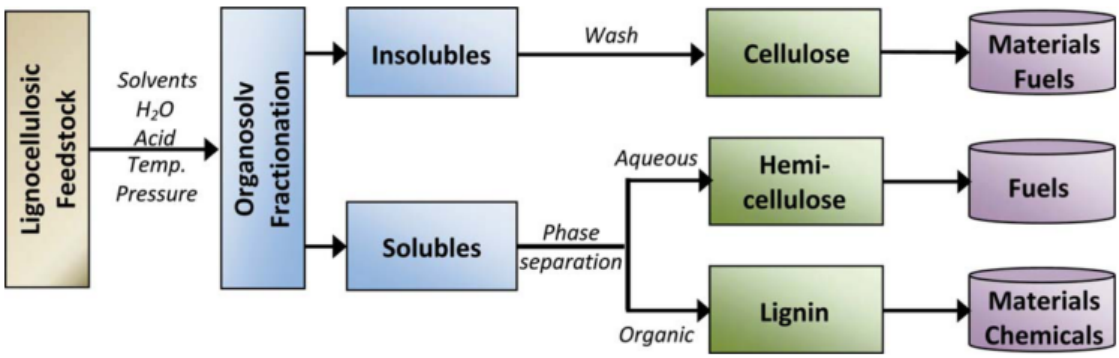

Figure 6. Organosolv fractionation process (Baker et al., 2013).

The organosolv fractionation removes non-cellulose components and separates the lignin from the hemicelluloses. This pretreatment also reduces the crystallinity of the cellulose and creates a specific surface area. Finally, a pure, high-quality lignin is recovered useable for further processing steps like melt spinning. The properties of organosolv lignin differ from other technical lignin. The major features are low molecular weight and high chemical purity (Lora et al., 2002).

2.5. Lignin Fiber Spinning and Conversion to Carbon Fiber

Fiber formation from polymers can basically be divided into three main methods as the dry, the wet, and the melt spinning technique. Melt spinning is the most rapid, convenient and commonly used method of forming polymeric fibers. With melt-spinning techniques the use of solvents can be significantly reduced. Lignin is a thermoplastic polymer making melt spinning is an applicable method to spin fibers. In contrast to kraft lignin, organosolv lignin contains only a very small amount of inorganic material, which provides good melt spinning opportunities (Lora, et al. 1993). Inorganic materials are contaminants that will degrade carbon fiber properties and are a result of the lignin recovery process.

Melt spinning of lignin was mentioned first by Otani (1969) describing several methods of forming fiber from lignin using a one pot melt spinning method. Since that time many achievements arose and current technical improvements enable faster and relatively easy handling. Baker et al. (2012) successfully melt spun lignin fiber from both a kraft hardwood lignin and an organic purified hardwood lignin. They used an organic solvent purification process to dissolve the lignin from most impurities to enhance its melt spinnability. Produced fibers were then stabilized and carbonized to obtain lignin-based carbon fiber. The main drawback was the slow heating rates for fiber stabilization. They showed that oxidative

stabilization can only be achieved at heating rates smaller than 0.05°C/min. They further showed that decreasing heating rates significantly increased the glass transition temperature (T_G) and furthermore, allowed the lignin to crosslink and deliver stabilized fibers. The mechanical properties of the carbon fibers were poor, and, therefore, investigations are needed to decrease stabilization times and improve their properties.

The conversion of melt spun fibers into a final product requires a two phase controlled pyrolysis: stabilization and carbonization (Huang, 2009). Thermal stabilization aims to stabilize the molecules of treated material at high temperature to enhance their properties, i.e. mechanical and decomposition resistance. In fiber production the goal is to transform a spun fiber from thermoplastic to a thermoset character using cross-linking, oxidation and cyclization reactions. A significant breakthrough towards commercial manufacture of lignin-based carbon fiber was described by Baker (2009), showing the feasibility of continuously melt spun fibers from organosolv lignin with a diameter as low as 10 μm. Norberg et al. (2013) investigated the stabilization of softwood kraft lignin and hardwood based kraft lignin in the presence of oxygen. They successfully stabilized and carbonized lignin in a one-step process in the presence of air and found that this approach offered a great potential to reduce the processing costs for a future commercialization of lignin (Norberg et al., 2013).

2.6. Analysis of Lignin

To evaluate and predict the performance of a material, a set of different analytical measurements can be carried out. To determine process parameters in lignin for further processing, the elemental composition and ash content need to be measured. Common analysis of the melting properties and the detection of transitions help to classify lignins. To obtain good quality lignin-based carbon fiber it is necessary to start with a high purity lignin with low ash content and a narrow thermal window between T_G and melting point (T_S) to ensure a low enough melt flow temperature but also high enough for fiber stabilization during melt-spinning. There are several methods to characterize lignin; these include analysis of purity (by Klason), thermal properties by DSC and carbonization properties by TGA. Melting properties can be measured with a Fisher-Johns melting point apparatus.

The moisture content as well as the ash content can be determined during the Klason analysis. The chemical structure and general functional group profile can be determined by nuclear magnetic resonance (NMR). NMR is a very detailed method of chemical analysis for organic compounds and can tell us the number of hydrogen atoms in a molecule and their related position in the carbon chain (Kadla et al., 2002).

Brebu et al. (2010) presented a review on the temperature range, kinetics and mechanism of thermal degradation, as well as on the type of degradation products to obtain valuable chemicals. Thermal analysis encompasses a broad range of applications and markets. It starts from the roots of the raw material all the way up the supply chain to the finished product. Thermal analysis is the investigation of a material on properties that change with temperature. There are many different methods to determine thermal properties focusing on temperature differences, volume changes, mechanical stiffness, thermal diffusivity or even optical properties.

2.6.1. Purity and Ash Content

Lignin purity is normally determined using a Klason analysis and was first reported by Klason in 1893 (Klason, 1920). The Klason process is gravimetric, and treats a biomass or lignin sample with 72% sulfuric acid at elevated temperature to hydrolyze residual sugars. The remaining insoluble material is dried and weighed and is defined as Klason or insoluble lignin. Later work has determined that a small amount of lignin is solubilized during this process. Thus, the hydrolysate from the Klason analysis is evaluated using UV spectroscopy to determine the amount of soluble lignin. The total lignin in the sample is the sum of Klason lignin and acid soluble lignin. Remaining lignin from Klason analysis can be used to determine the ash content in a lignin sample by incineration at 575°C. The ash content should be less than 0.1 % to be suitable for a carbon fiber precursor. (Kadla et al., 2002)

2.6.2. Elemental Analysis

The elemental analysis is used to determine the mass fraction of carbon (C), hydrogen (H) nitrogen (N) and sulfur (S) in an organic substance using a CHNS/O analyzer. Fadeeva et al. (2008) summarized results of many years of studies on the determination of carbon, hydrogen and nitrogen on automated CHNS analyzers. Amongst other properties the chemical and thermal stability and the incombustibility can be determined with a complex elemental composition characterization. Their aim was to display the efficiency of a universal CHNS analyzer by comparing three different models. They stated that any CHNS analyzer provides the complete decomposition of organic compounds and the determination of C, H, and N in substances of any elemental composition.

2.6.3. Melting Properties

The Fisher-Johns melting point apparatus is a very simple yet very effective measurement of melting behavior of materials. It handles materials with melting points from 20°C to 300°C and provides excellent temperature control and reproducibility.

2.6.4. Thermal Analysis by DSC

Differential scanning calorimetry is an analytical technique that measures the heat flow rate to or from a sample specimen as it is subjected to a controlled temperature program in a controlled atmosphere. Developed by E.S. Watson (Watson et al., 1964) in 1962 and introduced commercially at a conference "Analytical Chemistry and Applied Spectroscopy" (Wiberly, 1963) one year later, the DSC became a very famous technique in thermal analysis. DSC measures the heat absorbed (endothermic) or released (exothermic) as a sample is heated. These endotherms or exotherms can provide information such as T_S or T_G and the changes in heat capacity (ΔH). The measurement of the T_G is typically used for an amorphous material, whereas the measurement of the T_S is typically used for a semi-crystalline material. DSC also provides a rapid method for determining polymer crystallinity based on the heat required to melt the polymer. The result of a DSC is a curve that shows the phase transition of a material, and furthermore shows the temperature range for optimal processing. The DSC analysis sheds light on the behavior of a material under process conditions. In the melt spinning process the heating rate plays a significant role. The high speed DSC analysis enables the simulation of these conditions and provides highly quantitative measurements. To deliver accurate measurements this technique requires a nitrogen atmosphere in hermetically sealed aluminum pans using the sample (S) on the one side and a reference (R) sample (empty pan) on the other side. The sample is placed in a self-contained calorimeter that gives the used energy applied to or removed from the calorimeter to compensate the sample energy (Fyans et al., 1985).

2.6.5. Decomposition Analysis by TGA

Thermogravimetric analysis provides chemical and physical information about a material's decomposition behavior. TGA measures the change in the weight of a material as a function of linearly increasing temperature and/or time. Therefore, the composition of a material can be determined but also the thermal stability can be predicted. Physical phenomena such as crystalline transition and vaporization as well as chemical phenomenon as desolvation and

decomposition can be measured (Coats et al., 1963). The TGA is a very sensitive measurement that is based on a high degree of precision in temperature, and its change as well as mass changes. The weight of the sample is continuously monitored as it is heated to the desired temperature and shows the decreasing weight due to decomposition. It is common to use a constant heating rate although it can be individually adjusted. Kubo et al. (2008) utilized a temperature modulated TGA to study the kinetics of three industrial lignin preparations using a dynamic heating rate. Main conclusion in terms of accuracy and reduced experimental time was that lignin pyrolysis delivers best results at constant heating rate.Yang et al. (2009) reported the influence of heating rates on the TGA using wheat straw lignin. They found that there is a significant influence on the thermal decomposition at heating rates between 10°C and 50°C/min. Seo et al. (2010) studied the pyrolysis of biomass using TGA and concentration measurements of the evolved species. They used single and parallel models under non-isothermal conditions to investigate the pyrolytic behavior of sawdust and came to the conclusion, that the general constituents of biomass can be observed using TGA (Seo et al., 2010).

2.7. Mechanical and Optical Analysis of Lignin-Based Carbon Fiber

Mechanical properties of single fibers used in composites caused an enormous interest in the last decades. The characteristic of single fibers influence the mechanical properties of composites because they are the load carrying component (Ilankeeran et al., 2012).

The mechanical strength of fibers is commonly measured using an Instron testing machine according to an appropriate standard and then compared to other means. In carbon fiber analysis a standard test method for tensile strength and Young's modulus for high-modulus single-filament materials (ASTM D3379-75) can be conducted. Tensile strength or ultimate tensile strength is the maximum stress a material can withstand as it is stretched, whereas the Young's modulus or elastic modulus is the ratio of stress and strain also often referred to as stiffness. These two parameters are very important indicators for the comparison of carbon fiber properties. As the Young's modulus is a function of stress and strain as well as the diameter of tested fiber, the cross-section of a fiber is very important as well.

Stoner et al. (1994) investigated the effect of cross-sectional shape of carbon fiber received from pitch by extensive single-filament testing. Their conclusion was that the shape of the fiber does significantly influence the mechanical properties at a gauge length of 10mm or shorter. In addition to mechanical properties carbon fibers are also often verified on their optical characteristics and checked on their diameter using SEM microscopy.

CHAPTER III. MATERIALS AND METHODS

To present the data, their trends, correlation trend charts and box plots, JMP® Pro 10.0 (www.jmp.com) was used. Charts comparing severity with corresponding responses were fitted with a smoothing element showing a smooth curve through the data. The smoother is a cubic spline with a lambda of 0.05 and standardized X values. A cubic spline is a nonparametric spline constructed of piecewise third-order polynomials which pass through each set of *m* data points consecutively through all of the data (Bartels et al., 1987).

The performance charts of DSC and TGA were produced with PyrisSoftware 11.0. from PerkinElmer, Inc. The fiber diameter was determined using ImageJ 1.47v. Average values are given with one standard deviation using one decimal. [x.x (±y.y)]. For a simplified illustration of reaction parameters as sulfuric acid concentration, reaction temperature and residence time a combined severity (CS) factor according to Goh et al. (2011) was used.

3.1. Chemicals

The following chemicals were used to separate biomass into its three main fractions and complete the workup:

MIBK	Methyl isobutyl ketone [Fisher Scientific]
Ethanol	Ethanol 190 proof (UN 1170 Spec.) [Decon Laboratories, Inc.]
Water	Deionized water [tank at CRC, BEST]
Acid (Workup)	Sulfuric acid (H_2SO_4 95.0 to 98.0 w/w %) [Fisher Scientific]
Acid (Klason)	Sulfuric acid (H_2SO_4 72 w/w %) aqueous solution
Toluene	T323-4 (UN1294) [Fisher Scientific]
Ether	Ethyl ether anhydrous (E 138-4) [Fisher Scientific]
Salt	NaCl [Fisher Scientific]
Nitrogen	Ultra high purity
Argon	Ultra high purity

3.2. Analysis of Biomass

For this study, tulip poplar chips with a dimension of ~ 4cm^2 and a thickness of 0.5cm – 1cm were delivered from Oak Ridge Hardwoods, Oak Ridge, Tennessee (Figure 7). Switchgrass used for this study was harvested in East Tennessee (Figure 7). The size was reduced to an average length of 2cm – 5cm using a 2cm knife mill.

Moisture content of both biomass types was determined using the weight before and after drying for 12 hours in a 105°C oven. The theoretical lignin content of the biomass was measured using Klason and UV analysis after preparation of extractive-free wood according to the NREL standard (NREL/TP-510-42618) and was compared to actual yields. The preparation of extractive-free wood was carried out according to ASTM D01105-96 standard. Lignin content (purity) of every run was measured according to the same NREL standard (NREL/TP-510-42618).

Figure 7. Tulip poplar (left) and Alamo switchgrass (right).

3.3. Organosolv Reactor Preparation and Operation

3.3.1. Solvent System and Preparation

Solvent composition used for this thesis is based on previous studies on the efficacy of organosolv fractionation solvents (Bozell et al., 2011). The solvent consists of 16 wt% MIBK, 34 wt% ethanol and 50 wt% water as can be seen in Figure 8 and is designated as the -1 solvent as it is on -1 position along the phase transition curve containing less MIBK. The phase transition was determined using different ethanol/water mixtures and gradually adding

MIBK (Bozell et al., 2011). The solvent mixture contains 5% more ethanol to ensure a clear, single phase solution.

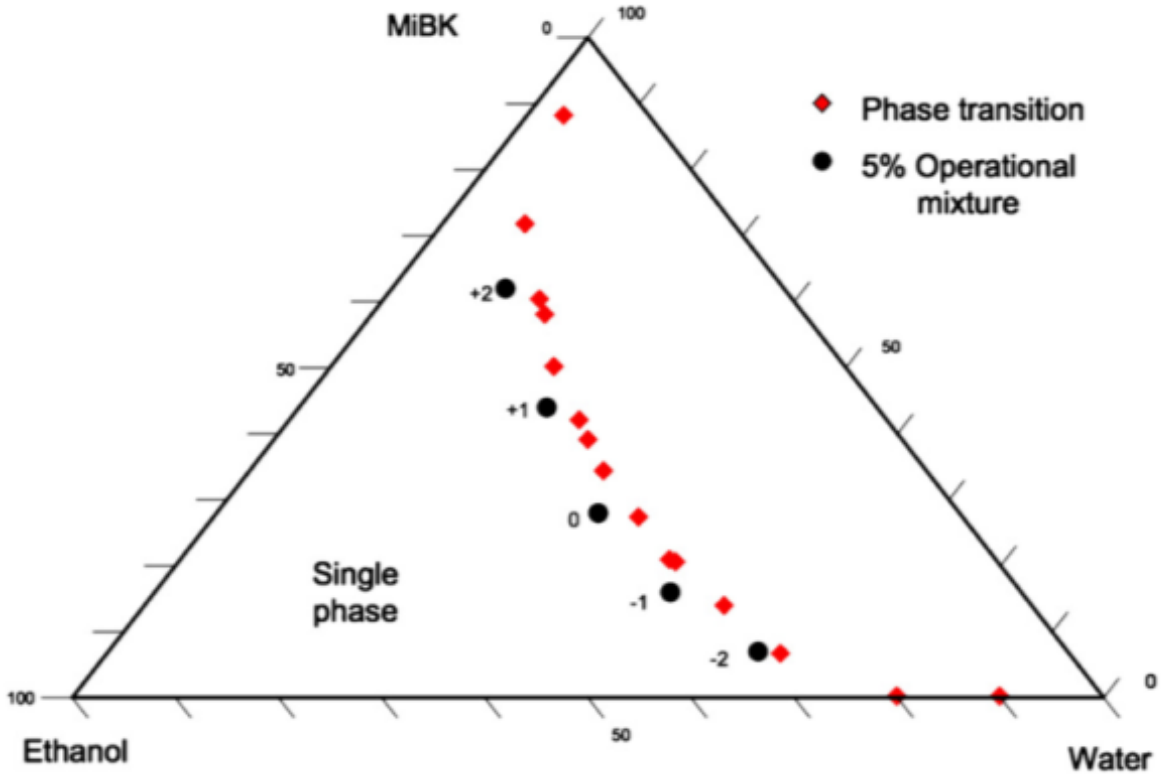

Figure 8. Ternary phase diagram of solvent (Bozell et al., 2011).

3.3.2. Reactor Operation

A Hastelloy C276 reactor is used to separate the biomass (Figure 9). For this study the reactor was filled with 430g switchgrass or 720g poplar. After the reactor is filled and sealed a vacuum is applied. The pulled vacuum is about -70 kPa and lasts for 20 minutes to enable a complete filling of the reactor with the solvent. The solvent is then pulled into the chamber using the vacuum. Before the reactor is heated to a temperature of 130 ºC - 170°C the vacuum is turned off. As soon as the reactor reaches operating temperature, additional solvent (11±1l) is pumped through. The feeding pump is set to a stroke length of 1.5 to ensure steady throughput. All data are monitored and controlled using Lab-VIEW 8.6 software in combination with a pressure transducer and an analog to digital converter. To ensure a consistent temperature throughout the entire run, Omega-C9000A temperature controllers are used. Filled and heated, the reactor runs for exactly 120 minutes to guarantee a complete separation of the feedstock. Gathered black liquor was transported into a wet laboratory where the separation was performed.

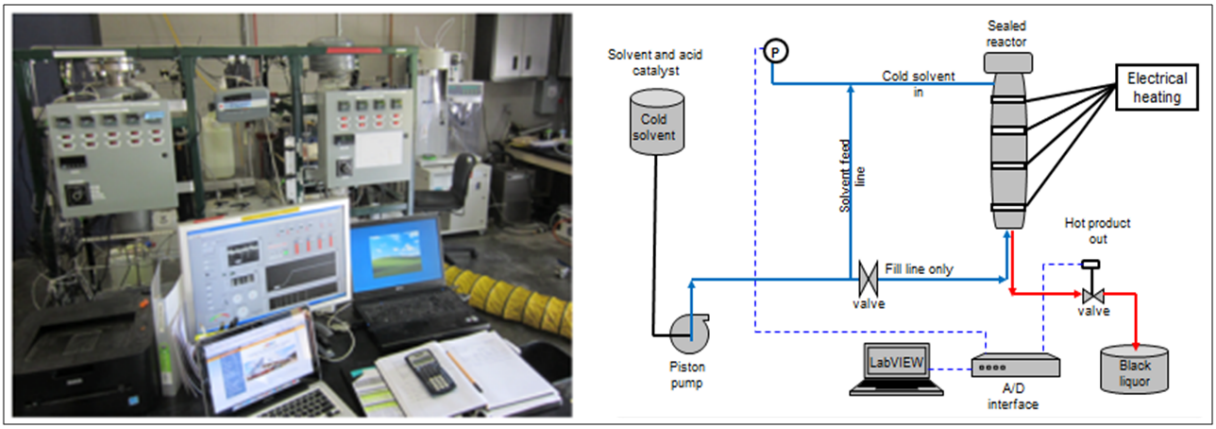

Figure 9. Organosolv fractionation reactor and schematic.

3.4. Recovery of Products from the Reactor and Black Liquor

The black liquor obtained from the fractionation was placed in a separatory funnel. Phase separation was induced by mixing the liquor with 15% solid NaCl based on the amount of water present in the fractionation solvent (Figure 10). The aqueous phase was drained, and the organic phase was further washed twice with about 30% DI water based on the amount of organic phase present. The organic phase was concentrated on the rotary evaporator to give a dark residue. The aqueous fraction was also concentrated on a rotary evaporator to remove most of the ethanol, which resulted in the precipitation of additional lignin. The aqueous phase was filtered using fast-flow paper to isolate the aqueous lignin. The aqueous lignin was combined with the organic residue and washed with ether to remove low-molecular weight material, filtered and pumped under high vacuum. This step was repeated until a free flowing brown powder was isolated. Finally, the combined lignin from the aqueous and organic phases was used for further analyses.

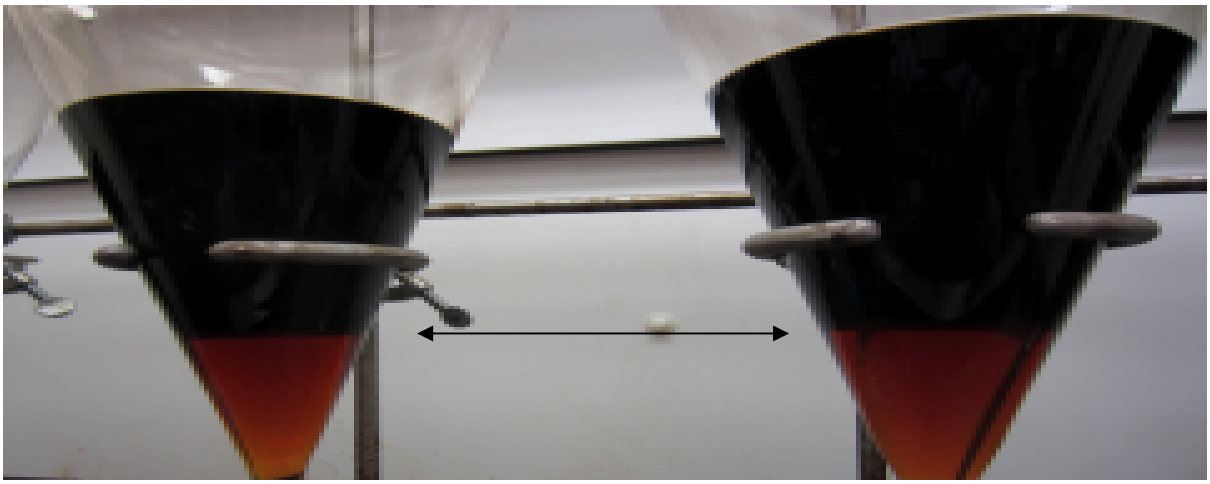

Figure 10. Separation of organic and aqueous phase.

3.5. Organosolv Fractionation of Tulip Poplar

Table 3 shows the experimental matrix and resulting run numbers used for production of lignin from tulip poplar via organosolv fractionation. Temperatures from 130 ℃ to 170°C and acid concentrations from 0.025 to 0.15M were employed over a total of 17 runs. Runs #169 and #172 shown in the Table were conducted prior to this work, but the data were included in this study for comparison. All runs were carried out for 120 minutes using 720g of feedstock and a solvent amount of 11±1L giving a liquid-solid ratio of 13.88. Due to evaporation during the run, a black liquor amount of about 9.5L is expected. An equilibrium pressure of 310kPa is observed at 130°C and 1450 kPa at 170°C.

Table 3. Tulip poplar runs

	Acid Concentration (M)				
	0.025	**0.05**	**0.075**	**0.1**	**0.15**
Temperature (°C)					
130	T005	T007	-	T008	-
140	T036	#169	T009	T010	T011
150	T012	T035	-	T014	-
160	T037	#172	T016	T017	T006
170	T019	T021	-	T022	-

A second set of experiments investigated the effect of different run times (Table 4). Longer run times were employed to improve the penetration of the solvent into the feedstock, increase the molecular weight distribution, improve the purity, and increase cleavage of the linkages between hemicellulose and lignin. These runs were carried out at a single temperature and acid concentration (140℃, 0.05M, -1 solvent) at run times from 60 to 360min.

Table 4. Time dependent runs of tulip poplar

Time (min)	60	120	180	240	360
Tulip Poplar	T023	#169	T024	T025	T026

3.6. Organosolv Fractionation of Alamo Switchgrass

The experimental matrix for Alamo switchgrass consisted of 16 runs including three carried out before this study, but included for comparison (Table 5). The range of conditions for these runs was almost identical to the tulip poplar runs except for the amount of feedstock and exclusion of runs at 170°C. Differences in the density and shape of switchgrass compared to poplar limited the amount of raw material used per run to 430g. Initial work at 170°C with poplar showed both the fractionation and isolation to be difficult, and thus, runs under those conditions were not included for switchgrass.

Table 5. Alamo switchgrass runs.

	Acid Concentration (M)				
	0.025	**0.05**	**0.075**	**0.1**	**0.15**
Temperature (°C)					
130	T015	T020	-	T027	-
140	T038	#178	T001	T018	T002
150	T028	T029	-	T030	-
160	T039	#171	T003	#177	T004

A group of switchgrass runs was also carried out at several different run times. (Table 6).

Table 6. Time dependent runs for Alamo switchgrass.

Time (min)	60	120	180	240	360
Alamo Switchgrass	T031	#178	T034	T032	T033

The impact of organosolv conditions on the properties of the resulting fractions was evaluated using a combined severity factor (Goh et al., 2011). This factor was based on the correlation of the pretretment as a function of treatment time (min) and temperature (°C), where T_{ref} = 100°C, as given in the following equation:

$$Log(R_O) = Log(t\ exp(T-T_{ref}))/14.7 \quad [1]$$

The effect of the acid concentration was taken into consideration by measuring the pH and was calculated as shown in the equation below:

$$\text{Combined severity (CS)} = \text{Log}(R_O) - \text{pH} \quad [2]$$

3.7. Lignin Characterization

Lignin received from organosolv fractionation was tested and compared by the methods listed in Table 7:

Table 7. Methods for lignin characterization.

	Method
Purity	Klason analysis, NREL/TP-510-42618
Elemental analysis	NREL/TP-510-42622
Ash content	NREL/TP-510-42622
Zero shear melt flow (T_S)	Fisher Johns melting point apparatus
Glass-liquid transition (T_G)	Differential scanning calorimetry
Decomposition temperature (T_d) and carbon yield	Thermogravimetric analysis
Analysis of lignin-based CF	ASTM D3379-75
Optical characterization	ASTM D3379-75
Mechanical properties	ASTM D1822-06

3.7.1. Purity and Ash Content

While Klason lignin is the standard method for determining the lignin content in wood, (Kirk and Obst, 1988) it can also be used directly on lignin to determine its purity.

NREL standard TP-510-42618 was used to determine the lignin purity, as content and the amount of acid soluble lignin (ASL). The oven dried weights (ODW) were measured on 0.300g ± 0.010g of lignin dried for 24 hours in a 105°C oven. After 24 hours the samples were mixed with 3ml of 72% H_2SO_4 in pressure bottles and then placed in a water bath for 1 hour. They were stirred every 10 minutes with a Teflon rod to ensure a complete acid to particle contact and uniform hydrolysis. Then the samples were mixed with 84.00 ± 0.04 ml deionized water to dilute the solution to 4% acid and were placed in an autoclave for one hour at 121°C to complete hydrolysis and liberation of sugars. After filtering, the samples were dried again and the percentage of acid insoluble lignin (AIL) could be determined.

In addition, the acid soluble lignin (ASL) was measured with UV to determine the lignin contained in the remaining liquid. Each sample was measured in duplicate at a certain wavelength and was diluted sufficiently to get an absorbance between 0.3 and 0.7 (dilutions were typically 1:6 to 1:30). Replicate purity measurements were carried out to achieve a difference of $\leq$ 1.5%. Replicates outside of this range were repeated.

The ash content was measured according to the standard developed by the National Renewable Energy Laboratory (NREL/TP-510-42622). A lignin sample of 600±50mg was heated at 575°C for 24 hours using a Lindberg/blue box-furnace with a maximum temperature of 1100°C and the weight of the remaining ash was measured using an AdventurePro balance model AV264C. Ash data according to the protocol could not deliver reasonable outcomes. Therefore, the sample amount was doubled (increased from 0.3g to 0.6g±0.05g).

3.7.2. Elemental Analysis

Elemental composition of the lignins was determined using a PerkinElmer Inc. 2400II CHNS/O combustion elemental analyzer equipped with a Perkin Elmer Inc. AD6 Autobalance microbalance. Carbon (C), hydrogen (H) and nitrogen (N) were determined on lignin samples dried for 24 hours at 80 °C under vacuum and compared with acetanilide, an organic analytical standard material. Samples were measured in triplicate. The additional sulfur content caused by the catalyst was neglected because of the very low contamination.

3.7.3. Fisher Johns

The softening properties of the lignin were measured using a Fisher-Johns melting point apparatus. A small amount of the lignin was sandwiched between two microscope cover glasses and placed on the heating stage. Prior to the measurements an initial rapid scan was carried out to find the approximate melting point. Afterwards, the temperature was set at 100°C and heating was carried out at 10°C/min. When the temperature was within about 15ºC of the melting point, the heating rate was lowered (1-3°C/min). The temperature was recorded at the following six different stages:

Discoloration	
Localized melting	(approximately 25% liquid)
Appreciable melting	(approximately 50% liquid)
Full melting	
Melt flow	(manual compression of the cover slips caused the sample to flow sideways)
High flow	(upper slip slides over the lower slip)

Anomalies (incomplete melting, darkening, bubbling, foaming) were also recorded.

3.7.4. Differential Scanning Calorimetry

Glass transition temperatures (T_G) of the lignins were determined on a PerkinElmer Pyris Diamond DSC instrument equipped with an Intracoller IIP. The lignin samples were dried at 80°C under vacuum for 24h and stored in a desiccator. Triplicate lignin samples (3mg±0.5mg) were prepared in an aluminum pan sealed with a lid using a universal sample press. The lignin sample was placed into the DSC cell with an empty pan as reference. Three cycles between 0°C to 200°C were carried out using a heating rate of 20ºC per minute. Finally, the average of the three cycles was recorded and the mean of the three measurements (Figure 11) provided the T_G.

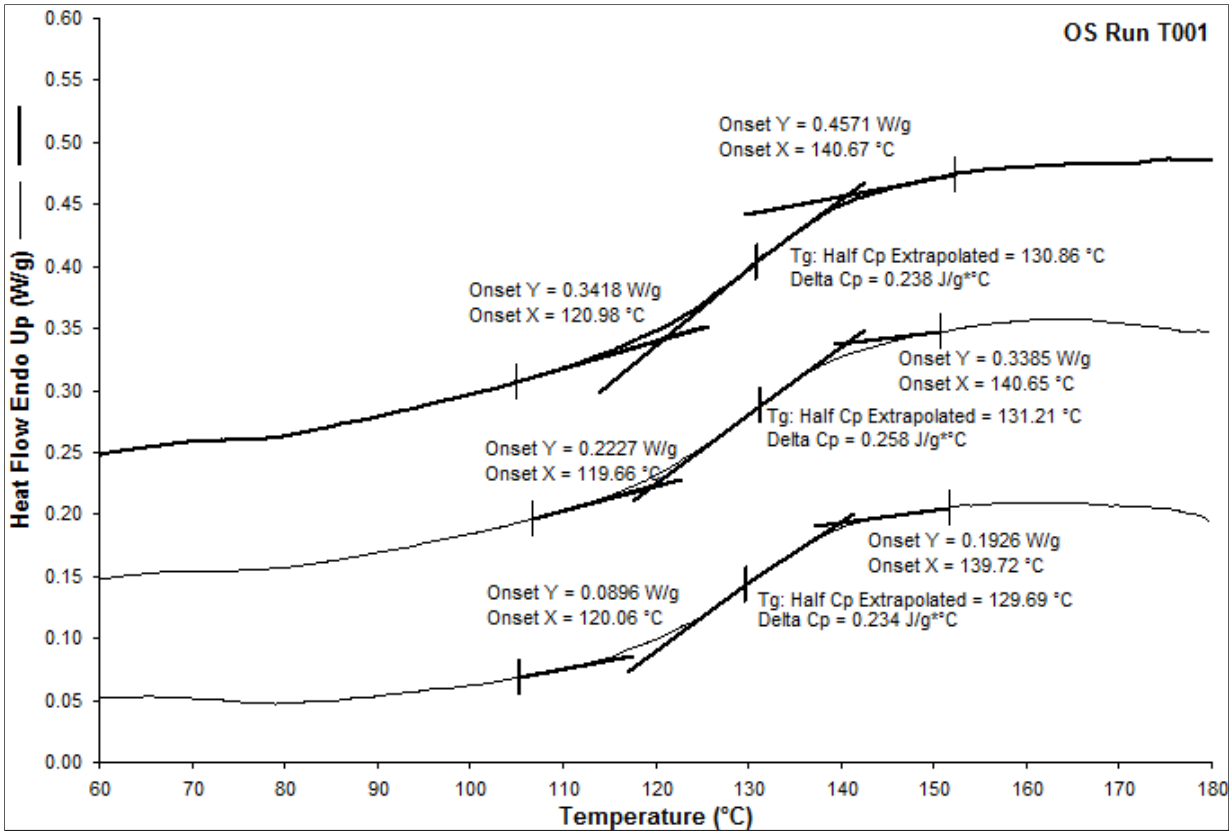

Figure 11. DSC chart showing the glass transition temperature of T001 sample.

In addition to the T_G measurements, the corresponding heat capacity as well as the onset and the width of calculated glass transition were recorded to allow making well informed estimations about the molecular weight distribution.

3.7.5. Thermogravimetric Analysis

Thermogravimetric analysis was carried out using a Pyris1TGA from PerkinElmer. Duplicate lignin samples (5mg±0.5mg, measured on a precision balance [0.001%]) were measured in flame-cleaned platinum pots. The TGA furnace was heated to 105ºC to allow moisture to evaporate and then the sample was heated from 105ºC to 925ºC at a rate of 5^{o}C/min affording a run time of 2.73 hours. Figure 12 shows a typical TGA trace. The red line shows the decreasing weight of the lignin sample. The blue line is the derivative of the red and gives information on the rate of decomposition. This chart also helps to understand the composition of a sample and if there are any impurities as remaining carbohydrates. Any mass remaining above 900°C was considered as char. With the help of the thermogravimetric analysis eleven points of interest were determined. To get a basic understanding of the decomposition of the lignin sample, five points (150°C, 200°C, 250°C, 300°C and 900°C) were measured and degradation was measured over time. The onset and the decomposition

temperature at 5% weight loss were recorded and analyzed (solid line). The derivative (dashed line) gives the slope of the performance line at every point and a maximum mass loss at the inflection point. This line can also indicate the presence of impurities and some low molecular weight volatiles.

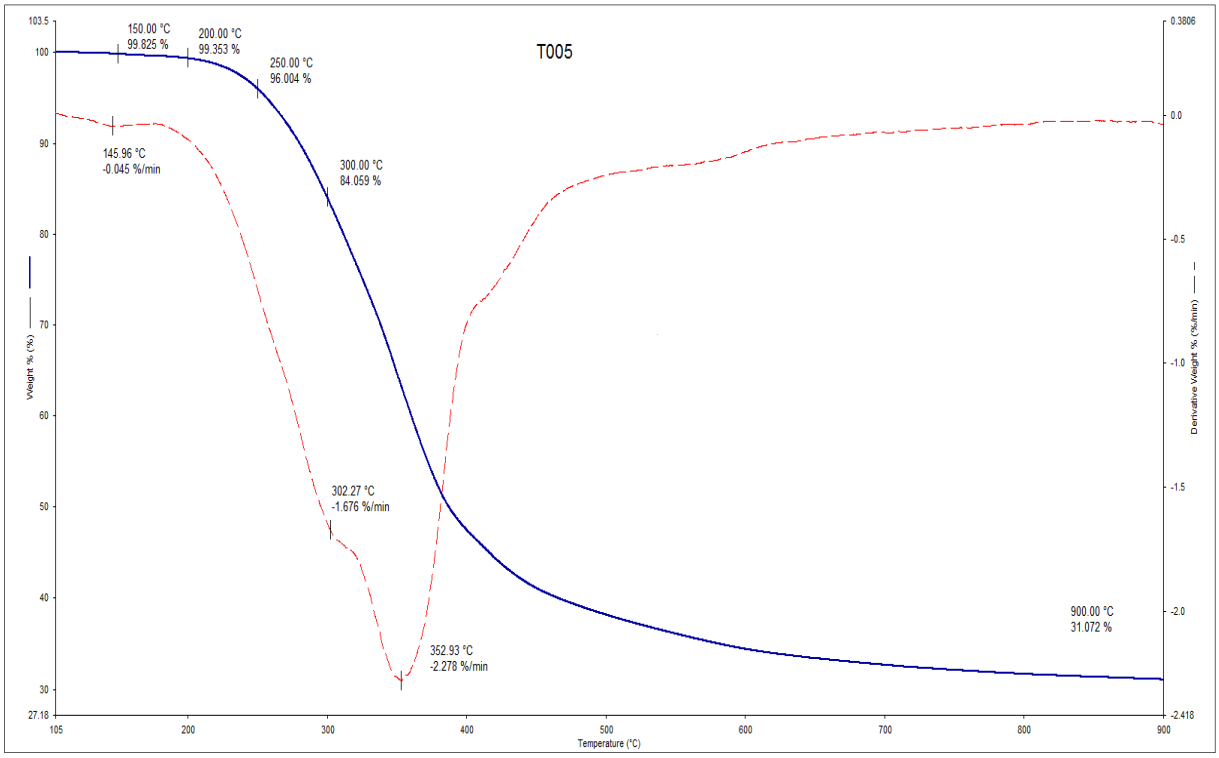

Figure 12. TGA chart showing the decomposition of T005 with five points of interest and the derivative.

3.8. Lignin Fiber Production and Analysis

Lignins from both poplar and switchgrass feedstocks were used for spinning. Lignin samples were dried for 12 hours at 80°C under vacuum using a Welch 1140 vacuum oven in combination with a Welch DuoSeal vacuum pump (VWR). A modified Haake MiniLab twin screw extruder (Typ 557-2190) was used to melt spin selected lignins into lignin fibers. The extruder was heated to the desired temperature using an Omega Benchtop Heater Controller controlled by a Haake Minilab Rheomex, CTW5. Prior to the spinning, the extruder and screws were cleaned and treated with silicon spray. The extruder was heated for approximately 30 min, and then the lignin sample was introduced, melted, and extruded at a screw rate of 100 rpm under argon at an applied pressure of 0.7kPa. The temperature and pressure were continuously controlled and the pressure did not exceed 70 N/cm^2. The melted lignin was extruded through a 200µm die and collected on a spool operating at 165 rpm to

give fibers of about 15μm diameter. Thereafter, the fibers were cut from the spool, labeled and stored for thermal treatments.

The lignin fibers were characterized as described and compared by ANOVA at a significance level of 0.05 to determine differences in fiber diameter. Lignin-based fibers were oxidatively thermostabilized by heating to 250ºC (0.05ºC/min) using a forced air convection furnace prior to carbonization. The samples were then placed in a 2.54 cm diameter Lindberg Blue tube furnace, which was first purged with nitrogen at 10L/min for 15 minutes. Carbonization of the stabilized fibers was then carried out under nitrogen at temperatures up to 1000ºC (3ºC/min), with a nitrogen flow rate of 1 L/min.

The stabilized and carbonized fibers were characterized using a scanning electron microscope (SEM) with at least a 400x optical magnification and an average of 30 measurements to determine their diameter, morphology and the degree of separation of the fiber. The mechanical strength of the fibers was measured using a common tensile strength test (Instron tensile testing machine model 5943) with 5 N load cell according to the ASTM standard D3379-75.

CHAPTER IV. RESULTS AND DISCUSSION

4.1. Organosolv Fractionation Runs

For this study, 46 organosolv fractionation runs were carried out using tulip poplar and Alamo switchgrass as feedstock. The average solid to liquid ratio was 1:13 for tulip poplar runs and 1:23 for Alamo switchgrass runs, equating to an average total solvent amount of 11.01 liter over all runs. The gathered black liquor, consisting mainly of hemicellulose and lignin, had an average volume of 9.72 liters. This difference led to the conclusion that the difference between solvent and black liquor (1.29 liter) resulted from evaporation during the run. The black liquor was then separated into an organic phase with an average amount of 640.1ml (±52.3) and an aqueous phase with 4975.15ml (±265.3). Lignin gained from both phases was then combined which resulted in an average lignin amount of 88.45g. The total average dry cellulose amount was 185.91g.

4.2. Biomass Characterization

Tulip poplar *(Liriodendron tulipifera)* is a genus from the *Magnoliaceae* "magnolia' family. It is the tallest eastern hardwood and widespread in the southeastern United States. It is easy to access and relatively inexpensive. Alamo switchgrass *(Panicum virgatum)* is a genus from the *Poaceae* "true grasses" family and it is adapted throughout the majority of the United States.

Moisture content of both feedstocks was determined after drying for 12h in a 105°C oven and had an average of 8%. In addition, the ash content averaged 0.19% for poplar and 0.10% for switchgrass based on oven dry weigh using protocol NREL/TP-510-42622. Adjusted for moisture content, the dry weight of the biomass had an average of 662.4g for poplar and 395.6g for switchgrass.

Extractive free biomass was measured for its theoretical lignin yield and showed that Alamo switchgrass has a maximum lignin content of 22.7% (±1.2) and tulip poplar a maximum lignin content of 24.26% (±0.1) with an ash content of 0.4% (±.0.2) and 0.4% (±0.3) respectively. The average lignin yield over all poplar runs was 115.7g and 61.2g for switchgrass runs. Therefore tulip poplar runs gave an average lignin yield of 17.46% and Alamo switchgrass 15.47% based on the oven dry biomass.

4.2.1. Organosolv Fractionation Runs of Tulip Poplar

All runs given in Table 10 were carried out using 720g of tulip poplar chips and a -1 solvent. The amount of the added H_2SO_4 ranged from 0.025 to 0.15 M and temperature from 130°C to 170°C. Average lignin content after fractionation of poplar was 117.2g (±20.6). The average amount of remaining dry cellulose was 241.6g (±89.1) with an average moisture content of 78.2% (±2.6%). Figure 13 summarizes the yield of cellulose and lignin as a function of fractionation temperatures and shows a very clear decreasing trend of the cellulose yield from low to high severity. The higher the temperature and acid level, the more cellulose is decomposed causing a lower yield. In contrast, the lignin yield increases at high severity but shows a constant level between 140°C and 160°C.

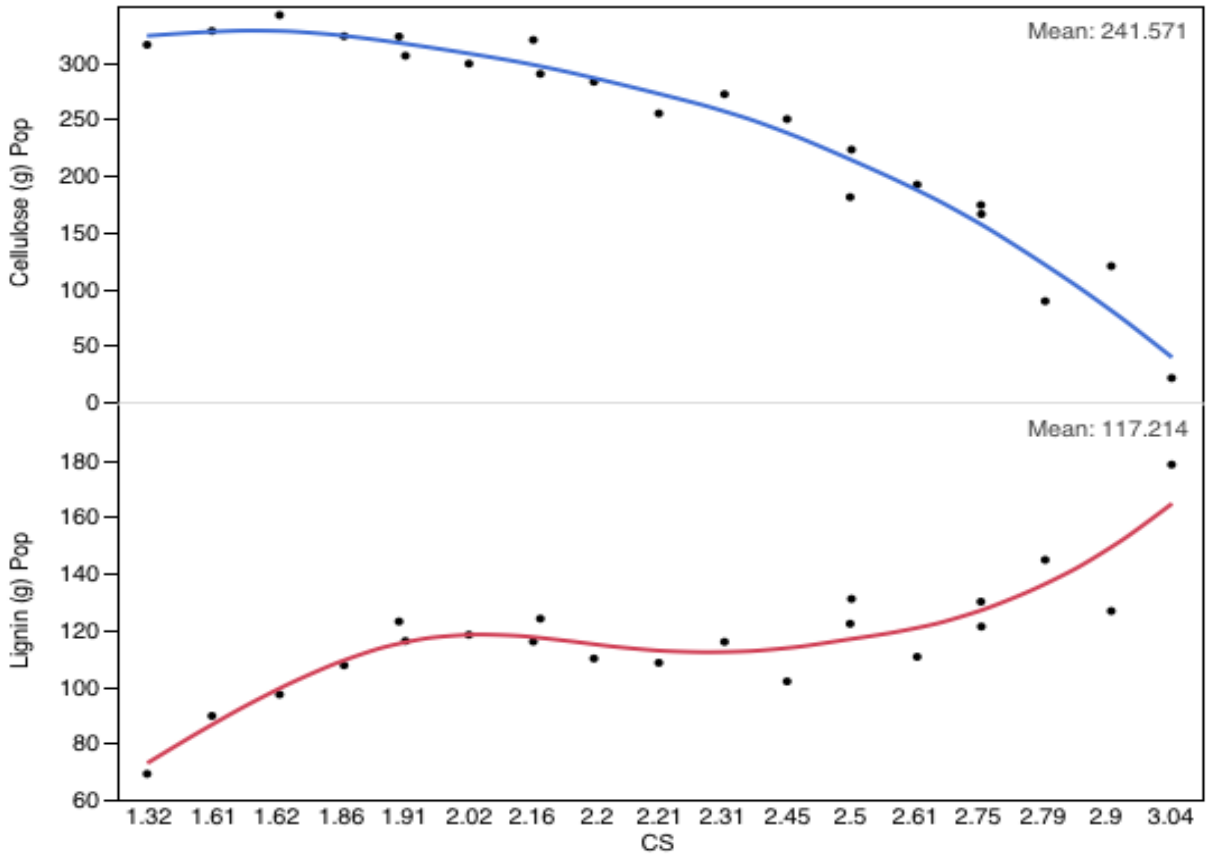

Figure 13. Pure cellulose and lignin yield of tulip poplar runs.

4.2.2. Time Dependent Runs on Tulip Poplar

The second approach of this study was to investigate runs with same conditions as a function of time (recall Table 11). Figure 14 illustrates the trend of lignin and cellulose yield from 60min to 360min for runs conducted at 140°C with an acid concentration of 0.5M using the standard -1 solvent.

The average lignin yield was 109.2g (±18.1) and cellulose yield was 301.0g (±19.3). Hence, the yield at 180min is 19.5g higher than average. At this point the longer penetration of the solvent into the biomass led to a higher lignin yield at 180min and caused a lower cellulose yield. A runtime longer than 180min causes the lignin yield to drop dramatically.

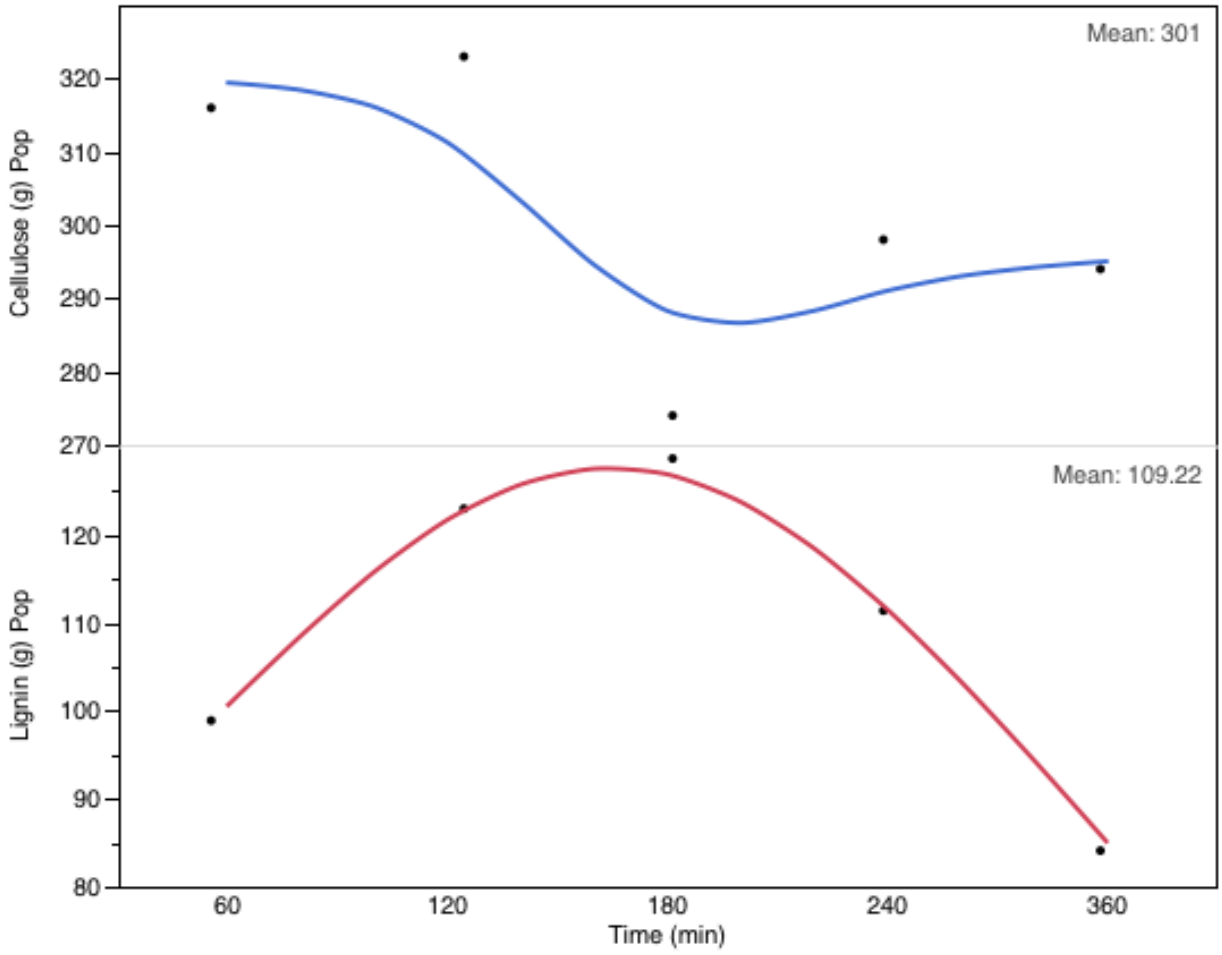

Figure 14. Time dependent runs of tulip poplar at 140°C using single values.

4.2.3. Organosolv Fractionation Runs of Alamo Switchgrass

All runs that were listed in Table 12 were carried out using 430g of switchgrass and a -1 solvent. The amount of the additional agent (sulfuric acid) ranges from 0.025 to 0.1M and the investigated temperature from 130°C to 160°C. The average lignin content of switchgrass runs excluding the time dependent runs was 61.5g (±6.03), which was 15.5% of the oven dry biomass. The average amount of remaining dry cellulose was 133.6g (±42.5) with a moisture content of 78.8% (±2.4).

The performance line in Figure 15 of the cellulose yield illustrates a distinct downward trend as acid concentration and temperature increase. There was no apparent trend in the

lignin yield, but the maximum in yield appeared around a temperature of 140°C. Therefore, fractionation runs using Alamo switchgrass should be conducted at 140°C giving a maximum lignin yield of 69g.

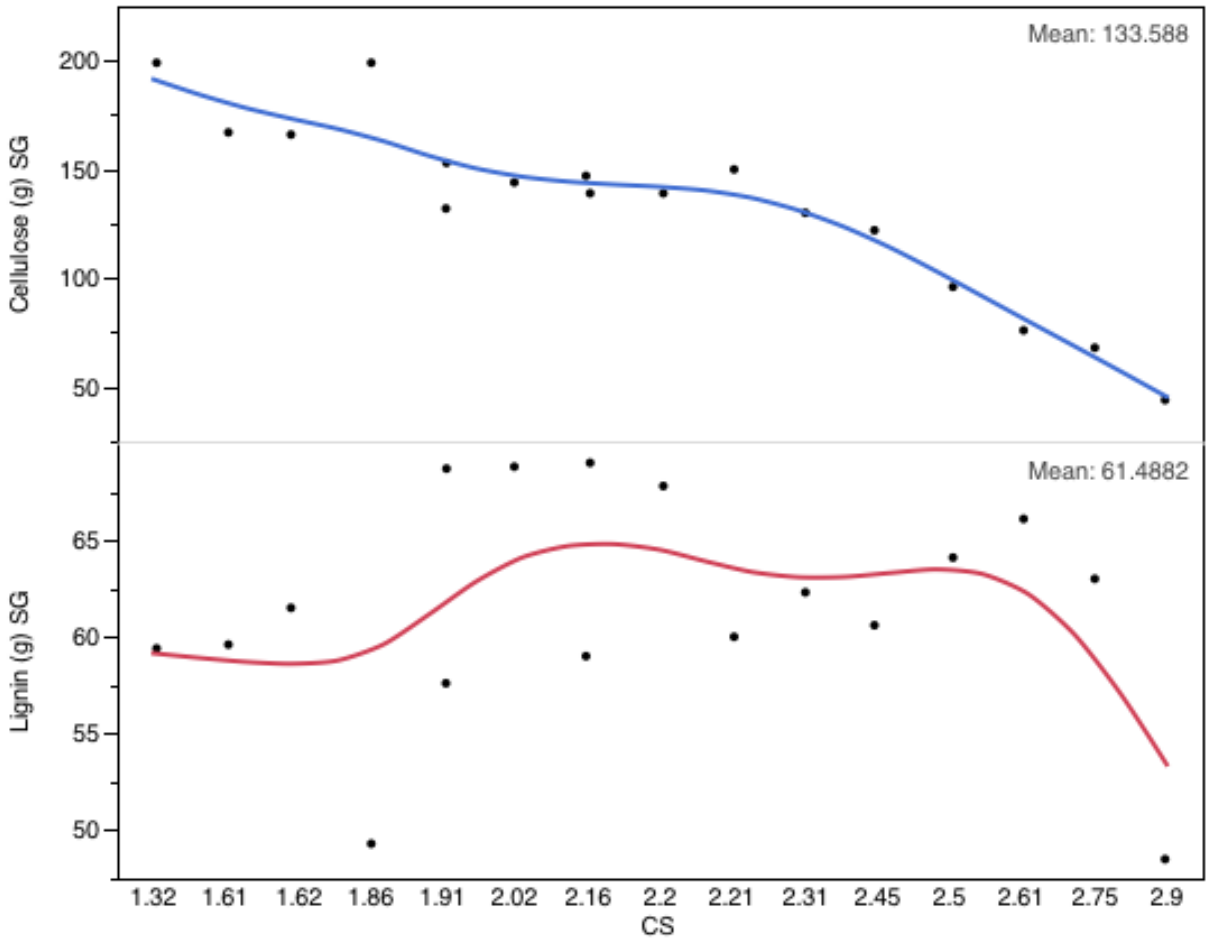

Figure 15. Pure cellulose and lignin yield of Alamo switchgrass runs.

4.2.4. Time Dependent Runs on Alamo Switchgrass

The second approach of this study was to investigate runs at a single set of conditions as a function of time. Figure 16 shows the trend of lignin and cellulose yield from 60min to 360min. These runs were conducted at 140°C with an acid concentration of 0.05M using the standard -1 solvent.

The average lignin yield was 60.3g (±6.2) and average cellulose yield was 148.0g (±17.3). The highest lignin yield for switchgrass from fractionation was achieved with a runtime of 120 minutes. The amount of residual cellulose seems to be lowest at 180min and increases with increasing runtime but is still relatively high compared to other run conditions. In contrast to poplar runs, the fractionation of switchgrass can be carried out at shorter runtimes.

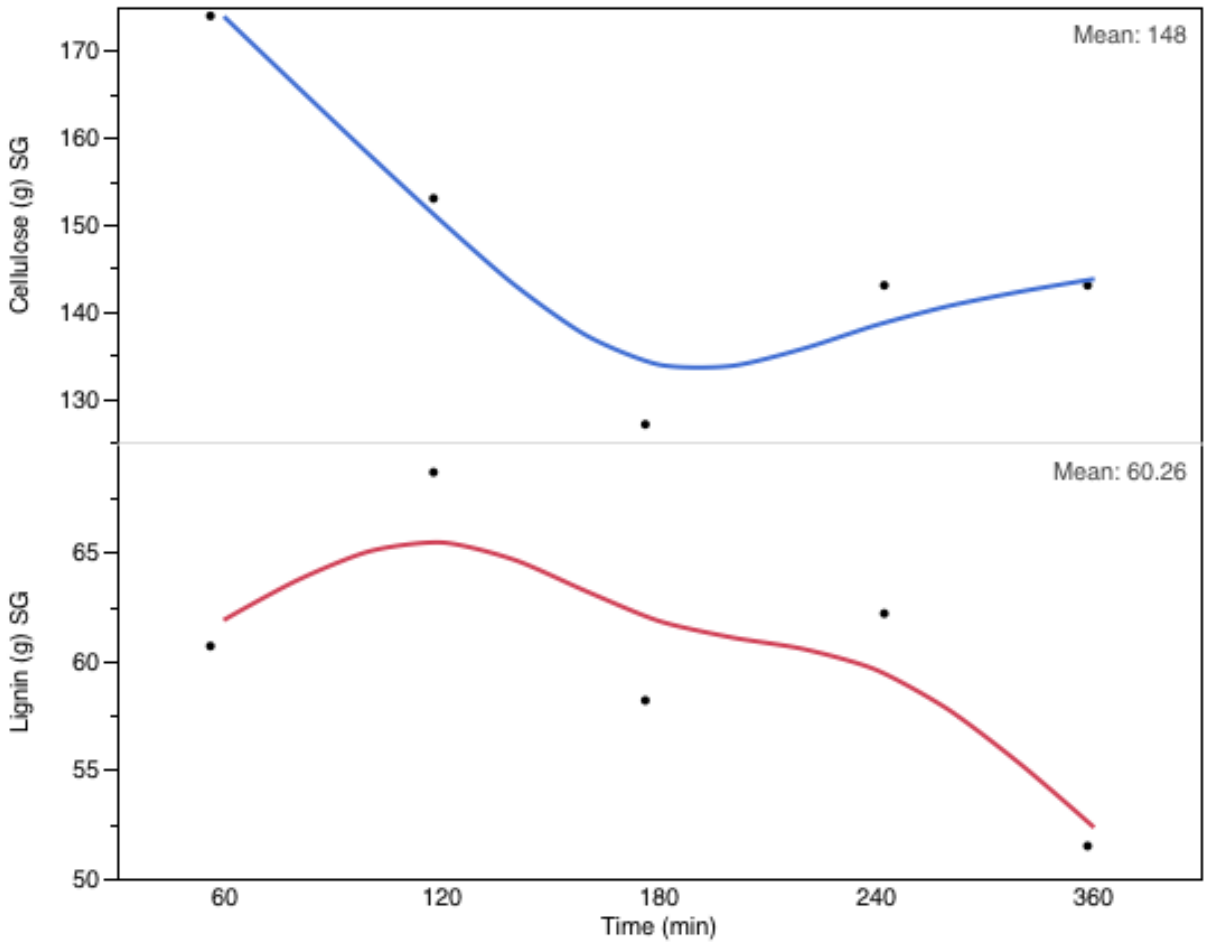

Figure 16. Time depending runs of switchgrass at 140°C using single values.

4.3. Comparison of Poplar and Switchgrass Fractionations

Figure 17 shows the lignin yields from both feedstocks as a function of temperature. Because the amount of the feedstock is limited by the maximum capacity of the reactor, the difference in the lignin yield is conclusive. However, the average over all runs gave 72.13% of the theoretical lignin content from tulip poplar and 68.22% from Alamo switchgrass. As illustrated, the highest yields were achieved at 140°C and 160°C for both feedstocks. To find if there is a significant difference, the yields were tested using a one way ANOVA as can be seen in Figure 19 and Figure 20.The one way ANOVA is considered a robust test against the normality assumption.

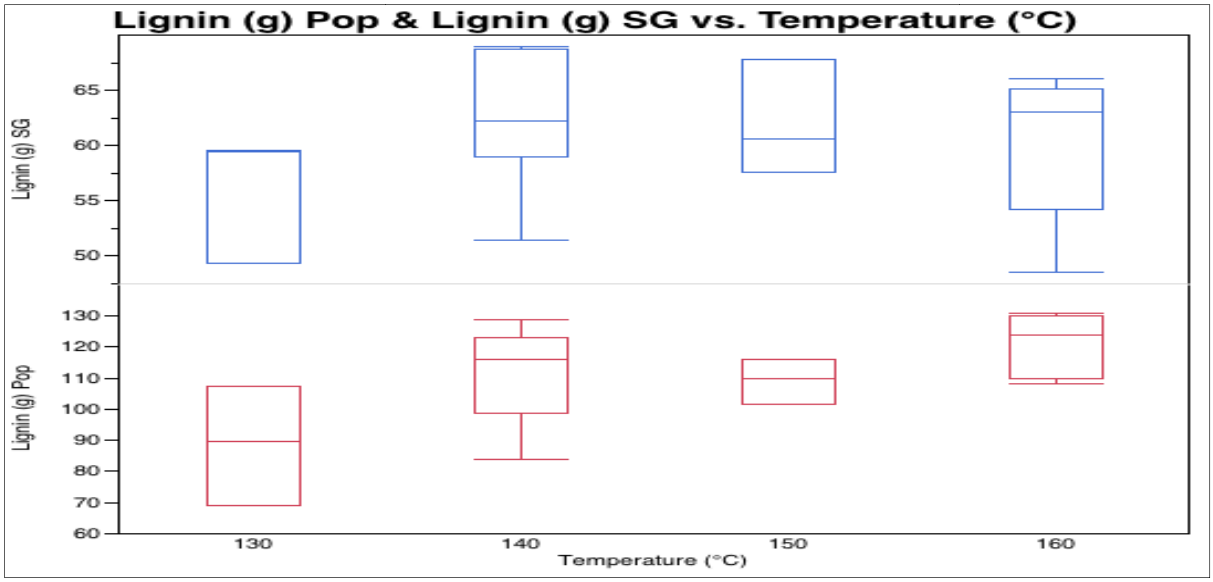

Figure 17. Lignin yield comparison as a function of temperature over all runs.

First, both datasets were statistically analyzed and indicate that data were normally distributed and could therefore be used for further statistical analysis (Figure 18). The histogram for lignin yields showed approximate normality of both feedstocks. Although the poplar yield box plot discloses two outliers and the switchgrass box plot indicates a slight negative skewness, both datasets are normally distributed and can be used for subsequent analysis.

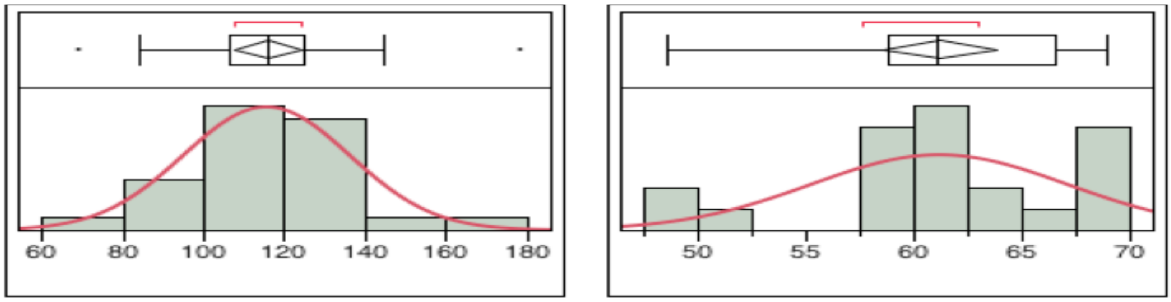

Figure 18. Histograms and box plots of lignin yield for poplar (left) and switchgrass (right).

The one way ANOVA for poplar identified a significant difference in lignin yield at 130°C compared to higher temperatures as can be seen in Figure 19 and Figure 20. There was no further significant difference for switchgrass yields at higher temperatures but the p-value of 0.1008 for a difference between 140°C and 130°C could be an indicator for proof of difference using replicates (Figure 20).

Figure 19 shows the distribution of the lignin yield for each temperature separately. JMP plots the means and 95% confidence intervals for each mean and generates the summary of fit

and the analysis of variance (Figure 21). The results suggest no significant difference in mean lignin yield for poplar across all means using Welch's ANOVA at an $\alpha = 0.05$. This may be due to unequal variances in each subgroup, even though the 130°C mean yield does appear lower than the other subgroups.

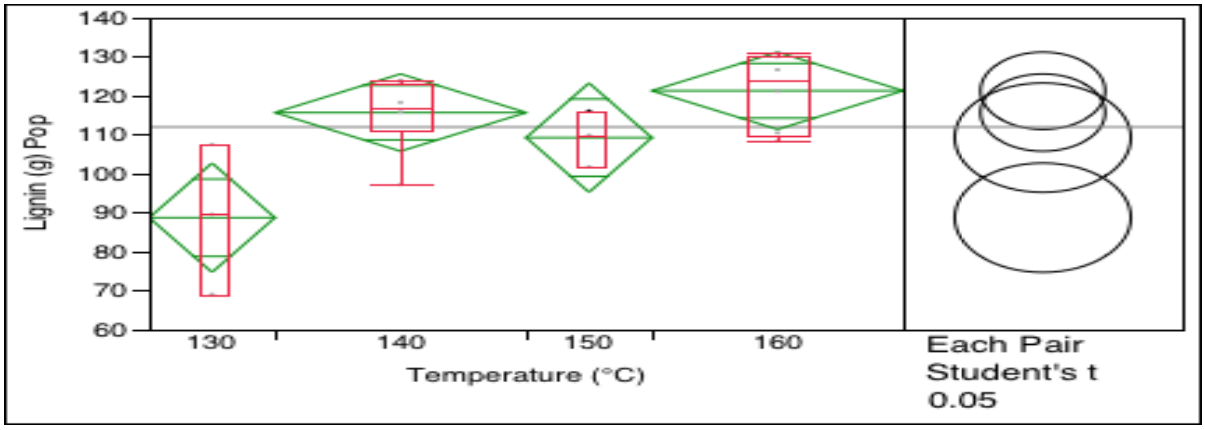

Figure 19. One way analysis of poplar lignin yield.

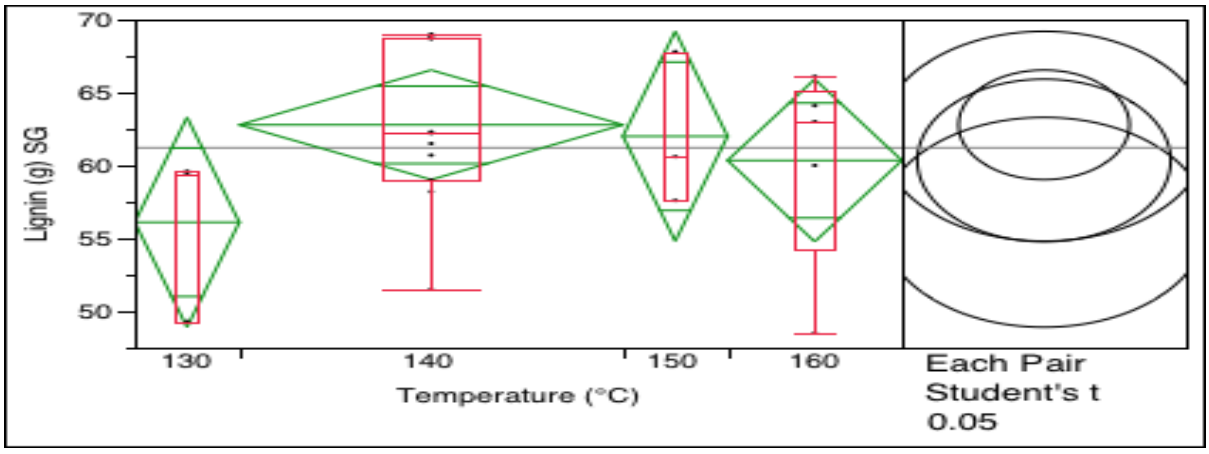

Figure 20. One way analysis of switchgrass lignin yield.

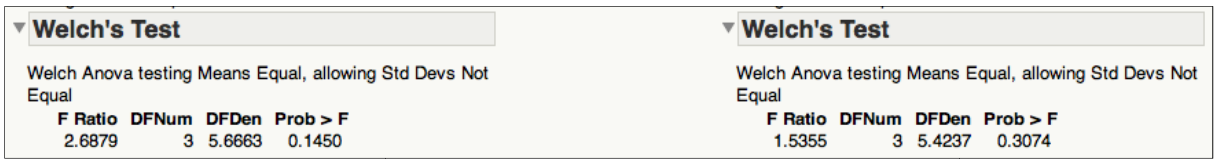

Figure 21. Welch's ANOVA of mean lignin yield across temperature for poplar (left) and switchgrass (right).

4.4. Characterization of Tulip Poplar Lignin

4.4.1. Purity and Ash Content

The average lignin purity for isolated tulip poplar lignin using the standard Klason analysis was 94.8% (±2.6). The highest purity [98.6% (±0.2)] was achieved at a temperature of 160°C using 0.1M sulfuric acid for 120 minutes. As can be seen in Figure 22 the purity of the lignin increases with temperature, has its peak at 160°C and decreases again at 170°C. All three acid concentrations exhibited the same trend. The average ash content is 0.12% (±0.1) but increases dramatically at temperatures higher than 160°C. For this reason, runs at 170°C were not carried out for switchgrass. One explanation could be that with very high temperature the materials in the reactor e.g. the Teflon basket, the wire or the reactor itself starts to degrade and causes the ash content to increase.

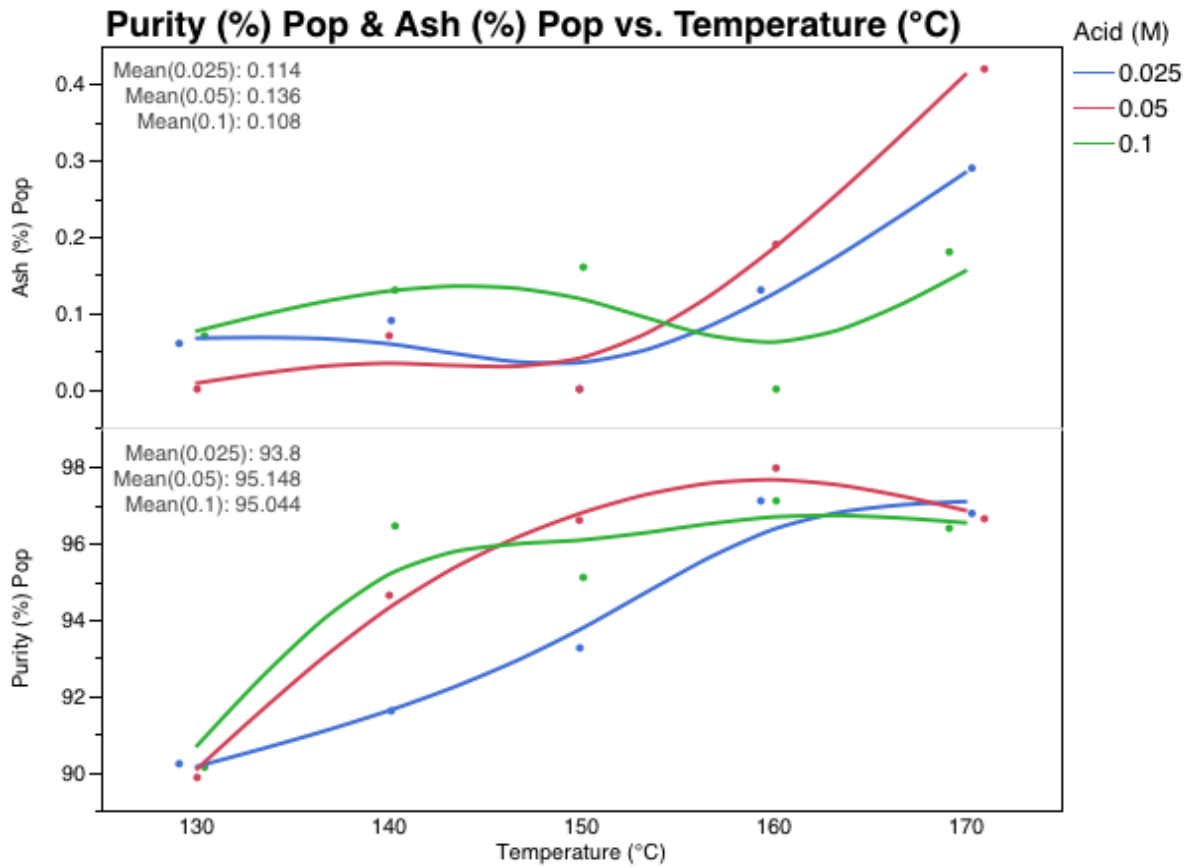

Figure 22. Purity and ash content as a function of time and acid concentration.

4.4.2. Elemental Analysis (CHNS/O)

The elemental composition of tulip poplar lignin gave an average carbon content of 63.67% (±1.1), hydrogen content of 6.0% (±0.2) and a nitrogen content of 0.28% (±0.04). The

remaining portion consists of inorganic material (ash), which averaged 0.19% (±0.1) and oxygen. The amount of oxygen is consequently 29.8%. The trend lines in Figure 23 show, that the carbon content increases while the hydrogen content decreases as a function of severity.

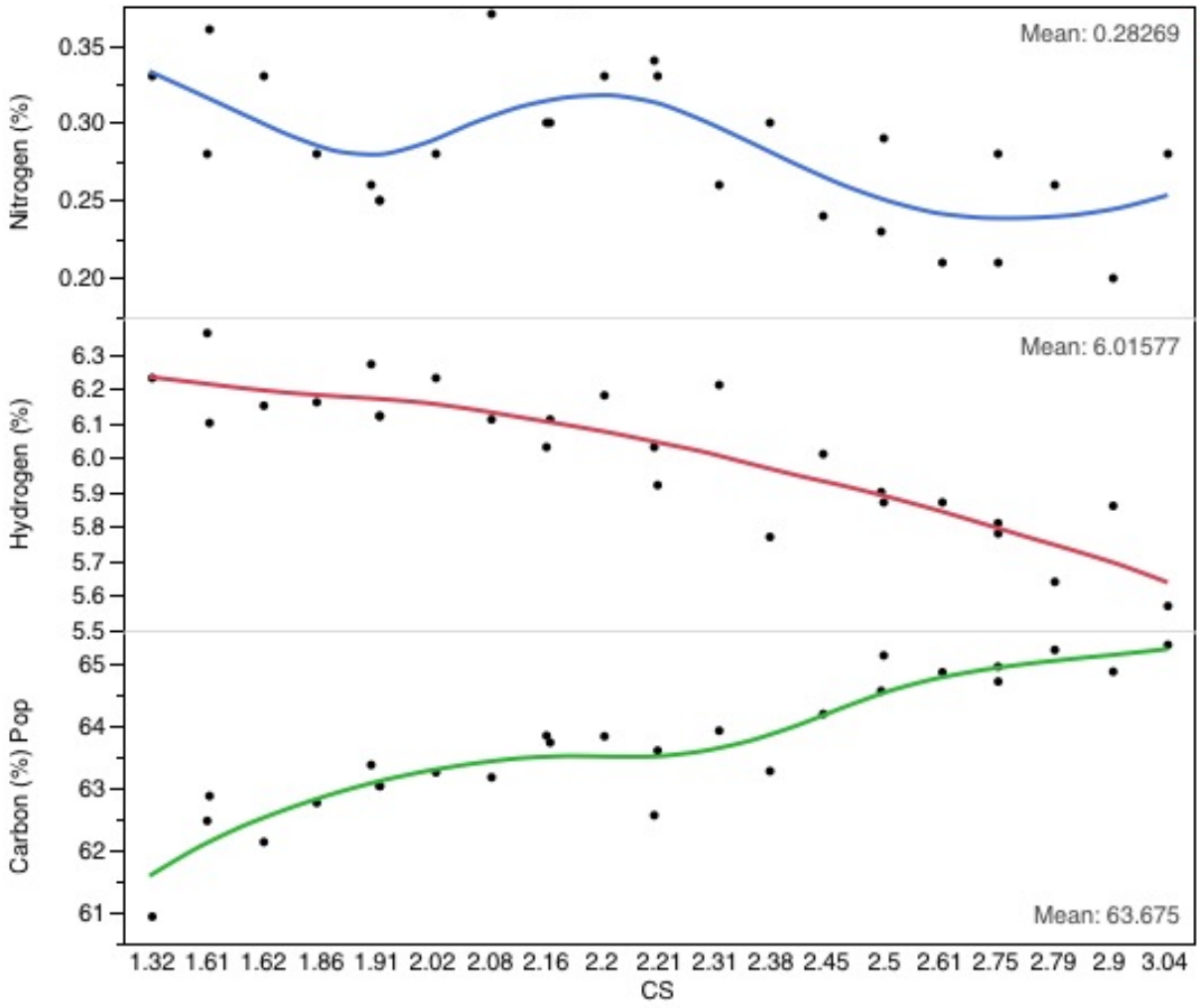

Figure 23. Elemental analysis of tulip poplar lignin.

4.4.3. Melting Properties (Fisher Johns)

All temperatures obtained with the Fisher Johns are given as average and can be seen in Table 18. The softening properties of the lignin samples were recorded over six stages of transformation: discoloration, localized melting, appreciable melting, full-melt, melt flow and high melt flow. Temperature ranges of interest are the appreciable melting (start of liquidation) with an average of 147.7ºC (±6.4) and the full melt with 152.9 ºC (±6.8). For melt spinning application each stage should be considered individually. Crosslinking seems to occur at temperatures of 200°C and above. All these measurements can be seen in Table 18.

4.4.4. Glass-Transition Measurement (DSC)

DSC results showed that poplar lignin exhibited an average glass transition at a temperature of 122.4°C (±4.8) and a heat capacity of 0.4 %(±0.1). The onset, where the lignin starts to change its aggregate state from solid to liquid, appeared to be at an average temperature of 110.3ºC (±3.9) and exhibited an average width of 22.1ºC (±5.2). The glass transition temperature performance line over all runs shows an increase as a function of severity indicating that the molecular weight increases with severity.

The heat capacity values apparently drop after 160°C as can be seen in Table 20 leading to the conclusion that the molecular weight distribution decreases as well. The onset decreases continuously as severity goes up but the width shows a clear upwards trend indicating a higher molecular weight distribution (Figure 24).

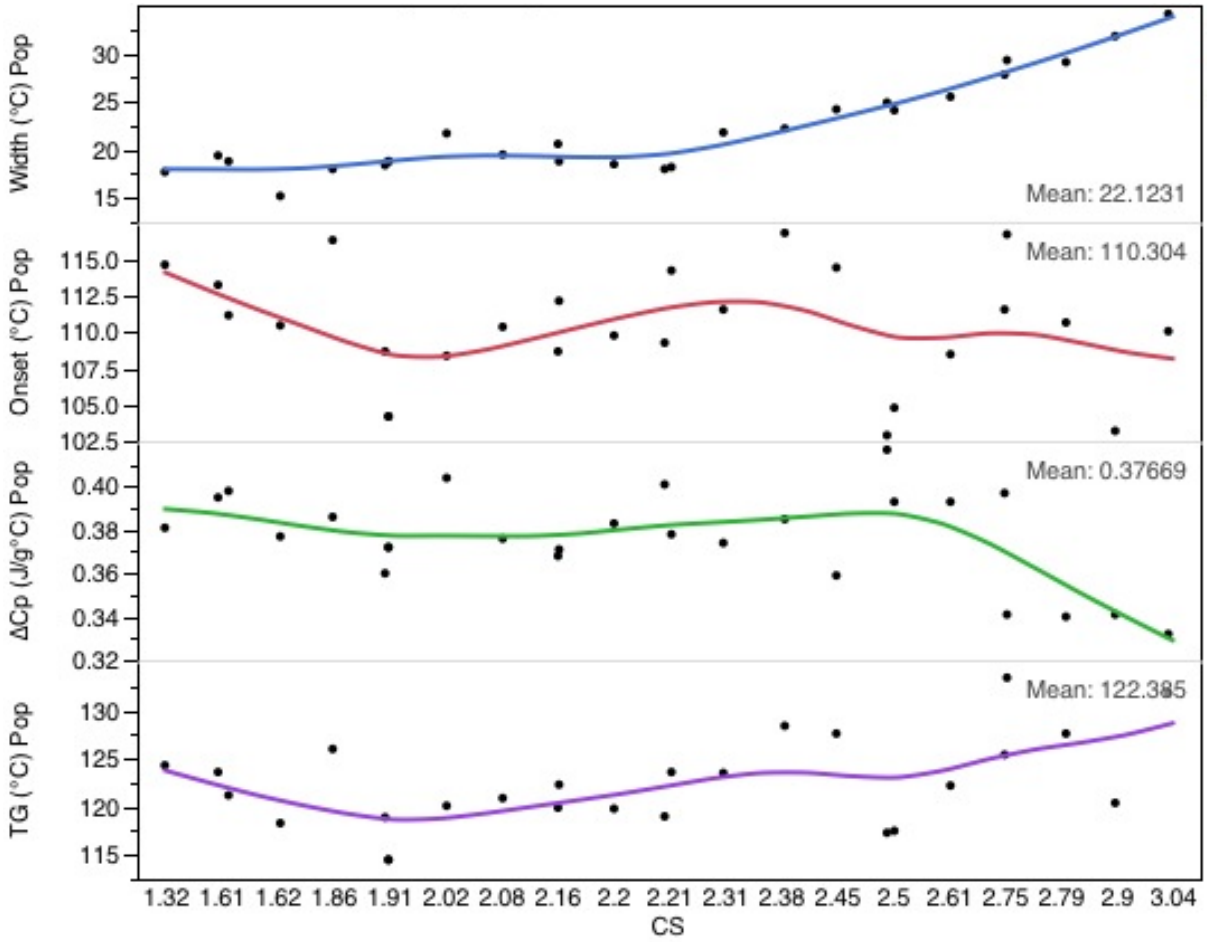

Figure 24. Transition measurements of tulip poplar showing glass transition temperature, heat capacity, onset of T_G and width of T_G as a function of CS.

4.4.5. Decomposition Measurements (TGA)

Results gained from TGA analyses showed that the decomposition of poplar lignin started at 274.6°C (±11.0) and a weight loss of 5% of the sample is already reached at 256.6°C (±5.1). The char content at 900°C is 36.2% (±3.3). The peak of the derivative curve (DTG), also referred to as the inflection point, is at 358.1°C (±3.6) as can be seen in Figure 25.

The trend of char content and the inflection point are expected, and the flattening trend of the onset and T_d can be explained by the percentage of purity. As shown before, the purity shows a peak at 160°C and drops down at 170°C and that causes the decrease in onset of the T_d and the T_d. Lower purity means higher impurities and that further means earlier decomposition, because impurities are mainly carbohydrates and those components that are volatile at these temperature ranges.

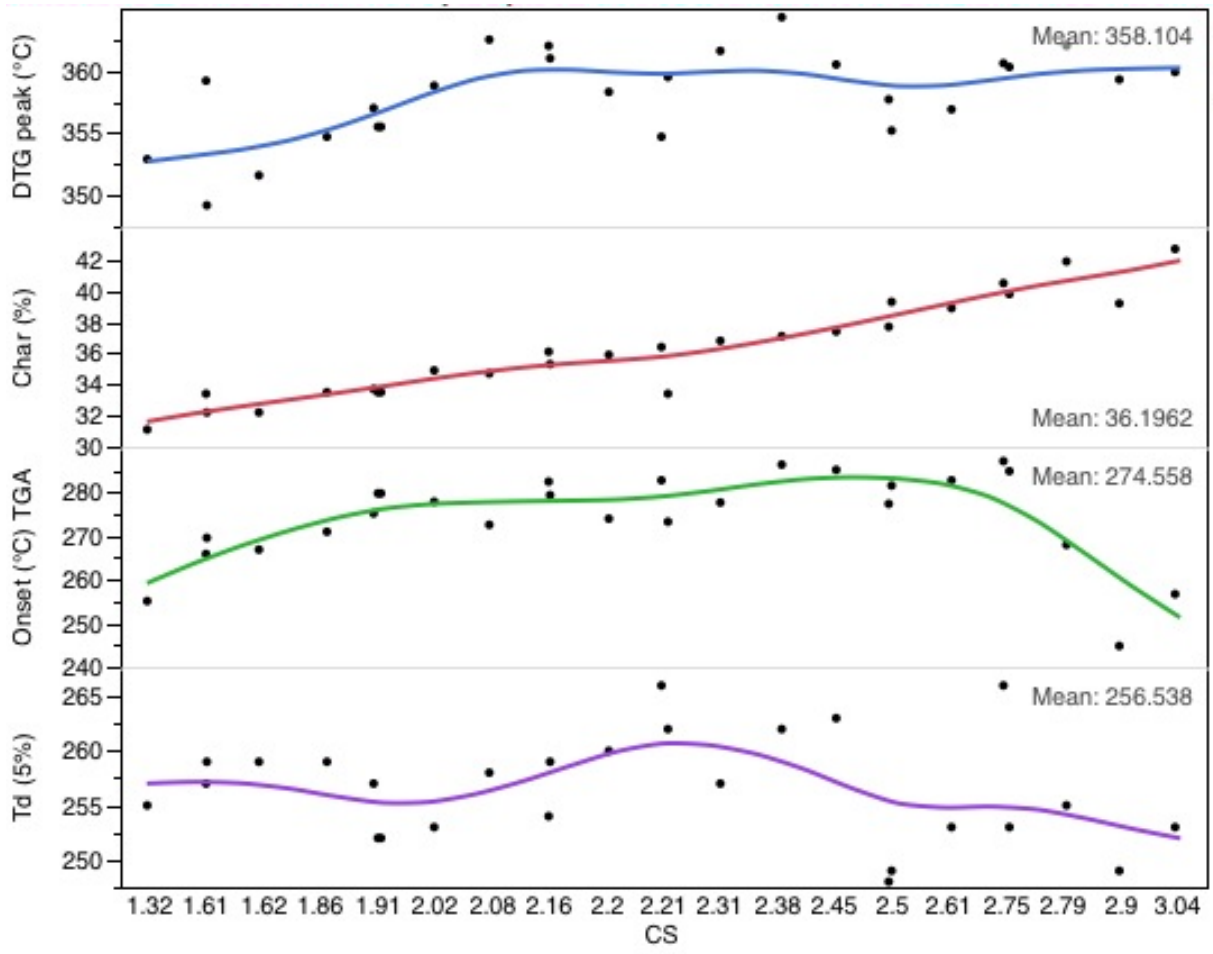

Figure 25. Decomposition measurements of tulip poplar showing decomposition temperature at 5% weight loss, onset of T_d, char content and inflection point.

Figure 26 compares the decomposition of poplar lignin at five different severities. Highest severity shows the highest char content (at 900°C) but also indicates slightly higher low molecular weight volatiles (at around 150°C). However, the char content continuously increases with higher temperature and acid concentration with a maximum amount of 42.7% at 170°C and 0.1M.

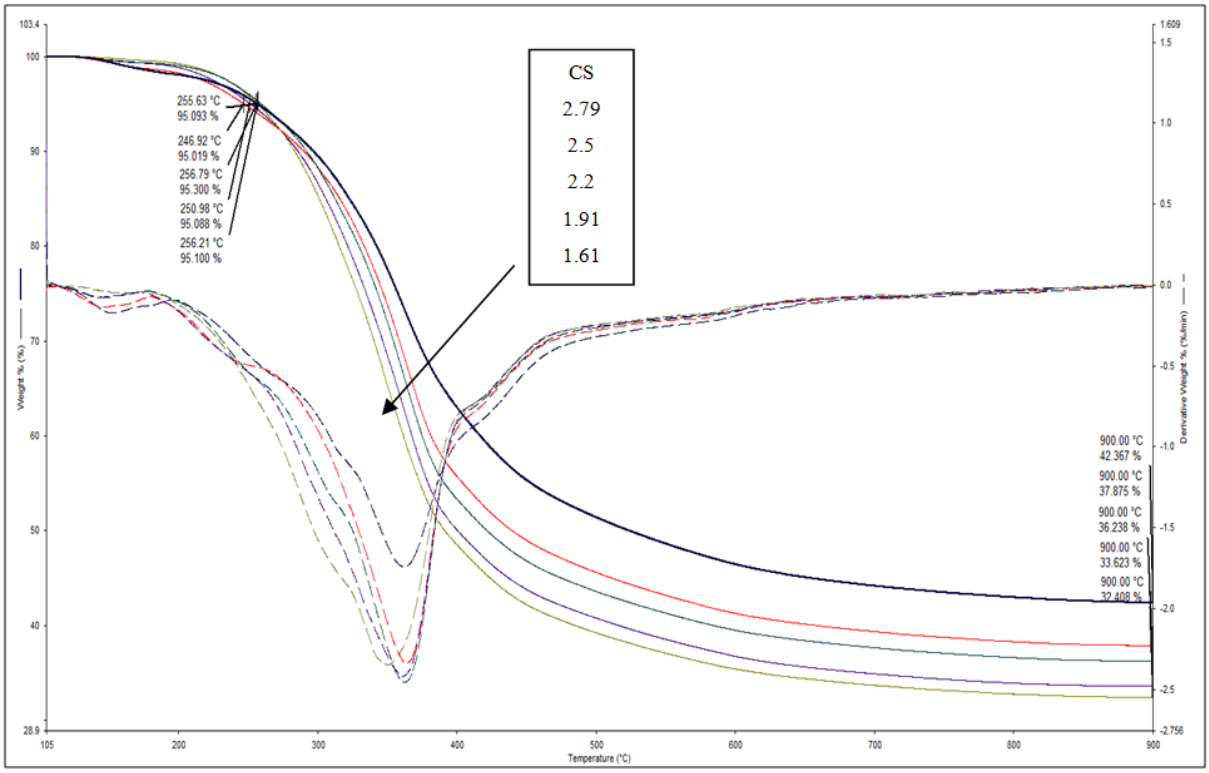

Figure 26. Decomposition of tulip poplar lignin at CS from 1.61 to 2.79.

4.5. Characterization of Alamo Switchgrass Lignin

4.5.1. Purity and Ash Content

Measurements of purity gave an average of 92.93% (± 3.17) with a maximum of 98.83% at 160°C with 0.1M acid concentration for 120min. As expected, the yield increases as severity increases. The ash content also increases with an average content of 0.1% (±0.1). The highest ash content was 0.2% found at 160°C using an acid concentration of 0.15M over 120min..

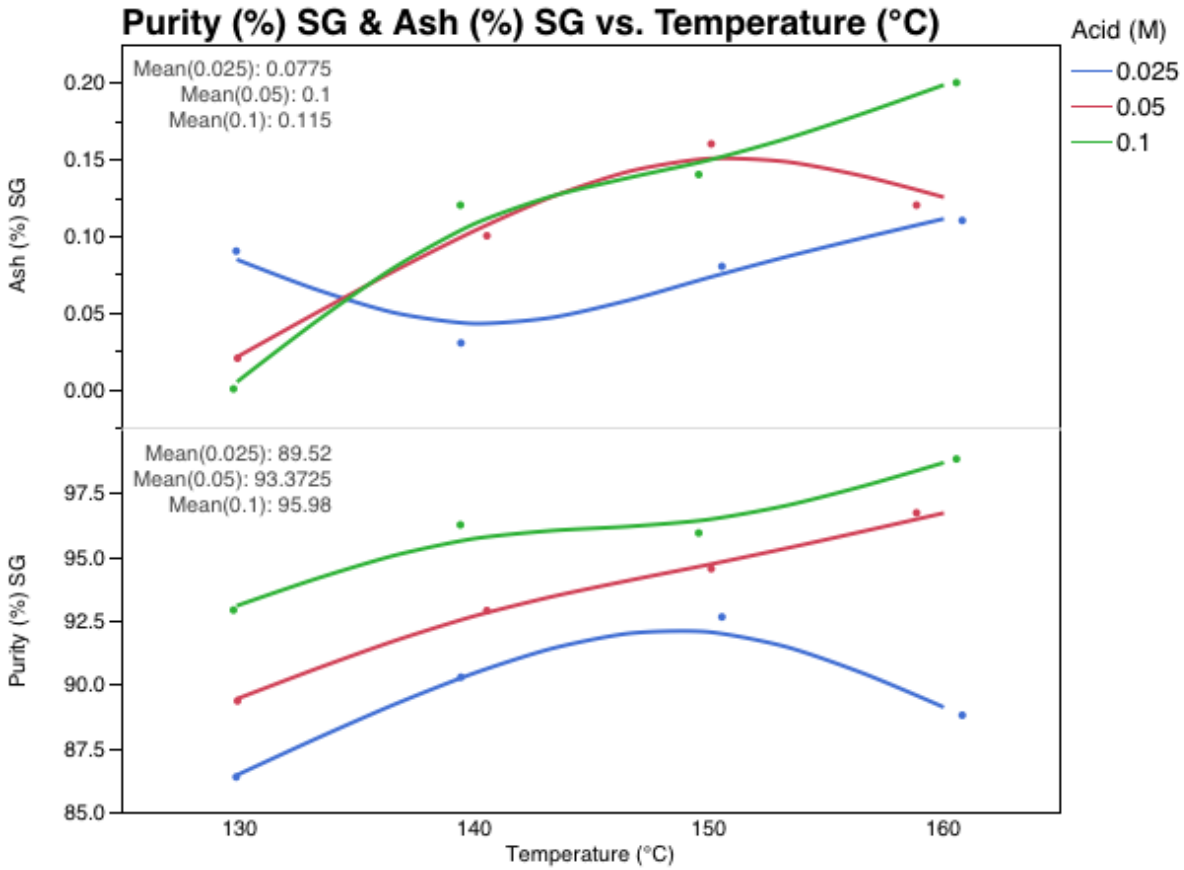

Figure 27. Purity and ash as a function of temperature and acid concentration.

4.5.2. Elemental Analysis (CHNS/O)

The elemental composition of Alamo switchgrass gave an average carbon content of 63% (±1.1), hydrogen content of 6% (±0.2) and a nitrogen content of 0.9% (±0.1). The remaining portion consists of inorganic material (ash), which was determined before with 0.1% (±0.1) and oxygen. The amount of oxygen is consequently 30.1%. Similar to poplar the trend lines for switchgrass show that the carbon content increases while the hydrogen content seems to decrease as a function of severity (Figure 28).

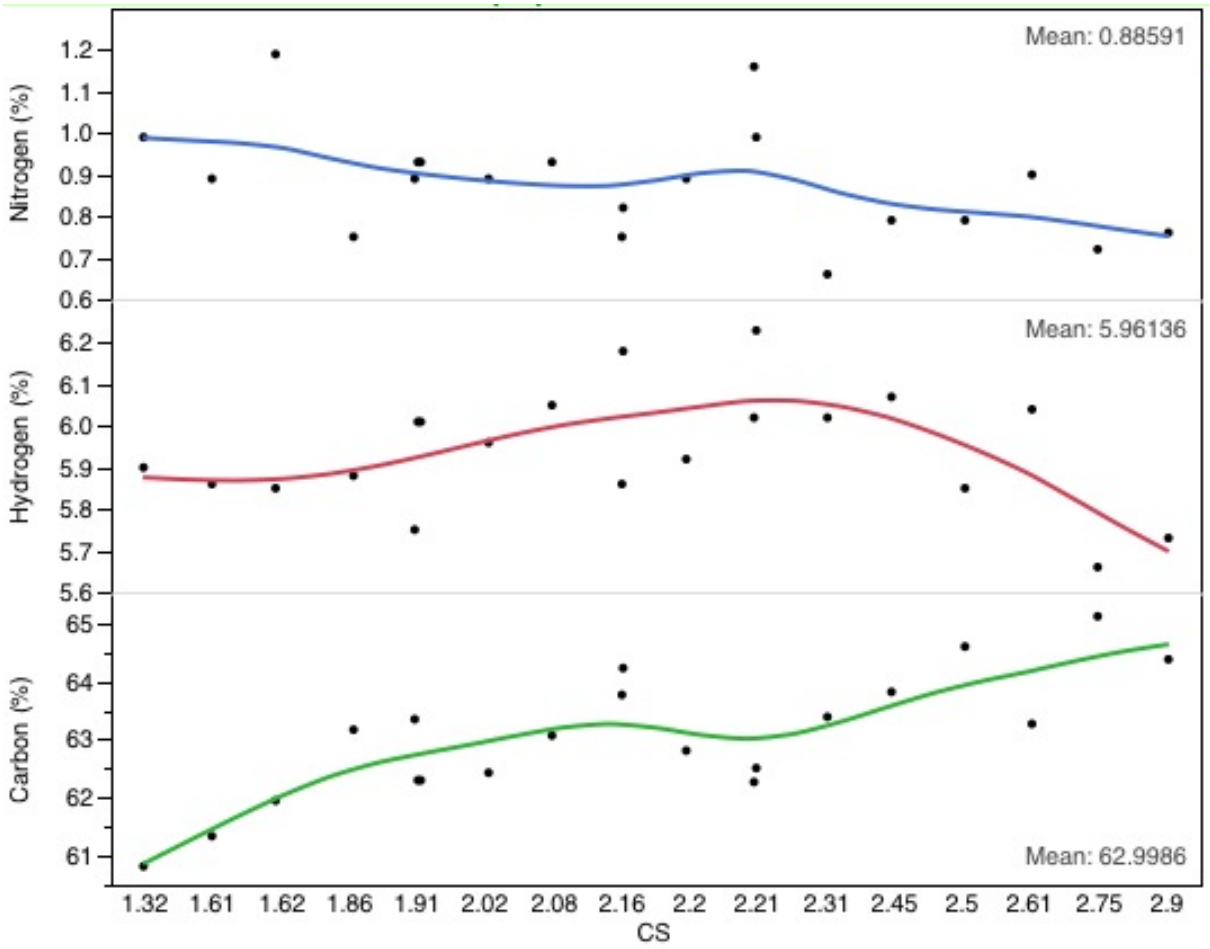

Figure 28. Elemental analysis of Alamo switchgrass showing carbon, hydrogen and nitrogen content.

4.5.3. Melting Properties (Fisher Johns)

All temperatures obtained with the Fisher Johns are given as average and can be seen in Table 19. The appreciable melt point was determined at 150.5°C (±5.1) and the full melt at 158.18°C (±6.4). The main observation for switchgrass melting behavior was that almost every sample showed a low viscosity but still included particles that did not melt rendering the sample not suitable for fiber spinning. Full melt temperature is 158.2°C (±6.4) Crosslinking was observed to occur at a temperature range from 180°C to 200°C.

4.5.4. Glass-Transition Measurements (DSC)

DSC results showed that switchgrass lignin exhibited an average glass transition at a temperature of 124.4°C (±5.0) and a heat capacity of 0.3 (±0.1). The onset appeared to be at a level of 111.4 (±5.2) and exhibited an average width of of 23.7 (±4.2). The glass transition

temperature in Figure 29 tends to decrease at high severity indicating the molecular weight increases as well.

The specific heat capacity generally increases showing a relatively pure lignin but drops after a severity of 2.61. That can be caused by a higher amount of impurities due to severe conditions.

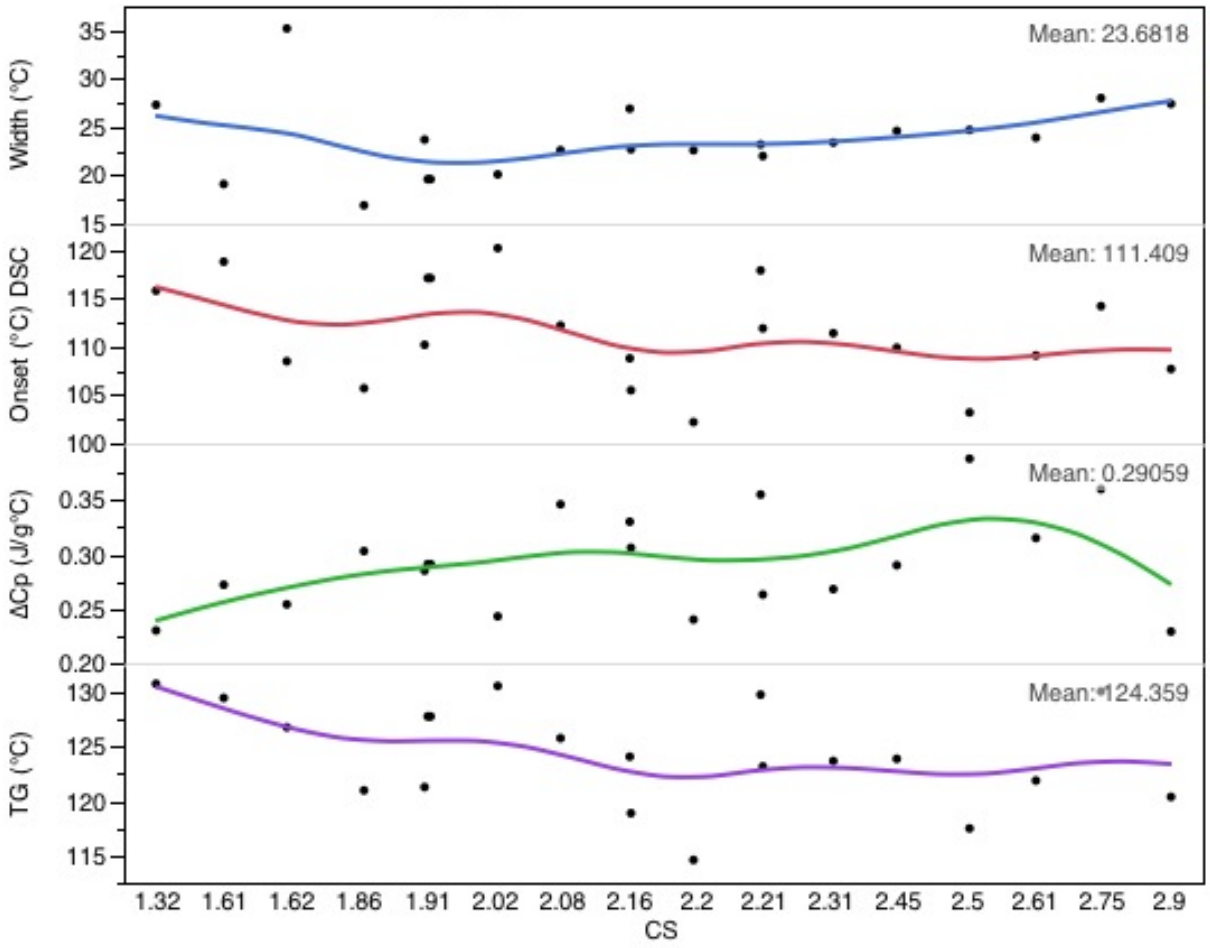

Figure 29. Transition measurements of Alamo switchgrass showing glass transition temperature, heat capacity, onset of T_G and width of T_G as a function of CS.

4.5.5. Decomposition Measurements (TGA)

Results gained from TGA analyses showed that the decomposition of switchgrass lignin started at 247.6°C (±15.9) and a weight loss of 5% of the sample is already reached at 237.9°C (±7.0). The char content at 900°C is 36.0% (±2.0). The peak of the derivative curve (DTG) is at 356.3°C (±5.1) as can be seen in Figure 30.

The trend line for the onset temperature seems to be constant but shows a decrease at high severity. That could be due to a low purity of the lignin at high severity. As shown in section 4.5.1 the purity at high temperature with low acid concentration was very low (88.79%)

causing the increasing trend to flatten out (Figure 30). The rising char content correlate with the already mentioned carbon content and causes the DTG showing similar behavior.

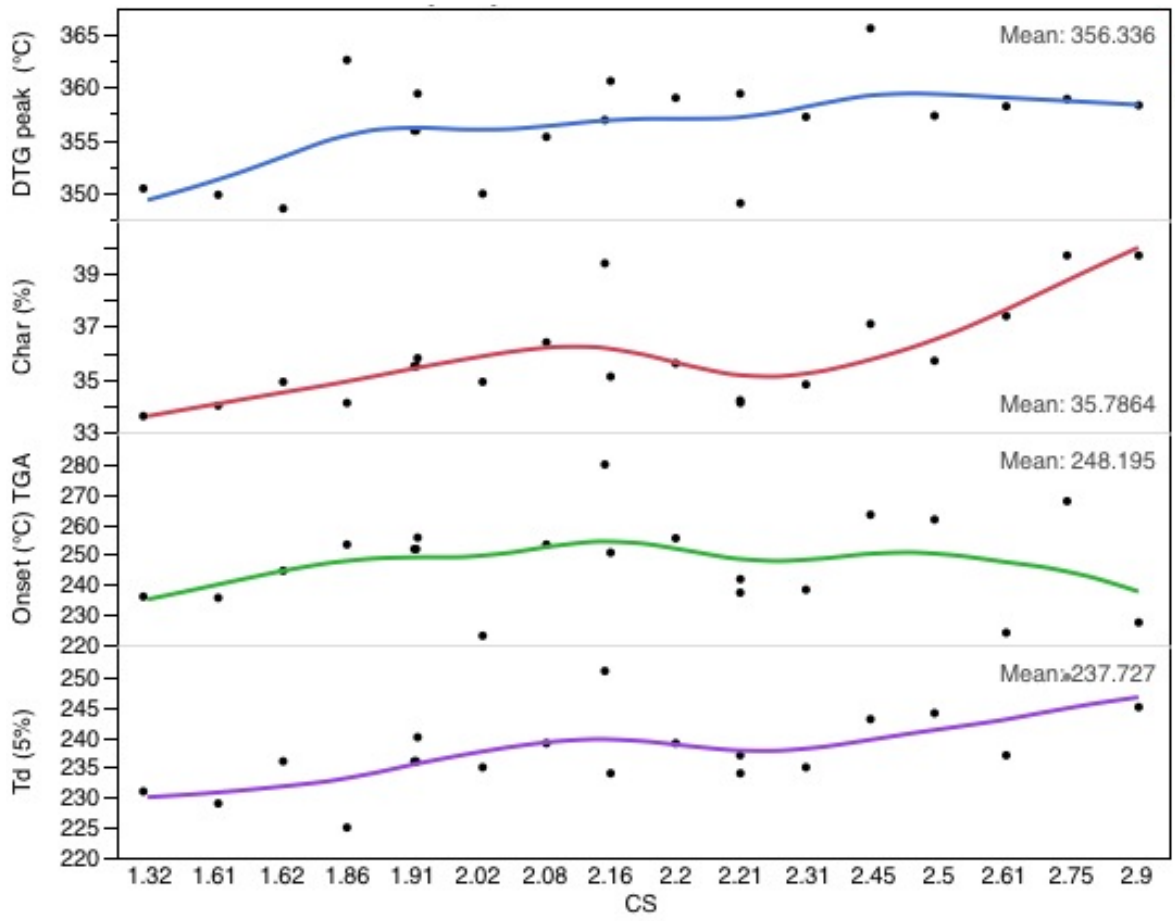

Figure 30. Decomposition measurements of Alamo switchgrass showing decomposition temperature at 5% weight loss, onset of T_d, char content and inflection point.

Figure 31 presents the changes in lignin decomposition due to higher severity. Higher severity basically means higher purity but at a severity of 2.9 the purity drops down (not shown in this figure) and therefore a later onset of decomposition (solid line). Later decomposition as well as higher char content therefore reduces the derivative trend line (dashed line) indicating less low molecular weight volatiles and carbohydrates. Consequentially, the decomposition rate is lower with higher severity.

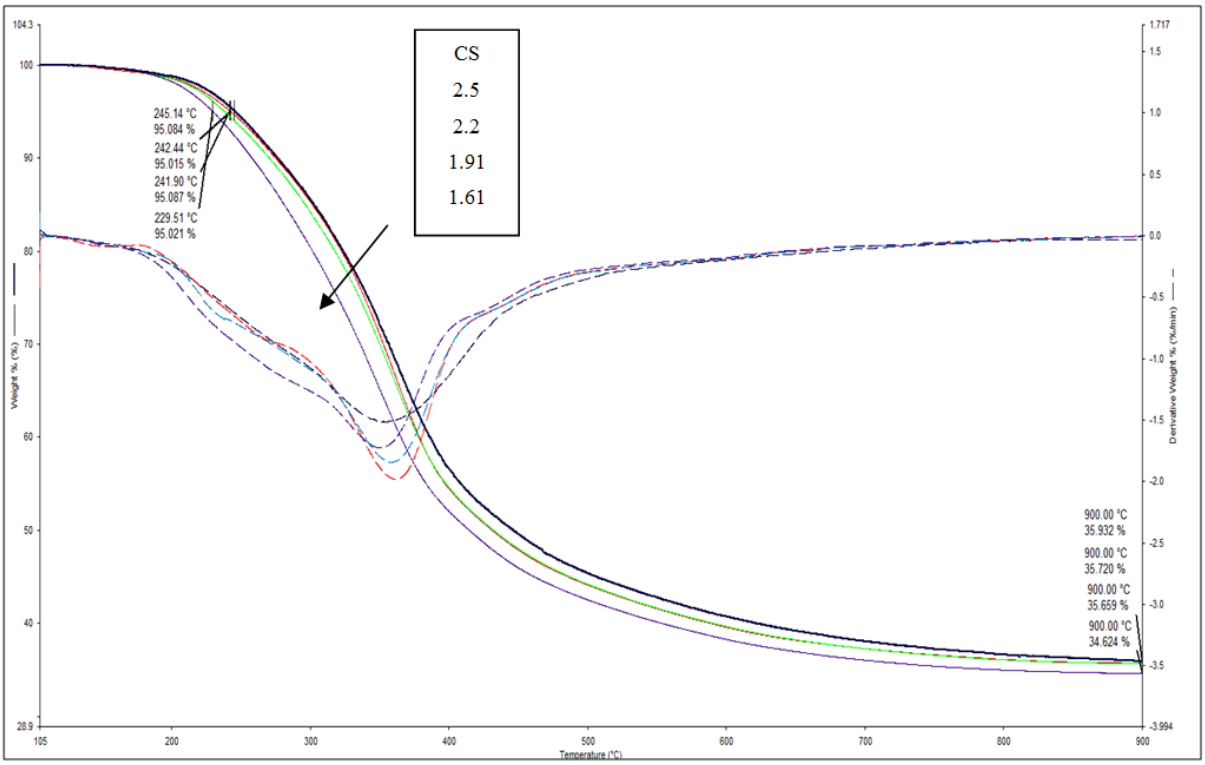

Figure 31. Decomposition of Alamo switchgrass lignin at CS of 1.61-2.5.

4.6. Comparison of Switchgrass and Poplar Lignin Characteristics

The purity of recovered lignin samples was found to be 86-98%, where poplar exhibited slightly higher values 94.64 (±2.45) than switchgrass 92.92% (±3.17). The highest purity was found at a severity of 2.75 for both feedstocks with 98.61% for poplar and 98.83% for switchgrass (Figure 32).

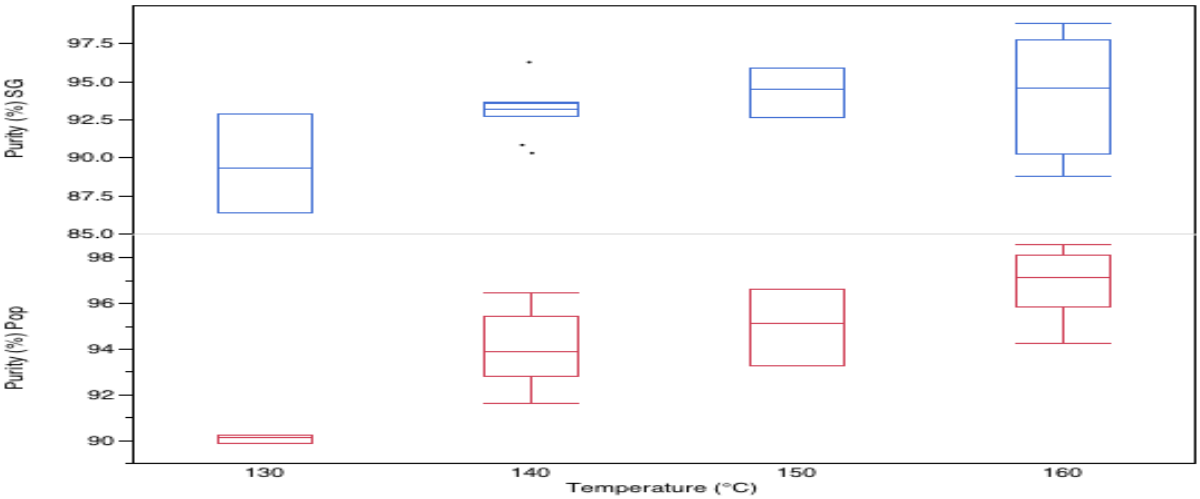

Figure 32. Comparison of poplar purity (bottom) and switchgrass purity (top).

The one way ANOVA for purity showed significant differences for poplar runs but not for switchgrass as can be seen in Figure 33 and Figure 34. The Student´s t-test gave highly significance between run temperatures of 130°C purity received at every single temperature step.

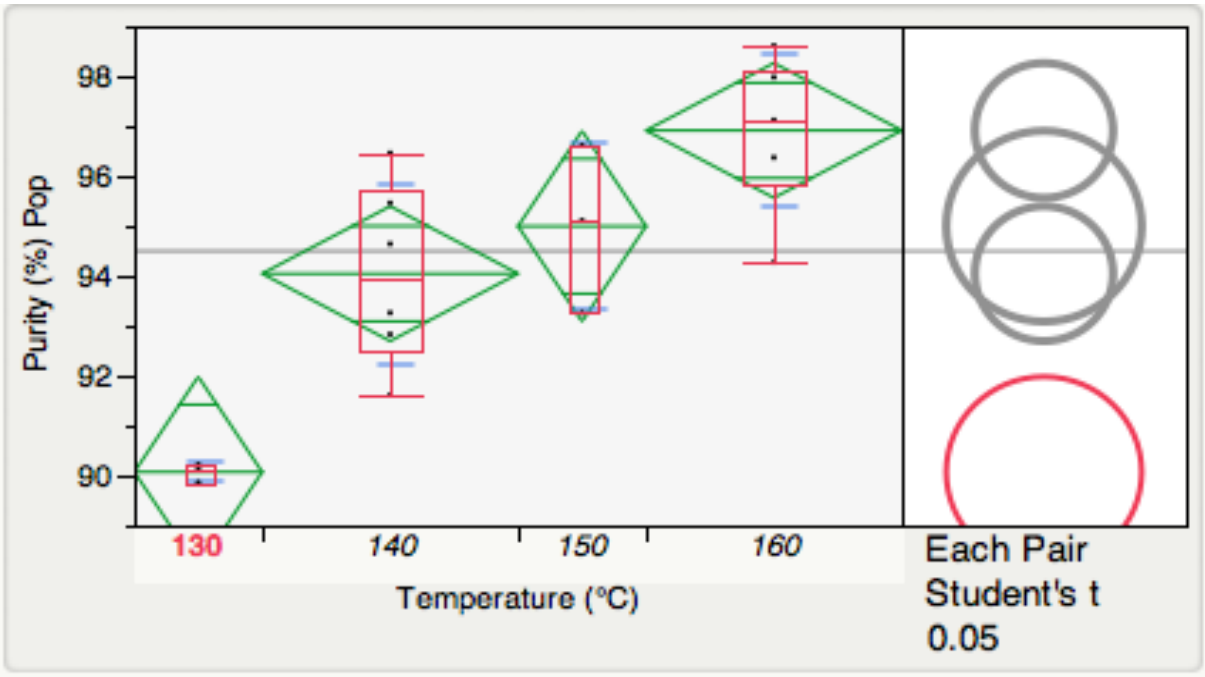

Figure 33. One way Analysis of poplar purity.

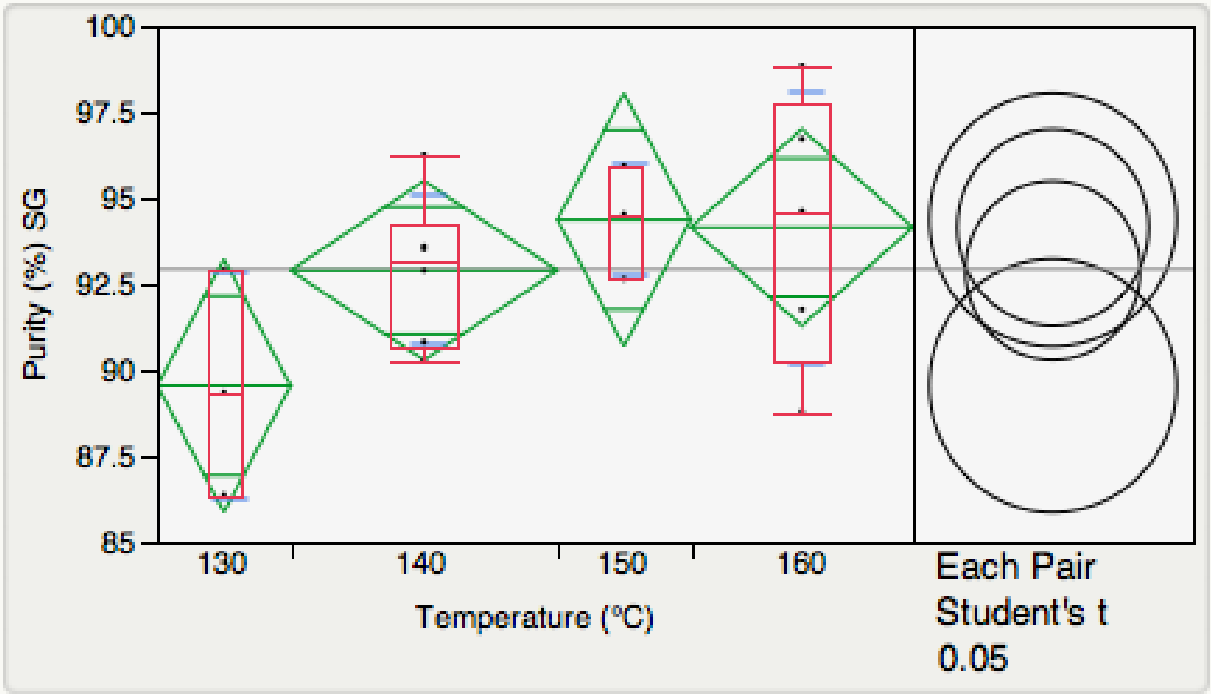

Figure 34. One way Analysis of switchgrass purity.

The Welch's ANOVA (3, 5.74) = 45.47, p<0.0002, also indicated a highly significant difference for poplar purity at 130°C as can be seen in Figure 35.

Figure 35. Welch's ANOVA of mean lignin purity across temperature for poplar (left) and switchgrass (right).

Even though the ash content of poplar lignin is more than double compared to switchgrass [0.2 % (±0.1) and 0.1% (±0.1)], some poplar lignin could achieve the highest purity but the elemental analysis could not find any profound differences between the feedstocks (Figure 36).

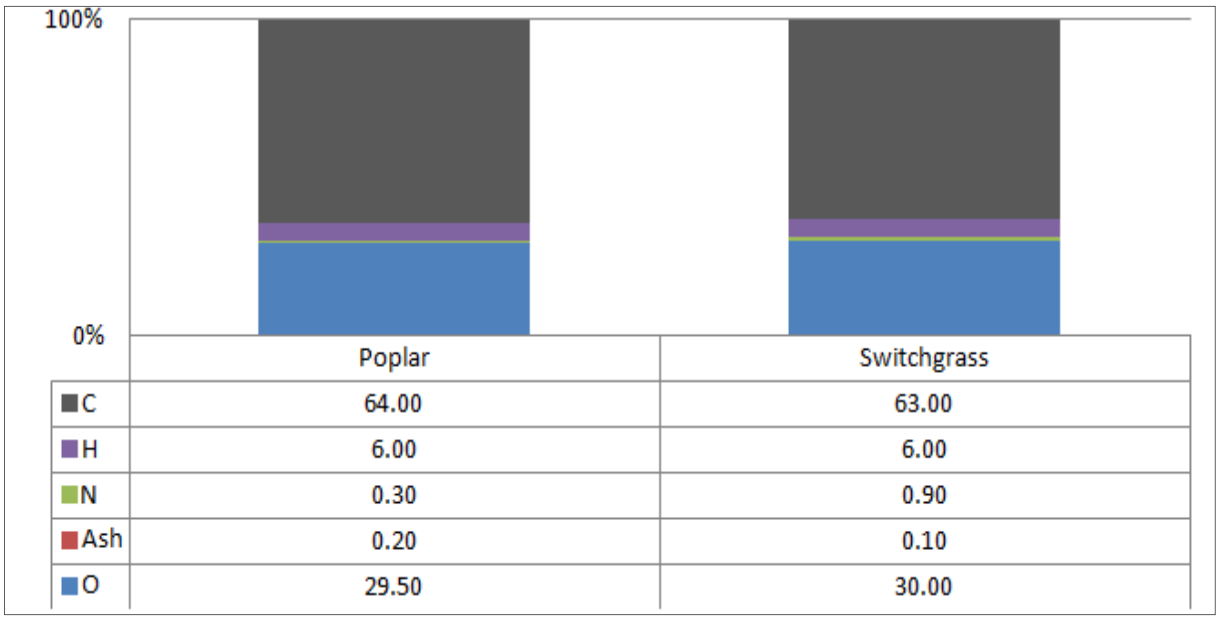

	Poplar	Switchgrass
C	64.00	63.00
H	6.00	6.00
N	0.30	0.90
Ash	0.20	0.10
O	29.50	30.00

Figure 36. Elemental analysis of poplar and switchgrass showing carbon, hydrogen, nitrogen, ash and oxygen content.

At low severity switchgrass showed a full melt at higher temperatures but at a severity of about 2.21 both feedstocks exhibited similar behavior. The integrity of the melting though was not complete and sporadically showed particles that did not show a melt at all and that made it complicated for melt spin applications.

All samples showed a clear glass transition. The difference of poplar and switchgrass transition temperature is minimal, even identical at a severity of 2.61 but the specific heat capacity is higher for poplar lignin.

Figure 37 shows that the change in heat capacity of poplar samples is almost the same as severity increases and declines at more than 2.75. That leads to the conclusion that these samples are relatively pure and that most of the material undergoes the transition, assuming that at a heat capacity of 0.4 most material transforms. In contrast, for switchgrass lignin the capacity is lower at lower severity but has considerable variation. Hence, less material changes from solid to liquid state.

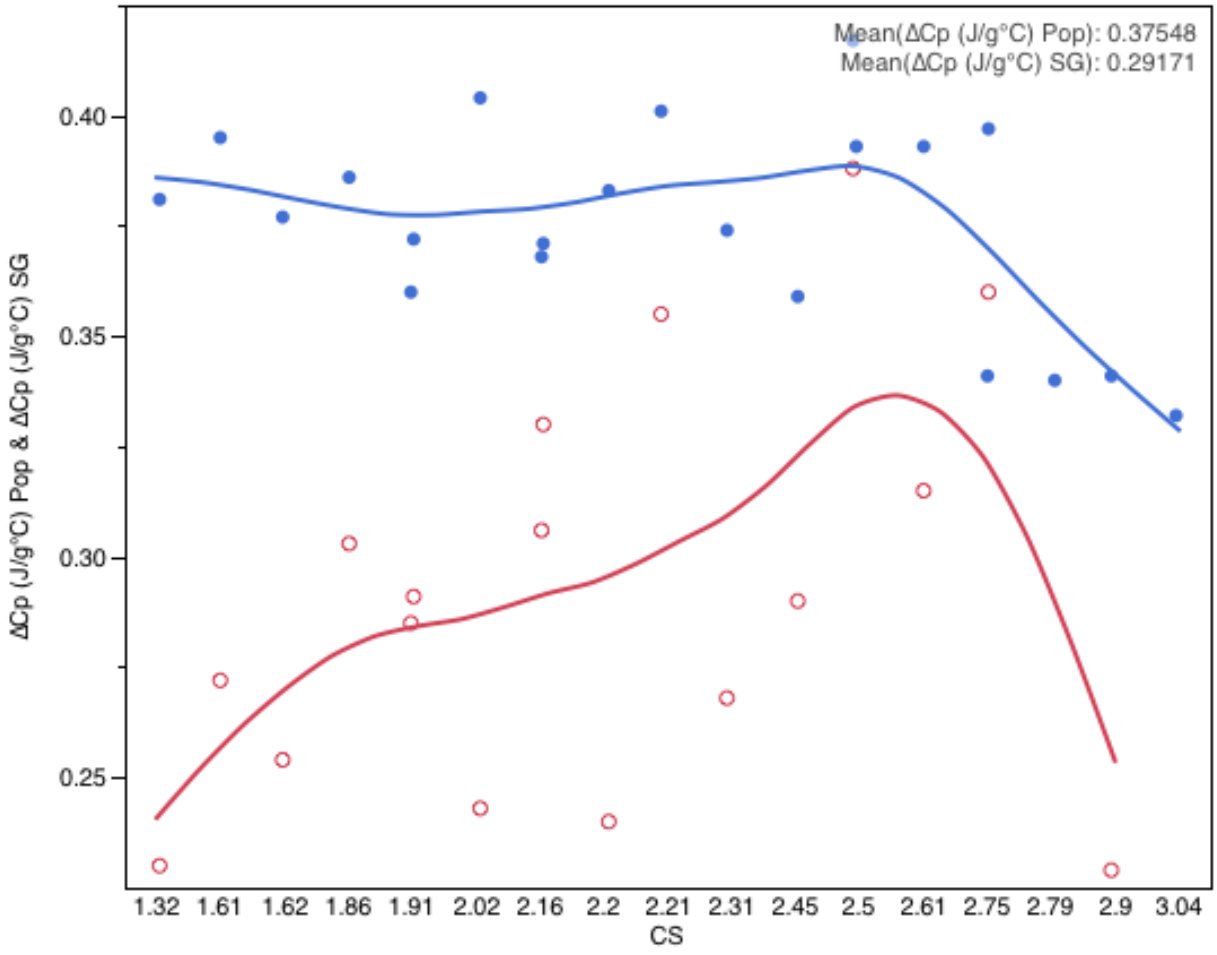

Figure 37. Comparison of heat capacity of poplar (upper line) and switchgrass (lower line)

Decomposition properties seem also very similar besides the T_d, the temperature where 5% of the sample weight decomposed. Figure 38 illustrates a flat, slightly downward trend for poplar, whereas the switchgrass trend exhibits the opposite.

However, switchgrass lignin shows fairly low T_d compared to poplar lignin, it can thus be concluded that switchgrass lignin contain a higher amount of impurities as low molecular

weight volatiles and carbohydrates also verified by decomposition measurements (recall Figure 30).

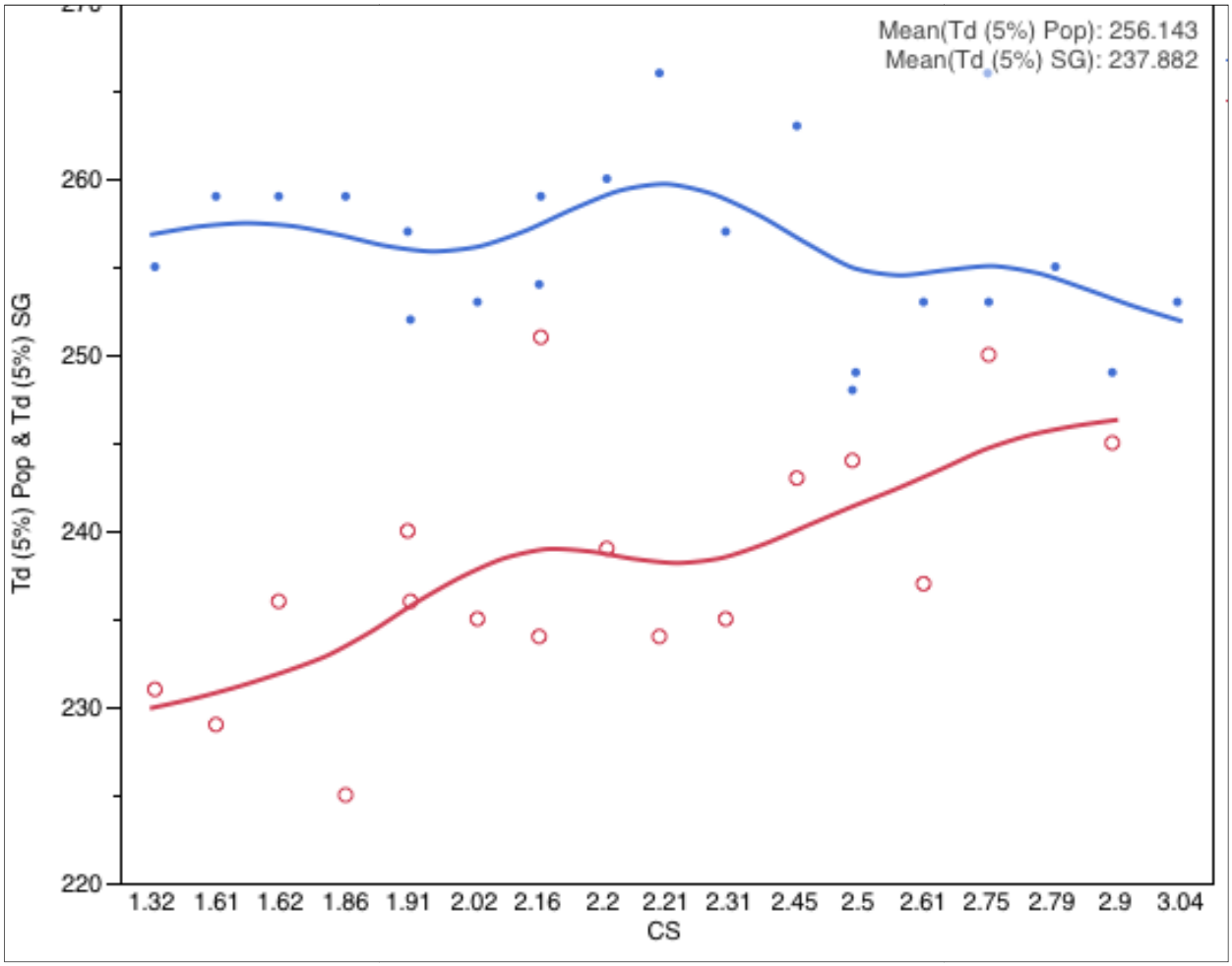

Figure 38. Comparison of decomposition temperature of poplar (upper line) and switchgrass (lower line).

4.7. Comparison of Time Dependent Runs

The second approach of this study discusses the changes of thermal properties over time and provided very interesting and trend-setting findings. The average purity of these runs is 94.0% (±1.3) for poplar and 93.2% (±0.4) for switchgrass. Heat capacity for poplar is 0.4 (±0.1) and 0.3 (±0.1) for switchgrass. These averages are very close to those from all runs described before but the peaks lead to the possibility to increase properties for both feedstocks. As can be seen in Figure 39, the purity of switchgrass lignin and the coherent heat capacity show a peak at 180 minutes runtime. The immense jump of the poplar purity seems very interesting but is just based on a single value; therefore a replicate test would be advised. The heat capacity for switchgrass shows an increase as well, from 120 to 360 minutes and indicates higher molecular weight and therefore could be beneficial for spinning applications.

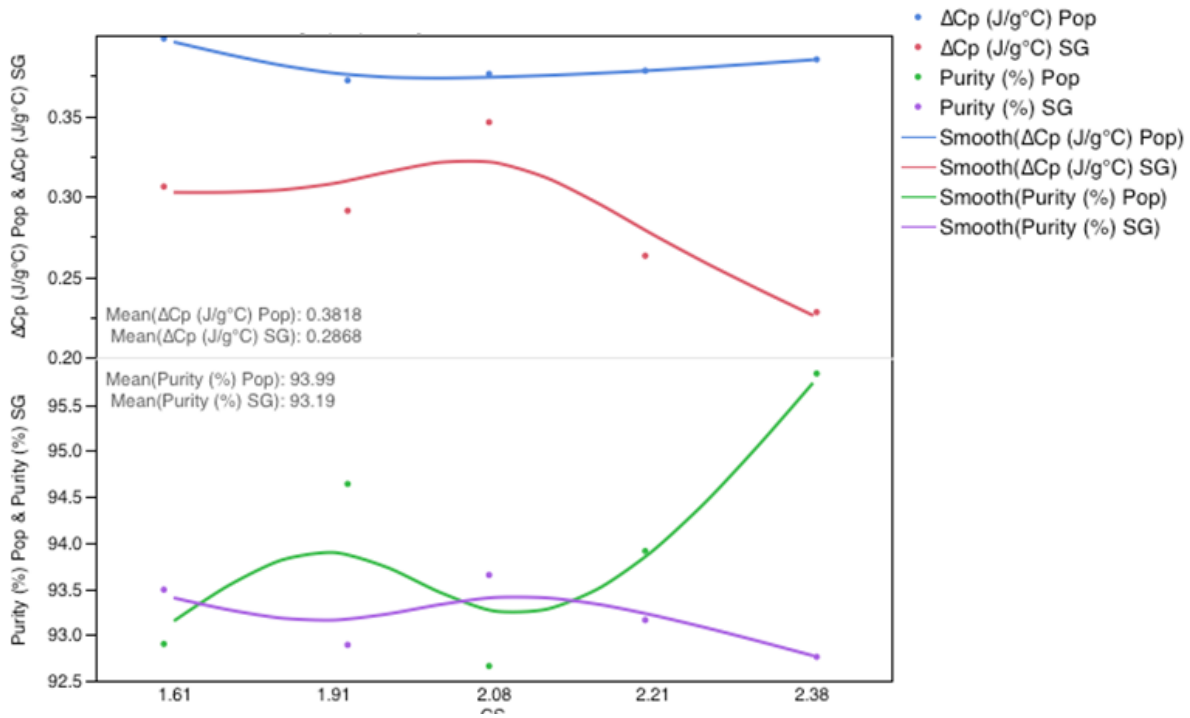

Figure 39. Comparison of purity and heat capacity of poplar and switchgrass.

4.8. Morphology of Fibers (SEM)

Fibers from both tulip poplar and Alamo switchgrass were melt spun with different diameters and images with a magnification of 100 to 600 were taken with an SEM showing the morphology. Impurities as low molecular weight volatiles could be determined but were not found in these fibers.

The diameter was measured for 70 fibers at each condition and was in a range of 15.1-23.55μm. Fibers with a fractionation severity of 2.5 reached a diameter as low as 15.1μm (±1.1) and also exhibited the best tensile properties as can be seen in the next section.

Figure 40 shows an image with a magnification of 400 of carbon fiber produced from tulip poplar with a severity of 2.5. The surface seems to be very smooth without impurities.

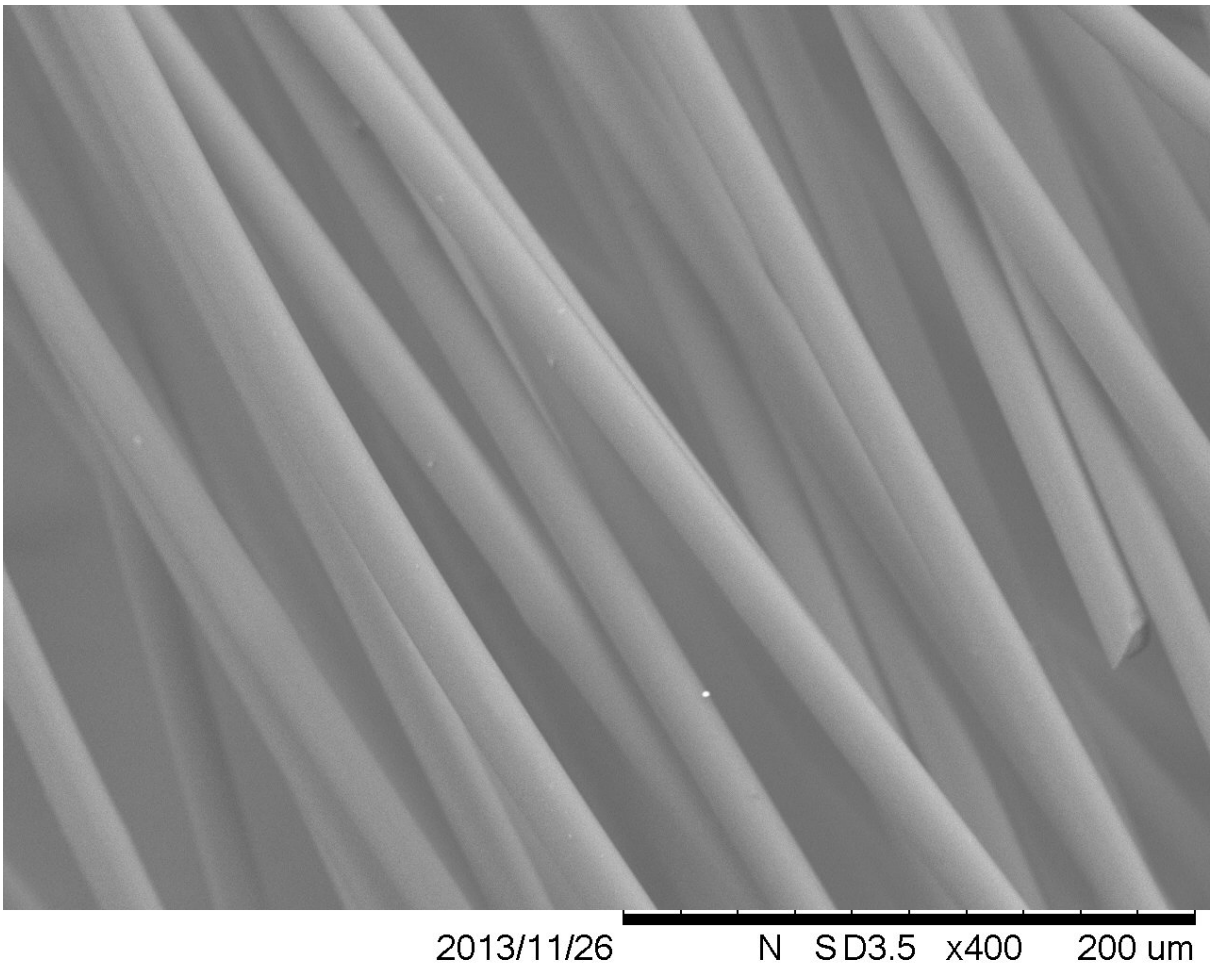

Figure 40. SEM image of carbon fiber from tulip poplar

Carbon fiber derived from switchgrass can be seen in Figure 41. This image has a magnification of 600 and shows in contrast to poplar fibers an uneven surface. These black pores are most likely due to impurities, which volatilized during the stabilization process.

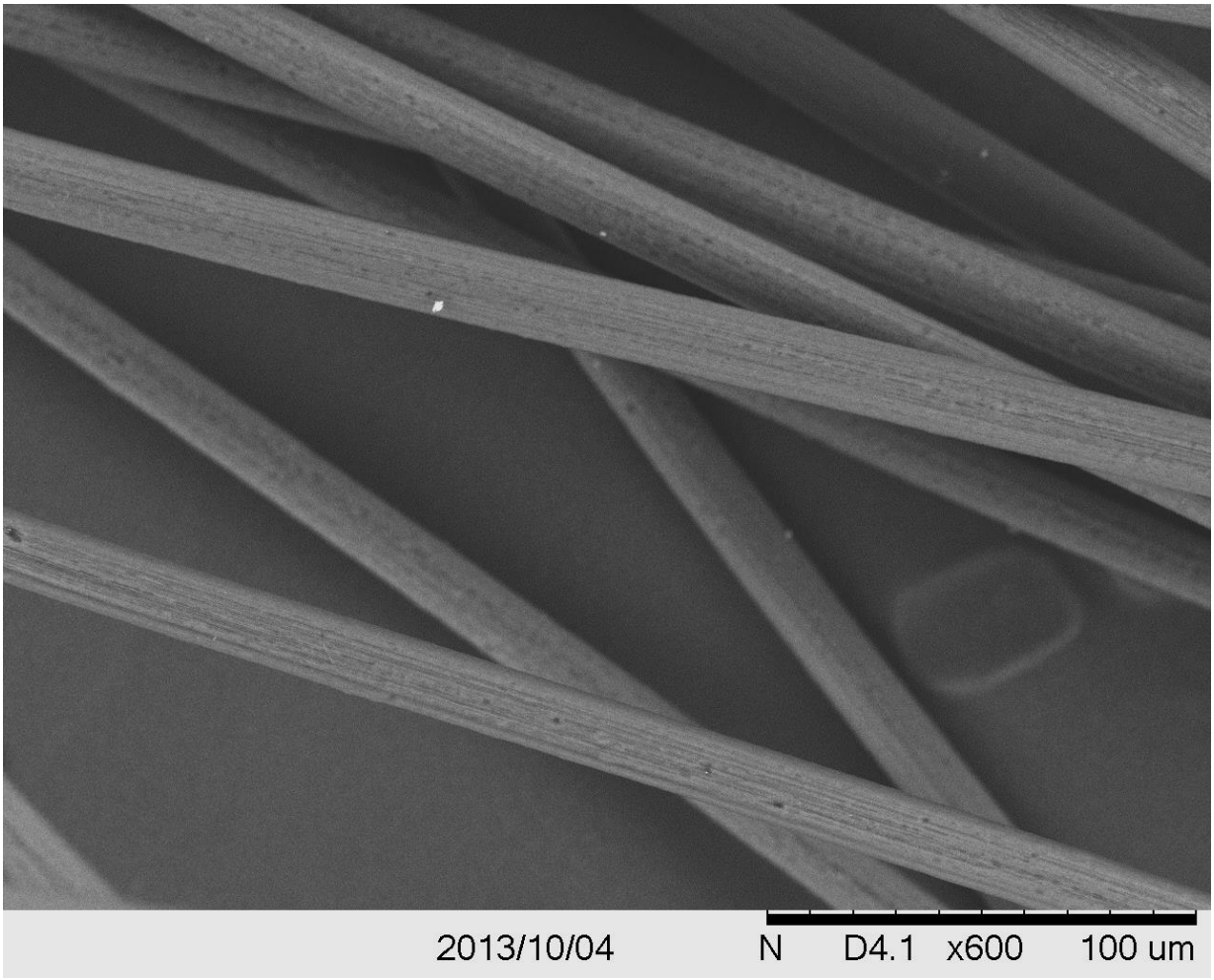

Figure 41. SEM image of carbon fibers from switchgrass.

4.9. Mechanical Properties of Lignin-Based Carbon Fiber

Mechanical properties of the fibers were measured by single filament testing according to the ASTM standard (ASTM D3379-75) and the results showed that the best fibers had a tensile strength of 640.1 GPa (±174.8) and a tensile modulus of 40.6 GPa (±4.6). For tulip poplar these condition were found to be at a CS of 2.2, 2.79 and 2.5. Carbon fiber derived from switchgrass could just be obtained from a CS of 2.5. For each condition, 35 fibers were tested and presented as an average as can be seen in Table 8. Due to a very good spinning performance, the speed of the rotating cylinder that collects the monofilament fiber could be increased to 600rpm delivering fibers with smaller diameter. Although the diameter of some fibers could be decreased the mechanical properties did not increase.

Table 8: Mechanical properties of carbon fiber

	Poplar	**Poplar**	**Poplar**	**Switchgrass**
CS	2.2	2.79	2.5	2.5
Spinning [rpm]	165	180	200	160
Diameter [µm]	21.2 (±2.3)	23.55 (±2.4)	17.7 (±1.3)	15.1 (±1.1)
Strength [MPa]	273.2 (±96.8)	470.6 (±99.2)	669.9 (±146.0)	476.0 (±90.7)
Modulus [GPa]	21.1 (±6.3)	34.4 (±5.8)	40.6 (±4.6)	34.1 (±3.8)

Table 9. Mechanical properties of different precursor processes.

Precursor	**Strength [Mpa]**	**Modulus [Gpa]**	**Reference**
Hardwood Kraft lignin	400-550	30-60	(Kadla et al., 2002)
Softwood organosolv lignin	355 (±53)	39.1 (±13.3)	(Uraki et al., 1995)
Phenolated steam exploded lignin	388 (±123)	40 (±14)	(Sudo et al., 1992)
Purified hardwood Kraft lignin (OP86)	1,069	82.7	(Baker et al., 2012)
Tulip poplar organosolv lignin	669.9 (±146)	40.6 (±4.6)	this research

CHAPTER V. CONCLUSIONS

Lignin for carbon fiber production should exhibit high purity as well as high carbon content but have specific thermal properties as discussed below,

The biomass itself was analyzed and gave an average lignin yield of 17.46% from theoretically 24.26% for tulip poplar and 15.47% from theoretically 22.7% indicating that there are improvement possibilities in the fractionation process. That could be due to incomplete fractionation or losses in the workup. Organosolv fractionation of both feedstocks showed an increase of cellulose decomposition with increasing severity, whereas the highest lignin yield could be obtained at temperatures of 140°C and 160°C. A one way ANOVA conducted on lignin yield of tulip poplar runs led to the conclusion that runs at 130°C are significantly lower in yield but an additional Welch's ANOVA was conducted given the unequal variances across the subgroups of temperature and indicated no significant difference at an $\alpha = 0.05$.

The same analysis carried out for differences in purity indicated that a significant difference could be discovered for tulip poplar runs at 130°C compared to other temperatures and therefore further investigations at this temperature can be excluded. Runs using switchgrass showed similar behavior but could not be statistically proven. Conditions for the highest lignin yields were found to be 170°C, 0.1M and 120min for tulip poplar and 140°C, 0.1M and 120min for Alamo switchgrass. Investigations over different runtimes gave a maximum lignin yield for tulip poplar at 180min with 128.7g and for Alamo switchgrass at 120min with 68.7g. Characterization measurements of lignin includes purity and ash content, elemental analysis, softening properties, and transition and decomposition temperatures. A purity as high as 98.6% and 98.8% using the same fractionation conditions, 160°C, 0.1M for 120min, could be achieved for poplar and switchgrass, respectively. The ash content of both feedstocks was very low in comparison to lignin obtained using other methods of biomass fractionation, therefore it can be neglected.

Softening behavior was similar for both feedstocks with an appreciable melt starting at 147.7°C and a full melt at 158.2°C, but crosslinking seems to be about 20°C lower for switchgrass. Elemental analysis showed that the carbon content increases steadily with higher severity whereas the hydrogen contents decreases but both feedstocks gave almost an identical elemental composition. Analysis on decomposition properties confirmed those results and gave an idea about the thermal treatability and impurities of the samples. Also the transition measurements supported those findings, especially the width of the glass transition analysis. It could be observed that with higher severity the onset, of the decomposition

temperature decreases and the coherent width of the T_G increases, showing higher low molecular weight volatiles as well as higher molecular weight distribution.

However, organosolv fractionation investigating time as variable offered some very interesting outcomes. This research indicates that enhanced spinning feasibilities of lignin exist,

SEM images gave information of carbon fiber integrity and were used to determine their diameter giving a lowest diameter of 15.1μm (±1.1). The best performing samples were used to produce carbon fiber which was further tested for their mechanical properties. Tensile strength of 476MPa for switchgrass and 669.9MPa for poplar and modulus of 34.1GPa for switchgrass and 40.6GPa for poplar could be reached.

Recall Table 9 summarized the mechanical properties of carbon fiber derived from different processes. Achieved properties documented in previous research suggested that properties could be exceeded. However, such achievements were not reached in this thesis research; therefore the research hypotheses of this thesis could not be supported. Possible reasons for this outcome could be the chemical structure of lignin used; as well as insufficient scale conditions of the melt spinning process. Research is ongoing to enhance these properties.

The mechanical properties achieved, although lower than the current recommended target properties of 1.72GPa tensile strength and 172GPa tensile modulus, represent a contribution towards the research of the continuous production of carbon fibers by melt spinning using a lignin precursor. This research hopefully provides initial data as a contribution for future research direction.

CHAPTER VI. FUTURE DIRECTIONS

The empirical nature of this research raises many experimental suggestions for improvement. Most of the findings rely on individual samples. Therefore a set of replicates of these samples would provide broader inference.

In this study a set of analytical methods was used to verify the accuracy of the findings but there are many other techniques that could be applied. Final carbon fiber can be measured with a DSC as well as TGA to check on changes in thermal behavior. NMR is a very detailed method of chemical analysis for organic compounds and can be used to analyze produced lignin.

To analyze lignin a pyrolysis gas chromatography mass spectrometry is commonly used and provides information to identify the evolved products and to assign corresponding fragments as well as impurities.

A statistically sound experimental design would enhance inference and allow for the investigation of interactions among the independent variables. This study may provide valuable direction on factors and levels of independent variables for a statistical experimental design.

All of the carbon fiber used in this study were manufactured on a mini screw extruder which has some disadvantages such as incomplete inert atmosphere. Comparing results from lignin produced on a larger scale extruder may provide an interesting assessment of the effect of scale on final carbon properties.

References

Adler, E. (1977). Lignin chemistry - past, present and future. *Wood Sci. Technol., 11*, 169-218.

Astner, F. A. (2012). Lignin yield maximization of lignocellulosic biomass by taguchi robust product design using organosolv fractionation. University of Tennessee, Knoxville, 137 pages.

Baker, D. A., Gallego, N. C., Baker, F. S. (2012). On the characterization and spinning of an organic-purified lignin toward manufacture of low-cost carbon fiber. *J. Appl. Polym. Sci.*, 227-234.

Baker, D. A., Rials, T. G. (2013). Recent advances in low-cost carbon fiber manufacture from lignin. *J. Appl. Polym. Sci., 130*, 713-728.

Bartels, R. H., Beatty, J. C., Barksy, B. A. *An introduction to splines for use in computer graphics and geometric modeling*. Morgan Kaufmann. San Francisco, CA, (1987).

Black, S. K., Hames, B. R., Myers, M. D., A. A. patent 5,730,838. M. R. Institute (1998).

Bozell, J. J., Black, S. K., Myers, M., Cahill, D., Miller, W. P., Park, S. (2011). Solvent fractionation of renewable woody feedstocks: Organosolv generation of biorefinery process streams for the production of biobased chemicals. *Biomass and Bioenergy, 35*, 4197-4208.

Bozell, J. J., Holladay, J. E., White, J. F., D., J. (2007). Top value-added chemicals from biomass: Results of screening for potential candidates from biorefinery lignin. *PNNL-16983, Pacific Northwest National Laboratory,* WA.

Brebu, M., Vasile, C. (2010). Thermal degradation of lignin - a review. *Cell. Chem. Technol., 44*, 353-363.

Candolle, A. P. d., Sprengel, K. P. J. *Elements of the philosophy of plants: containing the principles of scientific botany ... with a history of the science, and practical illustrations. by a. p. de candolle and k. sprengel. tr. from the german.* W. Blackwood. Edinburgh, (1821).

Cara, C., Ruiz, E., Ballesteros, I., Negro, M. J., Castro, E. (2006). Enhanced enzymatic hydrolysis of olive tree wood by steam explosion and alkaline peroxide delignification. *Process. Biochem., 41*, 423-429.

Chae, H. G., Choi, Y. H., Minus, M. L., Kumar, S. (2009). Carbon nanotube reinforced small diameter polyacrylonitrile based carbon fiber. *Compos. Sci. Technol., 69*, 406-413.

Chakar, F. S., Ragauskas, A. J. (2004). Review of current and future softwood kraft lignin process chemistry. *Industrial Crops and Products, 20*, 131-141.

Cheng, S., Zhu, S. (2009). Lignocellulosic feedstock biorefinery - the future of chemical and energy industry. *Bioresources, 4*, 456-457.

Christopher, L. P. (2009). Bioprocessing potential of integrated forest products biorefineries. *Abstr. Pap. Am. Chem. Sci., 238*.

Coats, A. W., Redfern, J. P. (1963). Thermogravimetric analysis. *Analyst, 88*, 906-924.

Council, N. R. *Biobased industrial products: research and commercialization priorities.* The National Academies Press. Washington, DC, (2000).

Davies, R. D. (1984). Pulp and paper-manufacture - an industry of the future. *S. Afr. J. Sci., 80*, 109-115.

de la Torre, M. J., Moral, A., Hernández, M. D., Cabeza, E., Tijero, A. (2013). Organosolv lignin for biofuel. *Industrial Crops and Products, 45*, 58-63.

Fadeeva, V. P., Tikhova, V. D., Nikulicheva, O. N. (2008). Elemental analysis of organic compounds with the use of automated chns analyzers. *J. Anal. Chem., 63*, 1094-1106.

Frank, E., Hermanutz, F., Buchmeiser, M. R. (2012). Carbon fibers: precursors, manufacturing, and properties. *Macromolecular Materials and Engineering, 297*, 493-501.

Fyans, R. L., Brennan, W. P., Earnest, C. M. (1985). The evolution of differential scanning calorimetry - a review. *Thermochim. Acta., 92*, 385-389.

Garrote, G., Dominguez, H., Parajo, J. C. (1999). Hydrothermal processing of lignocellulosic materials. *Holz Roh. Werkst., 57*, 191-202.

Goh, C. S., Tan, H. T., Lee, K. T., Brosse, N. (2011). Evaluation and optimization of organosolv pretreatment using combined severity factors and response surface methodology. *Biomass and Bioenergy, 35*, 4025-4033.

Hamaguchi, M., Kautto, J., Vakkilainen, E. (2013). Effects of hemicellulose extraction on the kraft pulp mill operation and energy use: review and case study with lignin removal. *Chemical Engineering Research and Design, 91*, 1284-1291.

Harmsen, P. F. H., Huijgen, W. J. J., Lopez, L. M. B., Bakker, R. R. C. *Literature review of physical and chemical pretreatment processes for lignocellulosic biomass.* Wageningen UR, Food and Biobased Research. Wageningen, (2010).

Helander, M., Theliander, H., Lawoko, M., Henriksson, G., Zhang, L. M., Lindstrom, M. E. (2013). Fractionation of technical lignin: molecular mass and ph effects. *Bioresources, 8*, 2270-2282.

Hergert, H. L., Pye, E. K. (1992). Recent history of organosolv pulping. *Notes Tech.*, 9-26.

Hongbin, C., Lei, W. *Lignocelluloses feedstock biorefinery as petrorefinery substitutes.* InTech. Canada, (2013).

Huang, X. (2009). Fabrication and properties of carbon fibers. *Materials. 2*, 2369-2403.

Ibrahim, M., Glasser, W. G. (1999). Steam-assisted biomass fractionation. part III: a quantitative evaluation of the "clean fractionation" concept. *Bioresource Technology, 70*, 181-192.

Ilankeeran, P. K., Mohite, P. M., Kamle, S. (2012). Axial tensile testing of single fibres. *Modern Mechanical Engineering, 2,* 151-156.

Johnson, D. J., Tomizuka, I., Watanabe, O. (1975). Fine-structure of lignin-based carbon-fibers. *Carbon, 13*, 321-325.

Kadla, J. F., Kubo, S., Venditti, R. A., Gilbert, R. D., Compere, A. L., Griffith, W. (2002). Lignin-based carbon fibers for composite fiber applications. *Carbon, 40*, 2913-2920.

Kamm, B., Schonicke, P., Kamm, M. (2009). Biorefining of green biomass - technical and energetic considerations. *Clean-Soil Air Water, 37*, 27-30.

Klason, P. (1920). Lignin and lignin-reactions (II). *Ber. Dtsch. Chem. Ges., 53*, 1862-1863.

Kubo, S., Kadla, J. F. (2008). Thermal decomposition study of isolated lignin using temperature modulated tga. *J. Wood Chem. Technol., 28*, 106-121.

Kubo, S., Uraki, Y., Sano, Y. (1998). Preparation of carbon fibers from softwood lignin by atmospheric acetic acid pulping. *Carbon, 36*, 1119-1124.

Li, J., Gellerstedt, G., Toven, K. (2009). Steam explosion lignins; their extraction, structure and potential as feedstock for biodiesel and chemicals. *Bioresource Technology, 100*, 2556-2561.

Lora, J. H., Glasser, W. G. (2002). Recent industrial applications of lignin - a sustainable alternative to non-renewable materials. *Journal of Polymers and the Environment, 10*, 39-48.

Lysenko, A. A., Lysenko, V. A., Astashkina, O. V., Gladunova, O. I. (2011). Resource - conserving carbon fibre technologies. *Fibre Chem., 42*, 278-286.

Manfred, M., Gerhard, W., Gottfried, P., Hildegard, S., Nikolaus, S., A. A. patent 3723609 B. Aktiengesellschaft (1973).

Mani, S., Tabil, L. G., Sokhansanj, S. (2006). Effects of compressive force, particle size and moisture content on mechanical properties of biomass pellets from grasses. *Biomass and Bioenergy, 30*, 648-654.

Maraun, H. (2013). Maximizing lignin yield using experimental design - analyzing the impact of solvent composition and feedstock particle size on the organosolv process in the presence of feedstock contamination. University of Tennessee, Knoxville, 124 pages.

Mason, W. H., A. A. patent 1,655,618. (1928).

Menon, V., Rao, M. (2012). Trends in bioconversion of lignocellulose: biofuels, platform chemicals and biorefinery concept. *Prog. Energ. Combust., 38*, 522-550.

Norberg, I., Nordström, Y., Drougge, R., Gellerstedt, G., Sjöholm, E. (2013). A new method for stabilizing softwood kraft lignin fibers for carbon fiber production. *J. Appl. Polym. Sci., 128*, 3824-3830.

Otani, S., Fukuoka, Y., Igarashi, B., Sasaki, K., A. A. patent 3,461,082. (1969).

Seo, D. K., Park, S. S., Hwang, J., Yu, T. U. (2010). Study of the pyrolysis of biomass using thermo-gravimetric analysis (tga) and concentration measurements of the evolved species. *J. Anal. Appl. Pyrol., 89*, 66-73.

Sjostrom, E. *Wood chemistry. Fundamentals and applications.* Gulf Professional. San Diego, (1993).

Stoner, E. G., Edie, D. D., Durham, S. D. (1994). An end-effect model for the single-filament tensile test. *J. Mater. Sci., 29*, 6561-6574.

Sudo, K., Shimizu, K. (1992). A new carbon-fiber from lignin. *J. Appl. Polym. Sci., 44*, 127-134.

Suhas, P. J. M., Carrott, M. M. L. R. (2007). Lignin - from natural adsorbent to activated carbon: a review. *Bioresource Technology, 98*, 2301-2312.

Uraki, Y., Kubo, S., Nigo, N., Sano, Y., Sasaya, T. (1995). Preparation of carbon-fibers from organosolv lignin obtained by aqueous acetic-acid pulping. *Holzforschung, 49*, 343-350.

Wang, X. T., Lu, L. S. (2010). Steam explosion pretreatment technique and application in biomass conversion. *Adv. Mater. Res-Switz, 113-114*, 525-528.

Warren, C. D., Paulauskas, F. L., Baker, F. S., Eberle, C. C., Naskar, A. (2009). Development of commodity grade, lower cost carbon fiber-commercial applications. *Sampe J., 45*, 24-36.

Watson, E. S., Justin, J., Brenner, N., Oneill, M. J. (1964). Differential scanning calorimeter for quantitative differential thermal analysis. *J. Anal. Chem., 36*, 1233-1256.

Wiberly, S. E. (1963). *On analytical chemistry and applied spectroscopy,* Paper presented at the 14th Annual Pittsburgh Conference, Pittsburgh, Pennsylvania.

Wyman, C. E., Goodman, B. J. (1993). Biotechnology for production of fuels, chemicals, and materials from biomass. *Appl. Biochem. Biotechnol., 39-40*, 41-59.

Yang, Q., Wu, S. B. (2009). Thermogravimetric characteristics of wheat straw lignin. *Cell. Chem. Technol., 43*, 133-139.

Appendices

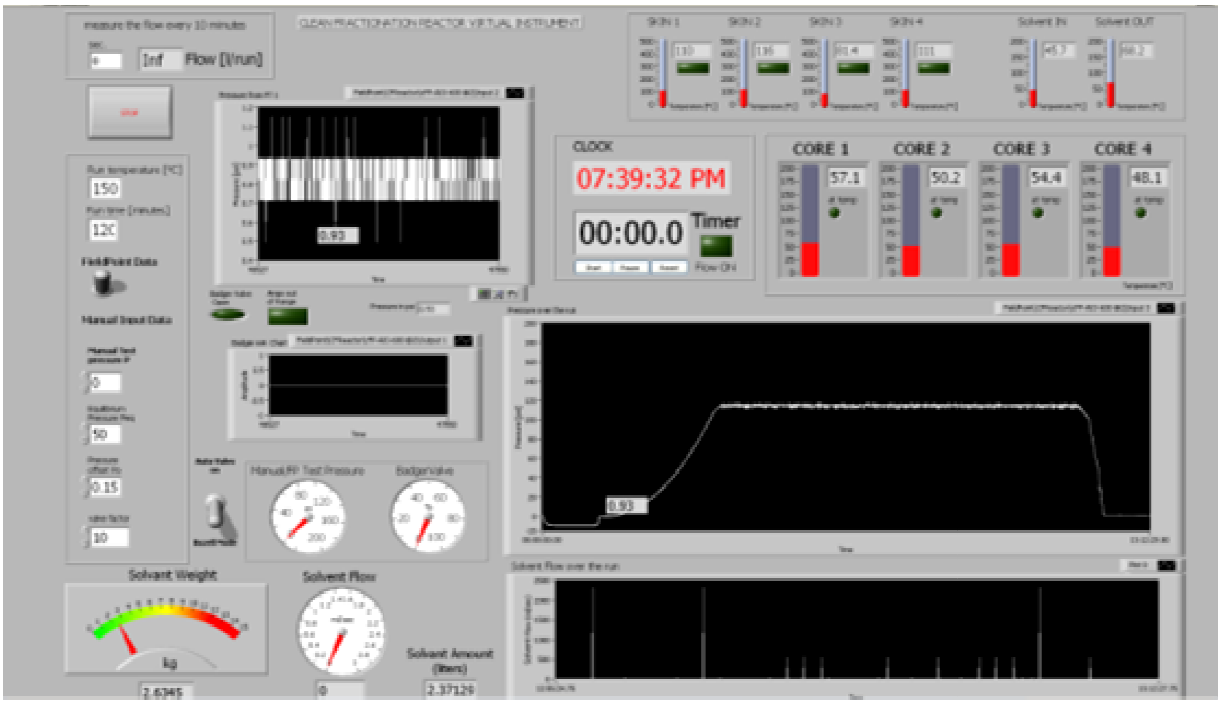

Figure 42: Pressure diagram of organosolv fractionation run

Table 10. Yield of tulip poplar runs.

Run #	Temp. [°C]	Acid Con. [M]	black L. [ml]	Lignin [g]	CL dry [g]
T005	130	0.025	9680	69.1	315
T007	130	0.05	10200	89.6	328
T008	130	0.1	10380	107.5	323
T036	140	0.025	10290	97.2	342
#169	140	0.05	N/D	123.0	323
T009	140	0.075	10290	118.3	299
T010	140	0.1	9750	115.9	290
#174	140	0.1	N/D	124.0	320
T011	140	0.15	9200	115.8	272
T012	150	0.025	9400	116.1	306
T035	150	0.05	9100	109.9	283
T014	150	0.1	8700	101.8	250
T037	160	0.025	9000	108.4	255
#172	160	0.05	N/D	131.0	223
T016	160	0.075	9000	110.5	192
#176	160	0.1	N/D	130.0	166
T017	160	0.1	9600	121.2	174
T006	160	0.15	9200	126.7	120
T019	170	0.025	9000	122.2	181
T021	170	0.05	9000	144.8	89
T022	170	0.1	9000	178.5	21

Table 11. Time dependent runs of tulip poplar at 140°C.

Run #	Time [min]	Solvent [kg]	s-l ratio	black L. [ml]	Lignin [g]	CL dry [g]	MC-Cel. [%]
T023	60	7.09	1 : 12.02	8360	98.9	316	79.7
#169	120	10.40	1 : 14.44	N/D	123.0	323	N/D
T024	180	9.70	1 : 13.47	12650	128.7	274	80.0
T025	240	10.16	1 : 14.11	9680	111.4	298	79.5
T026	360	10.28	1 : 14.28	9400	84.1	294	78.6

Table 12: Yield of Alamo switchgrass runs

Run #	Temp. [°C]	Acid M Con.	black L [ml].	Lignin [ml]	CL dry [g]	MC-Cel. [%]
T015	130	0.025	9880	59.4	199	77.9
T020	130	0.05	9800	59.6	167	78.2
T027	130	0.1	9600	49.3	199	74.5
T038	140	0.025	10000	61.5	166	79.3
#178	140	0.05	N/D	68.7	153	N/D
T001	140	0.075	10000	68.8	144	78.2
#175	140	0.1	N/D	69.0	139	N/D
T018	140	0.1	9900	59.0	147	78.0
T002	140	0.15	10290	62.3	130	78.5
T028	150	0.025	10000	57.6	132	81.5
T029	150	0.05	9250	67.8	139	79.4
T030	150	0.1	11000	60.6	122	79.8
T039	160	0.025	8500	60.0	150	78.0
#171	160	0.05	N/D	64.1	96	N/D
T003	160	0.075	9300	66.1	76	76.3
#177	160	0.1	N/D	63.0	68	N/D
T004*	160	0.15	9500	48.5	44	84.7

Table 13: Time dependent runs of Alamo switchgrass at 140°C

Run #	Time [min]	Solvent [kg]	s-l ratio	black L. [ml]	Lignin [g]	CL dry [g]	MC-Cel. [%]
T031	60	8.28	1 : 19.26	8300	60.7	174	81.3
#178	120	10.20	1 : 23.72	N/D	68.7	153	N/D
T034	180	10.27	1 : 21.88	10400	58.2	127	82.4
T032	240	10.6	1 : 24.65	10500	62.2	143	78.5
T033	360	10.37	1 : 24.12	11200	51.5	143	81.2

Table 14: Overview Klason

Klason Lignin Analysis

Run#		**T001**	**T002**	**T003**	**T004**	**T005**	**T006**	**T007**	**T008**	**T009**	**T010**	**T011**	**T012**	**T014**	**T015**	**T016**	**T017**
ODW	[g]	0.302	0.297	0.302	0.299	0.296	0.299	0.298	0.296	0.296	0.298	0.301	0.297	0.297	0.301	0.299	0.293
AIL	[%]	86.89	85.3	87.19	88.69	84.87	89.46	84.42	85.21	86.82	88.54	92.86	90.67	93.18	83.62	93.39	94.36
Ash Content	[%]	0.00	0.00	0.05	0.03	0.34	0.35	0.05	0.03	0.30	0.00	0.56	0.99	0.84	0.48	0.79	0.39
ASL	[%]	3.92	3.97	4.57	4.87	5.36	4.81	5.43	4.92	6.01	4.73	2.61	3.01	1.93	2.76	2.99	3.945
total Lignin	[%]	90.81	89.27	91.76	93.56	90.23	94.27	89.85	90.13	92.83	93.27	95.47	93.68	95.11	86.38	96.38	98.31

Run#		**T018**	**T019**	**T020**	**T021**	**T022**	**T023**	**T024**	**T025**	**T026**	**T027**	**T028**	**T029**	**T030**	**T031**	**T032**	**T033**
ODW	[g]	0.294	0.293	0.309	0.294	0.302	0.305	0.303	0.295	0.308	0.303	0.306	0.302	0.302	0.305	0.302	0.304
AIL	[%]	90.95	92.8	85.49	90.6	91.43	88.84	88.09	87.9	91.25	87.27	88.05	89.9	91.56	89.39	89.6	88.46
Ash Content	[%]	0.43	0.12	0.52	0.56	0.35	0.36	0	0.29	0.76	0.16	0	1.56	0	0.06	0	0.17
ASL	[%]	2.59	3.99	3.26	6.05	4.98	4.06	4.57	6.45	4.58	4.15	3.75	4.62	4.37	4.1	3.56	3.77
total Lignin	[%]	93.54	96.79	88.75	96.65	96.41	92.90	92.66	94.35	95.83	91.42	91.80	94.52	95.93	93.49	93.16	92.23

Run#		**T034**	**T035**	**T036**	**T037**	**T038**	**T039**	**#169**	**#172**	**#174**	**#176**	**#171**	**#175**	**#177**	**#178**
ODW	[g]	0.296	0.301	0.299	0.293	0.303	0.301	0.306	0.295	0.297	0.302	0.294	0.294	0.301	0.297
AIL	[%]	89.56	92.08	85.2	92.52	86.43	84.77	88.81	93.44	91.57	92.97	91.17	91.35	91.97	88.9
Ash Content	[%]	0.12	0.1	0	0.02	0.15	0	0	0	0	1.08	0.92	0.68	0.43	0.9
ASL	[%]	4.1	4.76	6.4	4.59	3.85	4.02	5.83	4.54	4.9	5.64	5.72	4.9	6.86	4.58
total Lignin	[%]	93.66	96.84	91.60	97.11	90.28	88.79	94.64	97.98	96.47	98.61	96.89	96.25	98.83	93.48

Table 15: Ash content of poplar and switchgrass runs

Temp (deg.C)	Acid (M)	Poplar ash (%)	Switchgrass ash (%)
130	0.025	0.06	0.07
130	0.05	0.00	0.02
130	0.1	0.07	0.00
140	0.025	0.09	0.03
140	0.05	0.07	0.10
140	0.075	0.00	0.00
140	0.1	0.13	0.12
140	0.1	0.00	0.10
140	0.15	0.00	0.00
150	0.025	0.00	0.27
150	0.05	0.00	0.16
150	0.1	0.16	0.14
160	0.025	0.13	0.00
160	0.05	0.19	0.12
160	0.075	0.07	0.09
160	0.1	0.00	0.20
160	0.1	0.21	N/D
160	0.15	0.19	0.23
170	0.025	0.09	
170	0.05	0.42	
170	0.1	0.18	
140 / 60min	0.05	0.09	0.13
140 / 120min	0.05	0.07	0.10
140 / 180min	0.05	0.09	0.18
140 / 240min	0.05	0.10	0.11
140 / 360min	0.05	0.16	0.17

Table 16: Elemental analysis of tulip poplar lignin

Carbon (%)	Hydrogen (%)	Nitrogen (%)
60.93 (0.32)	6.23 (0.11)	0.33 (0.03)
62.47 (0.09)	6.36 (0.10)	0.28 (0.03)
62.76 (0.27)	6.16 (0.06)	0.28 (0.04)
62.13 (0.27)	6.15 (0.10)	0.33 (0.01)
63.03 (0.11)	6.12 (0.18)	0.25 (0.01)
63.25 (0.14)	6.23 (0.05)	0.28 (0.03)
63.84 (0.30)	6.03 (0.06)	0.30 (0.06)
63.73 (0.04)	6.11 (0.05)	0.30 (0.05)
63.92 (0.14)	6.21 (0.18)	0.26 (0.02)
63.37 (0.07)	6.27 (0.04)	0.26 (0.02)
63.83 (0.24)	6.18 (0.06)	0.33 (0.02)
64.19 (0.14)	6.01 (0.10)	0.24 (0.02)
63.60 (0.29)	5.92 (0.01)	0.33 (0.02)
64.56 (0.09)	5.90 (0.07)	0.23 (0.05)
64.86 (0.18)	5.87 (0.09)	0.21 (0.02)
64.71 (0.13)	5.78 (0.04)	0.21 (0.02)
64.95 (0.04)	5.81 (0.01)	0.28 (0.03)
64.87 (0.06)	5.86 (0.04)	0.20 (0.01)
65.13 (0.05)	5.87 (0.05)	0.29 (0.02)
65.22 (0.17)	5.64 (0.06)	0.26 (0.06)
65.30 (0.13)	5.57 (0.05)	0.28 (0.04)
62.87 (0.26)	6.10 (0.04)	0.36 (0.02)
63.03 (0.11)	6.12 (0.18)	0.25 (0.01)
63.17 (0.03)	6.11 (0.06)	0.37 (0.02)
62.56 (0.15)	6.03 (0.05)	0.34 (0.04)
63.27 (0.16)	5.77 (0.07)	0.30 (0.03)

Table 17: Elemental analysis of Alamo switchgrass lignin

Carbon (%)	Hydrogen (%)	Nitrogen (%)
60.82 (0.22)	5.90 (0.14)	0.99 (0.01)
61.34 (0.17)	5.86 (0.04)	0.89 (0.03)
63.17 (0.06)	5.88 (0.01)	0.75 (0.03)
61.95 (0.22)	5.85 (0.10)	1.19 (0.05)
62.30 (0.04)	6.01 (0.14)	0.93 (0.03)
62.43 (0.15)	5.96 (0.03)	0.89 (0.06)
64.23 (0.25)	6.18 (0.09)	0.82 (0.03)
63.77 (0.16)	5.86 (0.08)	0.75 (0.04)
63.39 (0.19)	6.02 (0.11)	0.66 (0.04)
63.35 (0.31)	5.75 (0.02)	0.89 (0.01)
62.81 (0.25)	5.92 (0.06)	0.89 (0.05)
63.82 (0.08)	6.07 (0.07)	0.79 (0.02)
62.27 (0.24)	6.02 (0.03)	1.16 (0.03)
64.60 (0.11)	5.85 (0.16)	0.79 (0.02)
63.27 (0.16)	6.04 (0.04)	0.90 (0.01)
65.12 (0.24)	5.66 (0.09)	0.72 (0.04)
64.38 (0.05)	5.73 (0.04)	0.76 (0.01)
62.71 (0.23)	6.27 (0.01)	0.98 (0.01)
62.30 (0.04)	6.01 (0.14)	0.93 (0.03)
63.07 (0.27)	6.05 (0.03)	0.93 (0.04)
62.51 (0.20)	6.23 (0.04)	0.99 (0.02)
62.36 (0.28)	6.03 (0.09)	0.89 (0.03)

Table 18: Melt properties of tulip poplar lignin

Temp. (°C)	Acid Con.(M)	Discoloration	Localized melting	Appreciable melting	Full melt	Melt flow	High melt flow
130	0.025	144	147	150	155	160	171
130	0.05	137	142	147	153	160	178
130	0.1	142	145	149	153	160	175
140	0.025	132	138	142	147	152	178
140	0.05	130	135	140	144	148	170
140	0.075	135	140	145	151	155	173
140	0.1	138	141	145	150	159	180
140	0.1	140	144	147	150	154	178
140	0.15	140	145	149	154	160	174
150	0.025	135	138	141	145	152	170
150	0.05	130	135	140	145	152	180
150	0.1	145	152	156	162	170	185
160	0.025	132	137	142	147	153	177
160	0.05	140	143	147	150	154	173
160	0.075	140	145	152	158	167	177
160	0.1	151	157	166	169	177	195
160	0.1	148	153	157	162	176	195
160	0.15	143	146	150	157	167	178
170	0.025	135	138	142	148	159	170
170	0.05	141	146	152	160	170	195
170	0.1	142	148	155	162	175	200
140-1h	0.05	133	138	143	147	157	172
140-2h	0.05	130	135	140	144	148	170
140-3h	0.05	135	140	143	149	159	180
140-4h	0.05	138	143	146	152	160	178
140-6h	0.05	143	150	155	162	172	188

Table 19: Melt properties of Alamo switchgrass lignin

Temp. (°C)	Acid Con. (M)	Discoloration	Localized melting	Appreciable melting	Full melting	Melt flow	High melt Flow
130	0.025	145	155	160	170	177	185
130	0.05	146	152	155	161	167	176
130	0.1	135	143	150	160	166	172
140	0.025	134	141	151	166	172	178
140	0.05	138	145	150	156	164	175
140	0.075	150	157	161	169	174	179
140	0.1	130	135	141	147	153	160
140	0.1	138	142	150	155	162	170
140	0.15	142	147	154	166	172	182
150	0.025	137	144	150	160	165	172
150	0.05	134	139	146	152	159	177
150	0.1	135	140	145	151	160	170
160	0.025	140	151	155	160	166	172
160	0.05	130	135	140	148	155	175
160	0.075	142	145	148	152	158	163
160	0.1	142	148	154	163	175	N/A
160	0.15	142	148	154	163	175	N/A
140-1h	0.05	137	143	149	155	159	164
140-2h	0.05	138	145	150	156	164	175
140-3h	0.05	135	143	150	155	160	168
140-4h	0.05	138	143	148	155	162	170
140-6h	0.05	135	143	149	160	170	180

Table 20: Transition temperatures of tulip poplar lignin

T_G (°C)	ΔCp (J/g. °C)	Onset (°C)	End (°C)	Width (°C)
124.3 (0.5)	0.381 (0.004)	114.7 (0.8)	132.4 (0.2)	17.7 (0.8)
123.6 (0.4)	0.395 (0.020)	113.3 (0.5)	132.7 (0.1)	19.4 (0.5)
126.0 (0.6)	0.386 (0.010)	116.4 (0.5)	134.4 (0.5)	18.0 (0.1)
118.3 (0.0)	0.377 (0.011)	110.5 (0.5)	125.7 (0.1)	15.2 (0.3)
114.5 (1.6)	0.372 (0.012)	104.2 (1.8)	123.0 (1.8)	18.8 (1.6)
120.1 (1.2)	0.404 (0.023)	108.4 (0.7)	130.0 (1.1)	21.7 (1.2)
119.9 (0.7)	0.368 (0.020)	108.7 (0.5)	129.3 (1.0)	20.6 (1.0)
122.3 (0.3)	0.371 (0.010)	112.2 (0.9)	131.0 (0.6)	18.8 (0.2)
123.5 (0.6)	0.374 (0.010)	111.6 (0.9)	133.4 (0.1)	21.8 (0.8)
118.9 (0.2)	0.360 (0.002)	108.7 (0.2)	127.2 (0.4)	18.4 (0.6)
119.8 (0.3)	0.383 (0.005)	109.8 (0.3)	128.3 (0.4)	18.5 (0.2)
127.6 (1.1)	0.359 (0.012)	114.5 (0.7)	138.8 (0.4)	24.2 (0.7)
119.0 (0.7)	0.401 (0.017)	109.3 (0.7)	127.3 (0.8)	18.0 (1.4)
117.3 (1.2)	0.417 (0.018)	102.9 (1.0)	127.8 (1.0)	24.9 (0.1)
122.2 (0.5)	0.393 (0.011)	108.5 (0.9)	134.1 (1.8)	25.5 (2.0)
125.4 (0.5)	0.397 (0.017)	111.6 (0.8)	139.3 (0.8)	27.8 (0.9)
133.4 (1.9)	0.341 (0.017)	116.8 (1.7)	145.9 (2.3)	29.3 (2.4)
120.4 (1.1)	0.341 (0.010)	103.2 (0.6)	134.9 (0.6)	31.8 (0.7)
117.5 (0.1)	0.393 (0.016)	104.8 (1.0)	128.9 (0.3)	24.1 (0.7)
127.6 (0.6)	0.340 (0.006)	110.7 (0.3)	139.7 (0.4)	29.1 (0.7)
131.8 (0.6)	0.332 (0.004)	110.1 (1.7)	144.2 (0.8)	34.1 (0.9)
121.2 (0.3)	0.398 (0.006)	111.2 (0.6)	130.0 (0.4)	18.8 (0.2)
114.5 (1.6)	0.372 (0.012)	104.2 (1.8)	123.0 (1.8)	18.8 (1.6)
120.9 (0.5)	0.376 (0.001)	110.4 (0.2)	129.9 (0.5)	19.5 (0.2)
123.6 (0.7)	0.378 (0.007)	114.3 (0.7)	132.5 (0.8)	18.2 (0.6)
128.4 (0.5)	0.385 (0.018)	116.9 (0.5)	139.1 (0.2)	22.2 (0.3)

Table 21: Transition temperatures of Alamo switchgrass lignin

T_G (°C)	ΔCp (J/g. °C)	Onset (°C)	End (°C)	Width (°C)
130.8 (0.9)	0.230 (0.016)	115.8 (1.5)	143.1 (2.0)	27.3 (3.1)
129.5 (1.4)	0.272 (0.002)	118.8 (1.6)	137.9 (1.5)	19.1 (0.0)
121.0 (0.2)	0.303 (0.019)	105.7 (1.1)	132.7 (0.9)	16.9 (1.0)
126.8 (1.8)	0.254 (0.015)	108.5 (2.7)	143.6 (1.1)	35.2 (2.2)
127.8 (1.9)	0.291 (0.010)	117.1 (0.7)	136.7 (1.9)	19.6 (1.3)
130.6 (0.8)	0.243 (0.013)	120.2 (0.7)	140.4 (0.5)	20.1 (0.8)
118.9 (1.5)	0.306 (0.007)	105.5 (1.9)	128.2 (2.4)	22.7 (0.5)
124.1 (0.0)	0.330 (0.003)	108.8 (1.2)	135.7 (0.6)	26.9 (0.6)
123.7 (0.6)	0.268 (0.015)	111.4 (0.8)	134.7 (0.1)	23.4 (0.6)
121.3 (1.1)	0.285 (0.042)	110.2 (1.2)	133.9 (1.0)	23.7 (0.4)
114.6 (0.2)	0.240 (0.015)	102.2 (0.7)	124.9 (0.6)	22.6 (0.6)
123.9 (0.8)	0.290 (0.014)	109.9 (0.9)	134.4 (2.2)	24.6 (2.7)
129.8 (0.3)	0.355 (0.004)	117.9 (0.7)	141.1 (0.3)	23.2 (0.7)
117.5 (0.8)	0.388 (0.026)	103.2 (0.7)	127.9 (1.3)	24.7 (1.1)
121.9 (0.9)	0.315 (0.019)	109.1 (0.6)	133.0 (0.2)	23.9 (0.7)
130.1 (0.2)	0.360 (0.016)	114.2 (0.0)	142.2 (0.7)	28.0 (0.7)
120.4 (0.9)	0.229 (0.007)	107.7 (0.6)	135.1 (0.7)	27.4 (1.1)
123.9 (0.7)	0.306 (0.016)	111.3 (1.0)	135.2 (0.5)	23.9 (0.7)
127.8 (1.9)	0.291 (0.010)	117.1 (0.7)	136.7 (1.9)	19.6 (1.3)
125.8 (0.1)	0.346 (0.012)	112.2 (0.5)	134.8 (0.2)	22.6 (0.7)
123.2 (1.2)	0.263 (0.009)	111.9 (0.8)	133.8 (1.4)	22.0 (1.4)
122.5 (0.1)	0.228 (0.010)	112.3 (0.8)	135.9 (0.7)	23.6 (0.8)

Table 22: Decomposition temperatures of tulip poplar

Run Number	Onset (°C)	Td (5%)	Char (%)	DTG peak (°C)
T005	255.1	255.0	31.1	352.9
T007	269.6	259.0	32.2	349.2
T008	271.0	259.0	33.5	354.7
T036	266.9	259.0	32.2	351.6
169	279.8	252.0	33.5	355.5
T009	277.9	253.0	34.9	358.8
174	282.5	254.0	36.1	362.0
T010	279.4	259.0	35.3	361.0
T011	277.7	257.0	36.8	361.6
T012	275.2	257.0	33.7	357.0
T035	274.0	260.0	35.9	358.3
T014	285.2	263.0	37.4	360.5
T037	282.8	266.0	36.4	354.7
172	277.4	248.0	37.7	357.7
T016	282.8	253.0	38.9	356.9
T017	284.9	253.0	39.8	360.3
176	287.2	266.0	40.5	360.6
T006	244.8	249.0	39.2	359.3
T019	281.6	249.0	39.3	355.2
T021	268.0	255.0	41.9	362.0
T022	256.7	253.0	42.7	359.9
T023	265.9	257.0	33.4	359.2
169	279.8	252.0	33.5	355.5
T024	272.6	258.0	34.7	362.5
T025	273.3	262.0	33.4	359.5
T026	286.4	262.0	37.1	364.3

Table 23. Decomposition temperatures of Alamo switchgrass

Run Number	Onset (°C)	Td (5%)	Char (%)	DTG peak (°C)
T015	236.0	231.0	33.6	350.4
T020	235.6	229.0	34.0	349.8
T027	253.3	225.0	34.1	362.6
T038	244.6	236.0	34.9	348.5
178	251.8	236.0	35.5	355.9
T001	223.0	235.0	34.9	349.9
175	250.6	234.0	35.1	360.6
T018	279.9	251.0	39.4	356.9
T002	238.3	235.0	34.8	357.2
T028	255.6	240.0	35.8	359.4
T029	255.4	239.0	35.6	359.0
T030	263.2	243.0	37.1	365.6
T039	241.8	234.0	34.1	349.0
171	261.6	244.0	35.7	357.3
T003	224.0	237.0	37.4	358.2
177	267.7	250.0	39.7	358.9
T004	227.4	245.0	39.7	358.3
T031	264.2	237.0	34.5	355.3
178	251.8	236.0	35.5	355.9
T034	253.3	239.0	36.4	355.3
T032	237.3	237.0	34.2	359.4
T033	243.9	237.0	35.3	356.0

Table 24. Overview of tulip poplar runs showing conditions, yield, purity and elemental analysis

Yellow Poplar Runs												
Conditions						Yield		Klason		Elemental Analysis		
Run Number	Feedstock	Mass (g)	Temp (°C)	Acid (M)	Time (min)	Yield (g)	Cell Yield (g)	Purity (%)	Ash (%)	C (%)	H (%)	N (%)
T005	Y.Poplar	720	130	0.025	120	69.1	315	90.22 (0.25)	0.06	60.93 (0.32)	6.23 (0.11)	0.33 (0.03)
T007	Y.Poplar	720	130	0.05	120	89.6	328	89.86 (0.13)	0.00	62.47 (0.09)	6.36 (0.10)	0.28 (0.03)
T008	Y.Poplar	720	130	0.1	120	107.5	323	90.13 (0.02)	0.07	62.76 (0.27)	6.16 (0.06)	0.28 (0.04)
T036	Y.Poplar	720	140	0.025	120	97.2	342	91.61 (0.47)	0.09	62.13 (0.27)	6.15 (0.10)	0.33 (0.01)
169	Y.Poplar	720	140	0.05	120	123.0	323	94.64 (0.42)	0.07	63.03 (0.11)	6.12 (0.18)	0.25 (0.01)
T009	Y.Poplar	720	140	0.075	120	118.3	299	92.83 (0.96)	0.00	63.25 (0.14)	6.23 (0.05)	0.28 (0.03)
174	Y.Poplar	720	140	0.1	120	124.0	290	96.46 (0.32)	0.13	63.84 (0.30)	6.03 (0.06)	0.30 (0.06)
T010	Y.Poplar	720	140	0.1	120	115.9	320	93.26 (0.36)	0.00	63.73 (0.04)	6.11 (0.05)	0.30 (0.05)
T011	Y.Poplar	720	140	0.15	120	115.8	272	95.46 (0.21)	0.00	63.92 (0.14)	6.21 (0.18)	0.26 (0.02)
T012	Y.Poplar	720	150	0.025	120	116.1	306	93.26 (0.45)	0.00	63.37 (0.07)	6.27 (0.04)	0.26 (0.02)
T035	Y.Poplar	720	150	0.05	120	109.9	283	96.61 (0.47)	0.00	63.83 (0.24)	6.18 (0.06)	0.33 (0.02)
T014	Y.Poplar	720	150	0.1	120	101.8	250	95.11 (0.54)	0.16	64.19 (0.14)	6.01 (0.10)	0.24 (0.02)
T037	Y.Poplar	720	160	0.025	120	108.4	255	97.12 (0.15)	0.13	63.60 (0.29)	5.92 (0.01)	0.33 (0.02)
172	Y.Poplar	720	160	0.05	120	131.0	223	97.98 (0.12)	0.19	64.56 (0.09)	5.90 (0.07)	0.23 (0.05)
T016	Y.Poplar	720	160	0.075	120	110.5	192	96.37 (0.43)	0.07	64.86 (0.18)	5.87 (0.09)	0.21 (0.02)
T017	Y.Poplar	720	160	0.1	120	121.2	166	97.12 (0.39)	0.00	64.71 (0.13)	5.78 (0.04)	0.21 (0.02)
176	Y.Poplar	720	160	0.1	120	130.0	174	98.61 (0.18)	0.21	64.95 (0.04)	5.81 (0.01)	0.28 (0.03)
T006	Y.Poplar	720	160	0.15	120	126.7	120	94.27 (0.12)	0.19	64.87 (0.06)	5.86 (0.04)	0.20 (0.01)
T019	Y.Poplar	720	170	0.025	120	122.2	181	96.79 (0.16)	0.09	65.13 (0.05)	5.87 (0.05)	0.29 (0.02)
T021	Y.Poplar	720	170	0.05	120	144.8	89	96.65 (0.13)	0.42	65.22 (0.17)	5.64 (0.06)	0.26 (0.06)
T022	Y.Poplar	720	170	0.1	120	178.5	21	96.40 (0.50)	0.18	65.30 (0.13)	5.57 (0.05)	0.28 (0.04)
T023	Y.Poplar	720	140	0.05	60	98.9	316	92.90 (0.64)	0.09	62.87 (0.26)	6.10 (0.04)	0.36 (0.02)
169	Y.Poplar	720	140	0.05	120	123.0	323	94.64 (0.42)	0.07	63.03 (0.11)	6.12 (0.18)	0.25 (0.01)
T024	Y.Poplar	720	140	0.05	180	128.7	274	92.66 (0.84)	0.09	63.17 (0.03)	6.11 (0.06)	0.37 (0.02)
T025	Y.Poplar	720	140	0.05	240	111.4	298	93.91 (0.32)	0.10	62.56 (0.15)	6.03 (0.05)	0.34 (0.04)
T026	Y.Poplar	720	140	0.05	360	84.1	294	95.84 (0.10)	0.16	63.27 (0.16)	5.77 (0.07)	0.30 (0.03)

Table 25. Overview of tulip poplar runs showing trasition, melting and decomposition temperatures

Yellow Poplar Runs											
DSC					FisherJohns			TGA			
Tg (deg.C)	ΔCp (J/g°C)	Onset (°C)	End (°C)	Width (°C)	Appreciable melting	fullmelt (°C)	crosslink (°C)	Onset (°C)	Td (5%)	Char (%)	DTG peak (°C)
124.3 (0.5)	0.381 (0.004)	114.7 (0.8)	132.4 (0.2)	17.7 (0.8)	150.0	155.0	240.0	255.1	255.0	31.1	352.9
123.6 (0.4)	0.395 (0.020)	113.3 (0.5)	132.7 (0.1)	19.4 (0.5)	147.0	153.0	235.0	269.6	259.0	32.2	349.2
126.0 (0.6)	0.386 (0.010)	116.4 (0.5)	134.4 (0.5)	18.0 (0.1)	149.0	153.0	250.0	271.0	259.0	33.5	354.7
118.3 (0.0)	0.377 (0.011)	110.5 (0.5)	125.7 (0.1)	15.2 (0.3)	142.0	147.0	220.0	266.9	259.0	32.2	351.6
114.5 (1.6)	0.372 (0.012)	104.2 (1.8)	123.0 (1.8)	18.8 (1.6)	140.0	144.0	220.0	279.8	252.0	33.5	355.5
120.1 (1.2)	0.404 (0.023)	108.4 (0.7)	130.0 (1.1)	21.7 (1.2)	145.0	151.0	260.0	277.9	253.0	34.9	358.8
119.9 (0.7)	0.368 (0.020)	108.7 (0.5)	129.3 (1.0)	20.6 (1.0)	145.0	150.0	220.0	282.5	254.0	36.1	362.0
122.3 (0.3)	0.371 (0.010)	112.2 (0.9)	131.0 (0.6)	18.8 (0.2)	147.0	150.0	235.0	279.4	259.0	35.3	361.0
123.5 (0.6)	0.374 (0.010)	111.6 (0.9)	133.4 (0.1)	21.8 (0.8)	149.0	154.0	210.0	277.7	257.0	36.8	361.6
118.9 (0.2)	0.360 (0.002)	108.7 (0.2)	127.2 (0.4)	18.4 (0.6)	141.0	145.0	220.0	275.2	257.0	33.7	357.0
119.8 (0.3)	0.383 (0.005)	109.8 (0.3)	128.3 (0.4)	18.5 (0.2)	140.0	145.0	220.0	274.0	260.0	35.9	358.3
127.6 (1.1)	0.359 (0.012)	114.5 (0.7)	138.8 (0.4)	24.2 (0.7)	156.0	162.0	200.0	285.2	263.0	37.4	360.5
119.0 (0.7)	0.401 (0.017)	109.3 (0.7)	127.3 (0.8)	18.0 (1.4)	142.0	147.0	220.0	282.8	266.0	36.4	354.7
117.3 (1.2)	0.417 (0.018)	102.9 (1.0)	127.8 (1.0)	24.9 (0.1)	147.0	150.0	220.0	277.4	248.0	37.7	357.7
122.2 (0.5)	0.393 (0.011)	108.5 (0.9)	134.1 (1.8)	25.5 (2.0)	152.0	158.0	220.0	282.8	253.0	38.9	356.9
125.4 (0.5)	0.397 (0.017)	111.6 (0.8)	139.3 (0.8)	27.8 (0.9)	166.0	162.0	215.0	284.9	253.0	39.8	360.3
133.4 (1.9)	0.341 (0.017)	116.8 (1.7)	145.9 (2.3)	29.3 (2.4)	157.0	169.0	220.0	287.2	266.0	40.5	360.6
120.4 (1.1)	0.341 (0.010)	103.2 (0.6)	134.9 (0.6)	31.8 (0.7)	150.0	157.0	230.0	244.8	249.0	39.2	359.3
117.5 (0.1)	0.393 (0.016)	104.8 (1.0)	128.9 (0.3)	24.1 (0.7)	142.0	148.0	190.0	281.6	249.0	39.3	355.2
127.6 (0.6)	0.340 (0.006)	110.7 (0.3)	139.7 (0.4)	29.1 (0.7)	152.0	160.0	220.0	268.0	255.0	41.9	362.0
131.8 (0.6)	0.332 (0.004)	110.1 (1.7)	144.2 (0.8)	34.1 (0.9)	155.0	162.0	210.0	256.7	253.0	42.7	359.9
121.2 (0.3)	0.398 (0.006)	111.2 (0.6)	130.0 (0.4)	18.8 (0.2)	143.0	147.0	210.0	265.9	257.0	33.4	359.2
114.5 (1.6)	0.372 (0.012)	104.2 (1.8)	123.0 (1.8)	18.8 (1.6)	140.0	144.0	220.0	279.8	252.0	33.5	355.5
120.9 (0.5)	0.376 (0.001)	110.4 (0.2)	129.9 (0.5)	19.5 (0.2)	143.0	149.0	210.0	272.6	258.0	34.7	362.5
123.6 (0.7)	0.378 (0.007)	114.3 (0.7)	132.5 (0.8)	18.2 (0.6)	146.0	152.0	210.0	273.3	262.0	33.4	359.5
128.4 (0.5)	0.385 (0.018)	116.9 (0.5)	139.1 (0.2)	22.2 (0.3)	155.0	162.0	200.0	286.4	262.0	37.1	364.3

Table 26. Overview of Alamo switchgrass runs showing conditions, yield, purity and elemental analysis

Alamo Switchgrass Runs												
Contitions						Yield		Klason		Elemental Analysis		
Run Number	Feedstock	Mass (g)	Temp (°C)	Acid (M)	Time (min)	Yield (g)	Cell. Yield (g)	Purity (%) (SD)	Ash (%)	C (%) (SD)	H (%) (SD)	N (%) (SD)
T015	Alamo	430	130	0.025	120	59.4	199	86.37 (0.24)	0.07	60.82 (0.22)	5.90 (0.14)	0.99 (0.01)
T020	Alamo	430	130	0.05	120	59.6	167	89.35 (0.10)	0.02	61.34 (0.17)	5.86 (0.04)	0.89 (0.03)
T027	Alamo	430	130	0.1	120	49.3	199	92.91 (1.15)	0.00	63.17 (0.06)	5.88 (0.01)	0.75 (0.03)
T038	Alamo	430	140	0.025	120	61.5	166	90.28 (0.51)	0.03	61.95 (0.22)	5.85 (0.10)	1.19 (0.05)
178	Alamo	430	140	0.05	120	68.7	153	92.89 (0.07)	0.10	62.30 (0.04)	6.01 (0.14)	0.93 (0.03)
T001	Alamo	430	140	0.075	120	68.8	144	90.81 (0.23)	0.00	62.43 (0.15)	5.96 (0.03)	0.89 (0.06)
175	Alamo	430	140	0.1	120	69.0	139	96.25 (0.15)	0.12	64.23 (0.25)	6.18 (0.09)	0.82 (0.03)
T018	Alamo	430	140	0.1	120	59.0	147	93.60 (1.49)	0.10	63.77 (0.16)	5.86 (0.08)	0.75 (0.04)
T002	Alamo	430	140	0.15	120	62.3	130	93.51 (0.80)	0.00	63.39 (0.19)	6.02 (0.11)	0.66 (0.04)
T028	Alamo	430	150	0.025	120	57.6	132	92.64 (0.16)	0.27	63.35 (0.31)	5.75 (0.02)	0.89 (0.01)
T029	Alamo	430	150	0.05	120	67.8	139	94.53 (0.87)	0.16	62.81 (0.25)	5.92 (0.06)	0.89 (0.05)
T030	Alamo	430	150	0.1	120	60.6	122	95.93 (0.16)	0.14	63.82 (0.08)	6.07 (0.07)	0.79 (0.02)
T039	Alamo	430	160	0.025	120	60.0	150	88.79 (1.32)	0.00	62.27 (0.24)	6.02 (0.03)	1.16 (0.03)
171	Alamo	430	160	0.05	120	64.1	96	96.72 (0.63)	0.12	64.60 (0.11)	5.85 (0.16)	0.79 (0.02)
T003	Alamo	430	160	0.075	120	66.1	76	91.76 (0.58)	0.09	63.27 (0.16)	6.04 (0.04)	0.90 (0.01)
177	Alamo	430	160	0.1	120	63.0	68	98.83 (0.66)	0.20	65.12 (0.24)	5.66 (0.09)	0.72 (0.04)
T004	Alamo	430	160	0.15	120	48.5	44	94.61 (0.23)	0.23	64.38 (0.05)	5.73 (0.04)	0.76 (0.01)
T031	Alamo	430	140	0.05	60	60.7	174	93.49 (0.12)	0.13	62.71 (0.23)	6.27 (0.01)	0.98 (0.01)
178	Alamo	430	140	0.05	120	68.7	153	92.89 (0.07)	0.10	62.30 (0.04)	6.01 (0.14)	0.93 (0.03)
T034	Alamo	430	140	0.05	180	58.2	127	93.65 (0.44)	0.18	63.07 (0.27)	6.05 (0.03)	0.93 (0.04)
T032	Alamo	430	140	0.05	240	62.2	143	93.16 (0.12)	0.11	62.51 (0.20)	6.23 (0.04)	0.99 (0.02)
T033	Alamo	430	140	0.05	360	51.5	143	92.76 (0.67)	0.17	62.36 (0.28)	6.03 (0.09)	0.89 (0.03)

Table 27. Overview of Alamo switchgrass runs showing transition, melting and decomposition temperatures

Alamo Switchgrass Runs											
DSC					FisherJohns			TGA			
Tg (deg.C)	ΔCp (J/g°C)	Onset (°C)	End (°C)	Width (°C)	Appreciable melting	fullmelt (°C)	crosslink	Onset (°C)	Td (5%)	Char (%)	DTG peak (°C)
130.8 (0.9)	0.230 (0.016)	115.8 (1.5)	143.1 (2.0)	27.3 (3.1)	160.0	170.0	185.0	236.0	231.0	33.6	350.4
129.5 (1.4)	0.272 (0.002)	118.8 (1.6)	137.9 (1.5)	19.1 (0.0)	155.0	161.0	195.0	235.6	229.0	34.0	349.8
121.0 (0.2)	0.303 (0.019)	105.7 (1.1)	132.7 (0.9)	16.9 (1.0)	150.0	160.0	200.0	253.3	225.0	34.1	362.6
126.8 (1.8)	0.254 (0.015)	108.5 (2.7)	143.6 (1.1)	35.2 (2.2)	151.0	166.0	185.0	244.6	236.0	34.9	348.5
127.8 (1.9)	0.291 (0.010)	117.1 (0.7)	136.7 (1.9)	19.6 (1.3)	150.0	156.0	185.0	251.8	236.0	35.5	355.9
130.6 (0.8)	0.243 (0.013)	120.2 (0.7)	140.4 (0.5)	20.1 (0.8)	161.0	169.0	200.0	223.0	235.0	34.9	349.9
118.9 (1.5)	0.306 (0.007)	105.5 (1.9)	128.2 (2.4)	22.7 (0.5)	141.0	147.0	180.0	250.6	234.0	35.1	360.6
124.1 (0.0)	0.330 (0.003)	108.8 (1.2)	135.7 (0.6)	26.9 (0.6)	150.0	155.0	195.0	279.9	251.0	39.4	356.9
123.7 (0.6)	0.268 (0.015)	111.4 (0.8)	134.7 (0.1)	23.4 (0.6)	154.0	166.0	220.0	238.3	235.0	34.8	357.2
121.3 (1.1)	0.285 (0.042)	110.2 (1.2)	133.9 (1.0)	23.7 (0.4)	150.0	160.0	200.0	255.6	240.0	35.8	359.4
114.6 (0.2)	0.240 (0.015)	102.2 (0.7)	124.9 (0.6)	22.6 (0.6)	146.0	152.0	180.0	255.4	239.0	35.6	359.0
123.9 (0.8)	0.290 (0.014)	109.9 (0.9)	134.4 (2.2)	24.6 (2.7)	145.0	151.0	190.0	263.2	243.0	37.1	365.6
129.8 (0.3)	0.355 (0.004)	117.9 (0.7)	141.1 (0.3)	23.2 (0.7)	155.0	160.0	195.0	241.8	234.0	34.1	349.0
117.5 (0.8)	0.388 (0.026)	103.2 (0.7)	127.9 (1.3)	24.7 (1.1)	140.0	148.0	200.0	261.6	244.0	35.7	357.3
121.9 (0.9)	0.315 (0.019)	109.1 (0.6)	133.0 (0.2)	23.9 (0.7)	148.0	152.0	190.0	224.0	237.0	37.4	358.2
130.1 (0.2)	0.360 (0.016)	114.2 (0.0)	142.2 (0.7)	28.0 (0.7)	154.0	163.0	200.0	267.7	250.0	39.7	358.9
120.4 (0.9)	0.229 (0.007)	107.7 (0.6)	135.1 (0.7)	27.4 (1.1)	154.0	163.0	200.0	227.4	245.0	39.7	358.3
123.9 (0.7)	0.306 (0.016)	111.3 (1.0)	135.2 (0.5)	23.9 (0.7)	149.0	155.0	200.0	264.2	237.0	34.5	355.3
127.8 (1.9)	0.291 (0.010)	117.1 (0.7)	136.7 (1.9)	19.6 (1.3)	150.0	156.0	220.0	251.8	236.0	35.5	355.9
125.8 (0.1)	0.346 (0.012)	112.2 (0.5)	134.8 (0.2)	22.6 (0.7)	150.0	155.0	190.0	253.3	239.0	36.4	355.3
123.2 (1.2)	0.263 (0.009)	111.9 (0.8)	133.8 (1.4)	22.0 (1.4)	148.0	155.0	190.0	237.3	237.0	34.2	359.4
122.5 (0.1)	0.228 (0.010)	112.3 (0.8)	135.9 (0.7)	23.6 (0.8)	149.0	160.0	200.0	243.9	237.0	35.3	356.0

Vita

Andreas Attwenger was born and raised in Gmunden, Austria. In the year 2008 he attended the University of Applied Sciences in Salzburg, where he earned his BSc in Engineering, in Forest Products Technology and Timber Construction researching the Improvement of Adhesive-systems in Ski production. After successfully completing his Bachelor's in 2011 he continued his studies at Salzburg University of Applied Sciences with his master program studying Forest Products Technology and Management.

Currently he is in a dual master's degree as a Graduate Research Assistant program with the Center for Renewable Carbon at the University of Tennessee and Salzburg University of Applied Sciences.

Andreas was studying under the advisory of Dr. Darren A. Baker and the supervision of Prof. Dr. Joseph J. Bozell and Prof. Dr. Timothy M. Young and his research is focused on lignin-based carbon fiber production using a novel organosolv fractionation process at the CRC.

He is looking forward to graduating from the University of Tennessee in May 2014 and the Salzburg University of Applied Sciences in January 2014.